

Electronic Theses and Dissertations, 2004-2019

2007

Using Electrochemical Monitoring To Predict Metal Release In Drinking Water Distribution Systems

Rajendra D. Vaidya
University of Central Florida

 Part of the [Environmental Engineering Commons](#)
Find similar works at: <https://stars.library.ucf.edu/etd>
University of Central Florida Libraries <http://library.ucf.edu>

This Doctoral Dissertation (Open Access) is brought to you for free and open access by STARS. It has been accepted for inclusion in Electronic Theses and Dissertations, 2004-2019 by an authorized administrator of STARS. For more information, please contact STARS@ucf.edu.

STARS Citation

Vaidya, Rajendra D., "Using Electrochemical Monitoring To Predict Metal Release In Drinking Water Distribution Systems" (2007). *Electronic Theses and Dissertations, 2004-2019*. 3391.
<https://stars.library.ucf.edu/etd/3391>

USING ELECTROCHEMICAL MONITORING TO PREDICT METAL
RELEASE IN DRINKING WATER DISTRIBUTION SYSTEMS

by

RAJENDRA VAIDYA

B.E (Civil) Walchand Institute of Technology India, 1996

M.S (Env. Engg.) Virginia Polytechnic Institute & State University, 2002

A thesis submitted in partial fulfillment of the requirements
for the degree of Doctor of Philosophy in Environmental Engineering
in the Department of Civil and Environmental Engineering
in the College of Engineering and Computer Science
at the University of Central Florida
Orlando, Florida

Fall Term
2007

Major Professor: James S. Taylor

© 2007 Rajendra Vaidya

ABSTRACT

Corrosion of distribution system piping and home plumbing materials is a major concern in the water community. Iron release adversely affects aesthetic water quality and the release of copper and lead is regulated by the Lead and Copper rule (LCR) and can adversely affect consumer health. Corrosion control is typically done by pH regulation and/or addition of corrosion inhibitors. Monitoring of corrosion control is typically done after the fact by monitoring metal release, functional group concentration of the selected chemical species or water quality. Hence, the associated laboratory analyses create a significant delay prior to the assessment of corrosion in drinking water systems. As corrosion in drinking water systems is fundamentally an electrochemical process, measurement of the electrical phenomena associated with corrosion can be used for real-time corrosion monitoring. This dissertation focuses on using parameters associated with electrochemical corrosion monitoring (EN) measurements in a field facility to predict and control the release of Iron, Copper and Lead in finished waters produced from ground, surface and saline sources with and without usage of corrosion inhibitors. EN data has not been used previously to correlate water quality and metal release; hence the use of EN data for corrosion control in drinking water systems has not been developed or demonstrated.

Data was collected over a one year period from a large field facility using finished waters that are distributed to each of the fourteen pilot distribution systems (PDSs),

corrosion loops and Nadles each. The PDSs have been built from aged pipes taken from existing distribution systems and contain links of PVC, lined cast Iron, unlined cast Iron and galvanized Steel pipe. The effluent for each PDS was split in two parts. One was delivered to the corrosion loops which are made from coiled copper pipe with lead-tin coupon inserted inside each loop and the other was delivered to the Nadles which housed the EN probes with electrodes for Fe or Cu or Pb-Sn. Finished water quality was monitored in and out of each PDS and total and dissolved Copper and Lead were monitored out of each corrosion loop. Photographs, scanning electron microscope (SEM) micrographs and energy dispersive x-ray spectroscopy (EDAX) conducted on all EN electrodes.

EN electrodes showed dark brown to blackish voluminous scales for Fe, and EDAX revealed occurrence of two scales in distinct areas for all Fe electrodes; one comprised of porous, spongy looking structures and scales with more Fe content where the other had denser and more compact scales richer in Ca and P or Si. Cu electrodes had an orange to dark brown thin scale with blue green spots. Small pits were consistently observed mostly in the centre of such blue green spots which were identified as copper carbonates. The Pb electrodes visually showed a thin shiny transparent film with a surface very similar to the unexposed electrodes. Numerous pits were visually for pH controls and not seen for inhibitors; but SEM revealed that all electrodes had pits but the inhibitors reduced number and size of pits compared with pH controls. Thin hexagonal hydrocerussite plates were observed to occur in distinct growth areas and the presence of P or Si inhibitor seemed to increase the occurrence of hydrocerussite.

Both Fe & Pb release were mostly in the particulate form while Cu release was mostly in the dissolved form. Total and dissolved Fe, Cu and Pb release models using EN parameters were developed by nonlinear regression. Fe release increased with localized corrosion (PF) and the EN model predicts that Fe release can be effectively controlled to the same degree by pH elevation or inhibitors. Cu release increased with general corrosion (LPRCR) and was also influenced by localized corrosion (ECNCR). However general corrosion was more significant for copper release which was mostly in the dissolved form. Pb release was depended on both general corrosion (LPRCR & HMCR) and localized corrosion (PF). The EN models predict that both Cu and Pb release is highest for pH control and all inhibitors reduced Cu and Pb release, which is consistent with the data. Inhibitors ranked by increasing effectiveness for reducing both Cu and Pb release are pH elevation, Si, ZOP, OP and BOP.

EN monitoring is faster and less labor intensive than water quality monitoring and represents a significant advance for controlling metal release in drinking water distribution systems. The EN models were found to be comparable to water quality models developed from this study for metal release, and since EN is a real-time technique it offers a tremendous advantage over traditional water quality sampling techniques. Remote access of EN monitoring equipment is possible and the system requires little to no maintenance with the exception of a power supply or battery. The rapid turn around of corrosion rates from EN can be used to estimate metal release in drinking water proactively and mitigating measures can be implemented before the full adverse impacts are realized.

ACKNOWLEDGEMENTS

I would like to express my gratitude to my advisor Dr. James S. Taylor, whose expertise, understanding and patience added considerably to my graduate experience. His able guidance has offered me many opportunities for personal growth which will remain with me for a lifetime. I would also like to thank Dr. Ni-Bin Chang, Dr. Yong-ho Sohn, Dr. Steven J. Duranceau and Dr. Andrew A. Randall for serving on my committee. Dr Dietz was responsible for field operations and Dr. Norris was the laboratory manager for this project, and their efforts and support resulted in a successful completion of this study. A sincere note of appreciation for Dr Dietz and Dr Duranceau for their involvement and aid in data interpretation.

A special thanks to the members of my field crew Avinash Shekhar, and Philip Lintereur for their dedication, team work and commitment to get field work completed every week and the entire TBW student team viz. Abdulrahman Alshehri, Jorge Arevalo, Xiatao Guan, Stephen Glatthorn, David McNevin, Bingjie Zhao, Erica Stone, Chandler Wilson, Mingda Zhang and Xiaoli Liu. I appreciate the contribution of Maria Pia Robert for formatting and coordinating the manuscript for TBW II project.

We all in the TBW team recognize and appreciate the contributions of Oswald Weisner and the late Dennis Marshall both Pinellas county Fla. employees for their help and support during field operations. I appreciate the support by AwwaRF and Tampa Bay Water for funding this project and support from the Civil and Environmental Engineering Department at UCF.

TABLE OF CONTENTS

LIST OF FIGURES	xii
LIST OF TABLES	xiv
LIST OF PHOTOGRAPHS	xvi
LIST OF ABBREVIATIONS	xvii
1 INTRODUCTION	1
1.1 Limitations of corrosion monitoring	2
1.2 Research Objectives and Scope	3
1.3 Document summary	4
2 LITERATURE REVIEW	5
2.1 Background	5
2.2 Electrochemical aspects of corrosion in drinking water	7
2.3 Localized corrosion	8
2.4 Corrosion indices	9
2.5 Copper corrosion	14
2.6 Iron corrosion	15
2.7 Lead corrosion	18
2.8 Brief overview of corrosion inhibitor studies	21
2.9 Corrosion monitoring studies in drinking water	27
2.10 Literature on Electrochemical-Noise	34

3	MATERIAL AND METHODS	36
3.1	Existing facilities	36
3.1.1	PDS components.....	38
3.1.2	Blends of finished waters used in TBW II.....	41
3.2	Corrosion inhibitors	43
3.3	Data collection and quality assurance/control	47
3.4	EN monitoring	49
3.4.1	EN equipment- SmartCET system.....	50
3.5	Theory of measurement of EN parameters	54
3.6	References.....	58
4	CORRELATING COPPER RELEASE WITH ELECTROCHEMICAL CORROSION MONITORING IN DRINKING WATER	65
4.1	Introduction.....	65
4.2	Background.....	66
4.3	TBW II study	67
4.4	Literature on copper corrosion rates	68
4.5	Materials and methods	70
4.5.1	Operation.....	73
4.5.2	Electrochemical corrosion rate measurement	75
4.5.3	Quality assurance & control.....	76
4.6	Results and discussion	77
4.6.1	Copper release by inhibitor and phase :	77
4.6.2	Observations by photographs and SEM/EDS.....	79

4.6.3	Water quality correlations with EN	82
4.6.4	Statistical model development	85
4.6.5	EN empirical model for copper concentration	87
4.6.6	Advantages of EN in estimating copper release.	95
4.7	Conclusions.....	96
4.8	Recommendations.....	97
4.9	Acknowledgements.....	97
4.10	References.....	98
5	MODELING TRANSIENT Cu RELEASE IN DRINKING WATER	100
5.1	Introduction.....	100
5.1.1	Background.....	100
5.1.2	Literature on transient Cu release	101
5.2	Materials and methods	103
5.2.1	Field facility	103
5.2.2	Electrochemical corrosion rate measurement	105
5.2.3	Operation.....	106
5.2.4	Quality assurance & control.....	109
5.3	Results and discussion	109
5.3.1	Corrosion rates with stagnation time	109
5.3.2	Cu corrosion rates	111
5.3.3	Development of transient Cu release models.....	113
5.3.4	Transient Cu release models	118
5.3.5	Model verification.....	122

5.4	Conclusions.....	125
5.5	Recommendations.....	125
5.6	Acknowledgements.....	126
5.7	References.....	126
6	CORRELATING ELECTROCHEMICAL CORROSION MONITORING FOR IRON WITH WATER QUALITY.....	130
6.1	Introduction.....	130
6.1.1	Background.....	131
6.1.2	Literature on Fe corrosion monitoring.....	132
6.2	Materials and methods	136
6.2.1	Field facility	136
6.2.2	Operation.....	139
6.2.3	Electrochemical corrosion rate measurement	140
6.2.4	Quality assurance & control.....	142
6.3	Results and discussion	142
6.3.1	Water quality variations by phase.....	142
6.3.2	Iron release by inhibitor and phase	144
6.3.3	Observations by photographs and SEM/EDS.....	147
6.3.4	Water quality correlations with EN	152
6.3.5	Statistical Fe release model development.....	160
6.4	Conclusions.....	166
6.5	Recommendations.....	167
6.6	Acknowledgements.....	168

6.7	References.....	168
7	CORRELATING Pb RELEASE WITH ELECTROCHEMICAL CORROSION MONITORING IN A CHANGING WATER QUALITY ENVIRONMENT	171
7.1	Introduction.....	171
7.1.1	Literature on Pb corrosion	173
7.2	Experimental.....	175
7.2.1	Field facility.....	175
7.2.2	Electrochemical corrosion rate measurement.....	176
7.2.3	Operation.....	177
7.2.4	Quality assurance and control.....	179
7.3	Results and discussion	180
7.3.1	Water quality variations by phase.....	180
7.3.2	Observations by photographs, SEM and EDS of electrodes.....	182
7.3.3	Water quality correlations with EN	185
7.3.4	Statistical EN models for Pb release.....	188
7.4	Conclusions.....	193
7.5	Acknowledgements.....	194
7.6	References.....	195
8	SUMMARY OF FINDINGS	197

LIST OF FIGURES

Figure 3.1 Tanker truck for surface water hauling and surface water storage tanks	37
Figure 3.2 Water production area and laboratory, storage, pilot RO and EN trailers	37
Figure 3.3 Pilot distribution systems and coupon cradles.....	37
Figure 3.4 Influent standpipes.....	40
Figure 3.5 Inhibitor tanks and feed pumps	40
Figure 3.6 Copper loops with lead coupons.....	40
Figure 3.7 Electrochemical Noise Trailer.....	40
Figure 3.8 The Nadles layout with the probes connected.....	50
Figure 3.9 SmartCET system and electrodes.....	51
Figure 3.10 Schematic of electrodes.....	51
Figure 3.11 Electrode probes detail	52
Figure 3.12 Probe connection details.....	53
Figure 4.1 Total copper release by PDS and phase.	79
Figure 4.2 PF_{Cu} vs. LR1T for TBW II data.....	84
Figure 4.3 EN model predicted versus actual total copper concentration	90
Figure 5.1 Comparison of $LPRCR_{Cu}$ with stagnation time.....	111
Figure 5.2 Time-series plots of TCu release.....	115
Figure 5.3 Model predicted transient TCu release against actual data	121
Figure 5.4 Transient TCu release model verification for phase II.....	123

Figure 6.1 PF_{Fe} graphs with water quality	155
Figure 6.2 PF model predicted versus actual TCl_2 -loss.....	159
Figure 6.3 Temperature vs T_{Fe} by phase.....	164
Figure 6.4 EN model predicted versus actual D_{Fe}	166
Figure 7.1 SEM of Pb-Sn electrodes.....	185
Figure 7.2 Water quality correlations with $LPRCR_{Pb}$ and PF_{Pb}	187
Figure 7.3 Temperature vs TPb by phase	191
Figure 7.4 EN model predicted TPb (top) and DPb (bottom) against actual data.	193

LIST OF TABLES

Table 2.1 ECNCR and water quality from other EN studies.....	31
Table 2.2 Guidelines for corrosion types with EN skew and kurtosis.....	35
Table 3.1 Blend ratios of GW, SW and RO used in TBW II.....	42
Table 3.2 Finished source water descriptions.....	42
Table 3.3 Pilot plant finished water treatment goals.....	43
Table 3.4 Variations of water quality, inhibitor and dose by project phase.....	45
Table 3.5 Inhibitor product properties.....	46
Table 3.6 PDS Influent and effluent monitoring frequency.....	48
Table 3.7 Numbering of electrodes.....	52
Table 3.8 Typical output from Electrochemical Noise Monitoring (Iron).....	54
Table 3.9 Output parameters from EN monitoring.....	54
Table 4.1 Summary of water quality and corrosion rates for copper from various studies	70
Table 4.2 TBW II Water quality by phase.....	74
Table 4.3 Output parameters from electrochemical noise monitoring.....	76
Table 4.4 Copper release EN models.....	88
Table 4.5 Corrosion current density (I_{corr}) comparison from LPR for Cu.....	94
Table 5.1 TBW II Water quality by phase.....	107
Table 5.2 TBW II Average inhibitor doses.....	108
Table 5.3 Output parameters from electrochemical noise monitoring.....	112

Table 5.4 Summary of water quality and Cu corrosion rates from various studies.....	112
Table 5.5 Average of last two observations by phase for total Cu release	117
Table 5.6 Transient TCu model results.....	119
Table 5.7 Summary of paired t-test for model verification	124
Table 6.1 Summary of water quality and corrosion rates for iron from various studies	135
Table 6.2 TBW II Water quality by phase	140
Table 6.3 TBW II Water quality by phase	141
Table 6.4 Paired t-tests for iron concentrations compared with pH _s	145
Table 6.5 Comparison of surface elemental composition from EDS by areas	152
Table 6.6 Total chlorine loss PF _{Fe} models	158
Table 6.7 Iron release EN models.....	162
Table 7.1 Output parameters from electrochemical corrosion monitoring.....	179
Table 7.2 TBW II Water quality by phase	182

LIST OF PHOTOGRAPHS

Photograph 4.1 Copper corrosion loops.....	72
Photograph 4.2 EN probe connection in Nadle	73
Photograph 4.3 Copper electrodes, left OP (1 mg P/L) and right ZOP (2 mg P/L).....	80
Photograph 4.4 SEM & EDAX of electrode exposed to BOP at 1 mg /L of P	81
Photograph 5.1 Copper corrosion loops.....	105
Photograph 5.2 EN probe connection in Nadle	105
Photograph 6.1 Pilot Distribution Systems.....	138
Photograph 6.2 EN probe connection in Nadle	138
Photograph 6.3 Fe electrodes, clockwise from top left BOP (0.5 mg P/L), ZOP (2 mg P/L), pH _s and pH _{s+0.3}	148
Photograph 6.4 SEM & EDS of Fe electrodes exposed to BOP. Top & middle are for exposure to 1 mg P/L and bottom is for exposure to 0.5 mg P/L.	150
Photograph 7.1 Copper corrosion loops (top) & EN probe connection in Nadle (bottom)	177

LIST OF ABBREVIATIONS

AC	Alternating Current
AMPAC	Advanced Materials Processing and Analysis Center
ANOVA	Analysis of Variance
AOC	Assimilable Organic Carbon
avg	Average
AWWA	American Water Works Association
AWWARF	American Water Works Association Research Foundation
B	Stearn Geary coefficient
Ba	Anodic tafel slope
Bc	Cathodic tafel slope
BOP	Blended Ortho-Phosphate
CET	also SmartCET, Patented Corrosion Monitoring Electro-noise Equipment
cm	Centimeter
COM	Communications port
CPU	Cobalt-platinum color units
CR	Corrosion Rate
CSMR	Chloride to sulfate mass ratio
°C	Degrees Celsius
DC	Direct Current
DO	Dissolved Oxygen
DV	Dummy Variable
Ea	Activation energy
ECN	Electrochemical Noise
ECNCR	Electrochemical Noise Corrosion Rate
EDS	Energy Dispersive X-ray Spectroscopy
EIS	Electrochemical Impedance Spectroscopy
EN	Electrochemical corrosion parameters
EPA	Environmental Protection Agency
F	Faraday's constant
G	Galvanized Steel
gpm	Gallons per Minute

GW	Groundwater
HDA	Harmonic Distortion Analysis
HMCR	Harmonic Distortion Analysis Corrosion Rate
HRT	Hydraulic Residence Time
I	Current
ICP	Inductively- (or Ion-) Coupled Plasma spectroscopy
IKRT	Kurtosis of the current
ISKW	Skew of current
k	Rate Constant
k ₂₀	Rate constant at 20 °C
LCI	Lined Cast Iron
LCR	Lead and Copper Rule
LPR	Linear Polarization Resistance
LPRCR	Linear Polarization Resistance Corrosion Rate
LR	Larson's Ratio
LR1T	Larson's Ratio with Temperature
LRM	Modified Larson's Ratio
LSI	Langelier Saturation Index
Max	Maximum
MCF	Material Characterization Facility
meq/L	Milli-Equivalents per Liter
MG	Member Government
MGD	Million Gallons per Day
mg/L	Milligrams per Liter
Min	Minimum
mL	Milli-Liter
mpy	Mills per year
µg/L	Micrograms per Liter
NA	Not Applicable
NPDOC	Non-Purgeable Dissolved Organic Carbon
NTU	Nephelometric Turbidity Unit
OP	Ortho-Phosphate
Pb/Sn	50/50 Lead/Tin Alloy
PDS	Pilot Distribution System
PF	Pitting Factor
pH	Potential Hydrogen
pH _s	Saturation pH

PKRT	Kurtosis of the potential
ppb	Parts per billion
ppm	Parts per million
PSKW	Skew of potential
PVC	Polyvinyl Chloride
QA	Quality Assurance
QA/QC	Quality Assurance/Quality Control
QC	Quality Control
R	Resistance
R _N	Noise Resistance
RO	Reverse Osmosis
R _P	Electrode resistance
RSOL (Rs)	Solution resistance
SEM	Scanning Electron Microscope
Si	Silica based inhibitor
SW	Surface Water
T16	Averaged 16 hour temperature in PDS before sampling
T, Temp	Temperature
TBW	Tampa Bay Water
TBWI	Tampa Bay Water 1
TBWII	Tampa Bay Water 2
TCP	Tailored Collaboration Project
TDS	Total Dissolved Solids
TOC	Total Organic Carbon
TP	Total Phosphorus
UCF	University of Central Florida
UCI	Unlined Cast Iron
US	United States
USEPA	United States Environmental Protection Agency
V	Potential
v	volts
WQ	Water Quality
XPS	X-ray Photoelectron Spectroscopy
Z	Impedance
ZOP	Zinc Ortho-Phosphate

1 INTRODUCTION

Control of distribution system pipe corrosion has long been a challenge for the water treatment industry. Corrosion of system pipes has economic, hydraulic and aesthetic impacts including water leaks, corrosion product buildup and water quality deterioration. All electrochemical corrosion monitoring is collectively termed 'EN' in this study. EN has been previously used as a corrosion monitoring technique for different types and rates of corrosion, but field applications have been very scarce (Dolterly et al., 1990, NACE Vol3A 1993). Advances in EN monitoring have enabled real-time measurement of corrosion rates but the author is not aware of a single field application in drinking water distribution systems. Use and development of EN technology to measure corrosion parameters and develop models that predict distribution system water quality offer the water community a tremendous advantage to identify and mitigate adverse impacts before they are fully realized. The EN data can be gathered much faster than traditional data and hence provide a means of mitigating corrosion before traditional monitoring techniques.

The Stochastic fluctuations of the corrosion potential, and corrosion current spontaneously generated by corrosion reactions is known as electrochemical noise (ECN). By measuring electrochemical noise at the open circuit i.e. free corrosion potential the corrosion system is not disturbed by any external voltage or current source; therefore, no additional corrosion effects are induced. Other techniques apply a small

current or voltage to metal surfaces and measure the response current or voltage. Linear polarization resistance (LPR) uses a direct current while Harmonic distortion analysis (HDA) uses an alternating current.

1.1 Limitations of corrosion monitoring

The goal of maintaining non corrosive water in distribution systems largely concerns with limiting the concentrations of metals to an acceptable level. With the implementation of Lead and Copper rule of EPA, tap water concentrations for these metals must be limited to acceptable concentrations. Corrosion and its kinetics though being the cause of the source of metals do not bear a simple or direct relation to tap water concentrations. This is due to the complex physio-chemical and biological transformations of the corroded ions in the distribution and service lines; and is further complicated by particulate release of metals. The formation of scale on corroded metal surface is affected by an array of parameters chiefly oxidants as dissolved oxygen or free and combined chlorine, temperature, oxidation-reduction potential, anions as sulfate and chlorides, pH. The scaling tendency of water with respect to calcium carbonate also plays a key role in scale properties. In general homogeneous adherent scales with few imperfections are less likely to break and release scale as corrosion products (CPs) or expose the bare metal surface to water. Water quality changes on any scales may adversely affect CP release if the existing scales are incompatible with the change; hence it is difficult to relate corrosion rates and types to CP release and ambient metal levels in drinking water. Though the aim of corrosion monitoring programs is to quantify and predict corrosion rates in relation to water quality and is directly useful as an operating

parameter for utilities, prediction of metal levels cannot be achieved. The aim of this study is to relate corrosion monitoring by on-line techniques with a view to correlate and predict metal concentrations.

1.2 Research Objectives and Scope

The primary goal of this study was to correlate EN parameters with metal release in form of total and dissolved Fe, Cu and Pb. Predominance of general or localized corrosion for these metals was identified. Statistical models for predicting metal release using EN were developed. The advantage of EN is a rapid turn around which offers the opportunity for proactive control of adverse water quality mitigation. Transient Cu and Pb release which occurred during water quality changes from one phase to another in this study was evaluated and EN models were developed to predict the response time for the change in metal concentration. This response time would be available for real systems to exercise control by applying mitigatory measures. The data for EN taken during this study was in stagnant waters and ranged from a continuous monitoring from 6 hours to approximately 18 hours. Specific objectives of this study are listed as:-

- Compare the corrosion rates obtained during stagnation by time.
- Correlate EN parameters to water quality for Fe, Cu and Pb. Evaluate the correlations based on corrosion theory and identify meaningful correlations for use in real systems.
- Develop statistical models for metal release using EN parameters. Identify the importance of general and localized corrosion from these models. Compare

various inhibitor types and dose by using these EN parameters and present observations. Discuss applicability of EN measurements for field use.

- Develop transient Cu and Pb release models and evaluate the ability of EN to predict the response time for the change in release over time during water quality changes.

1.3 Document summary

The document comprises of nine chapters. The first chapter gives an introduction to the scope of this particular research work. Chapter 2 presents the available literature on EN monitoring applicable to drinking water industry. Chapter 3 discusses the materials and methodology including field facilities at the Tampa Bay Water site, EN equipment and parameters. The next four chapters comprise of results and discussions. Chapter 4 includes an evaluation of correlation Cu release with EN and presents EN models to predict Cu release. Chapter 5 includes an evaluation of transient Cu release concentrations during water quality changes and the ability of EN to predict this response. Chapter 6 presents correlation of Fe release concentration and water quality with EN parameters and presents EN models to Fe release and chloramine residual loss in the hybrid PDSs. Chapter 7 includes an evaluation of correlation of Pb release with EN and presents EN models to predict Pb release. Chapter 8 briefly summarizes the findings of relationship of EN with water quality and metal release from this study.

2 LITERATURE REVIEW

2.1 Background

Electro-chemical corrosion monitoring (EN) measures the corrosion current which represents electron transfers due to all oxidation reactions on a metal surface, without regard to whether metal is released to the water or incorporated in an oxidized scale. Numerous reactions are expected to occur on a metal surface in drinking water environment. Metal scale formation, oxygen consumption, hydrogen generation, chlorine reduction, biological oxidation and oxidation of metals other than Fe, Cu or Pb are examples of reactions that change surface potential (voltage) and result in current flow, which generates EN and are not direct measurements of Fe, Cu or Pb release. Hence all corrosion does not lead to metal release. The release of corrosion products are controlled by the identity and the type of solids that form on the surface. Scales that are highly scalable, conductive, porous and friable are considered problematic and vice-versa. Scale characteristics are controlled by water quality, flow conditions and temperature. The primary goal of corrosion mitigation program is to identify and achieve the desired water quality changes that result in the formation of a better scale.

Changes in water chemistry can however disrupt this equilibrium and generate reactions with pipe materials and deposits in distribution systems, which cause discoloration and other water quality concerns (McIntyre and Mercer 1993). Conditions

prevailing in distribution systems favorable to bacterial proliferation include reduction in residual disinfectant, higher temperature, long residence time and a high ratio of pipe surface to volume of water. These conditions are typical for service lines especially after overnight stagnation. In a utility study by Prevostet (1997), for most consumers flushing for a few minutes brought HPC levels down to service line influent concentrations. This suggested that steady shear conditions and after thorough flushing the biofilms in service lines does not contribute significant to the bacteria found in bulk water. In cases of longer residence times higher HPC were found at tap, even after 15 minutes of flushing. This suggests that not only the factors regulating biofilms are important for maintaining water quality at tap; but also any factors which lower the potential for regrowth play a major role for longer residence times. Inhibitor evaluation from such a regrowth potential may be a key factor for selection of the corrosion control strategy for a utility.

A study by Edwards et al., (1999) for utilities confirmed an optimum alkalinity of about 30 (mg/L as CaCO_3) in mitigating lead CP release at pH above 8.5. An adverse effect of increasing the Chlorides to Sulfate mass ratio (CSMR) on lead CPs was reported when CSMR was in excess of 0.58; and typically exceeded the action level of LCR. Utilities with CSMR below 0.58 generally met Lead compliance but observed an adverse effect of detectable color on Copper CP release. The authors also reported that solubility models accurately predicted trends in CP release at populations of utilities; they were poor quantitative predictors at individual utilities. Vasquez et al., (2006) reports increased lead CP release for chloramines than free chlorine irrespective of water quality changes in alkalinity, sulfates, chlorides and nitrates. The authors observed that the ORP was reduced in presence of chloramines with respect to free chlorine and explained the

increased CP release based on Pourbaix diagram. The controlling solid in presence of free chlorine is Lead dioxide (PbO_2) which has a lower solubility while in presence of chloramines it is hydrocerussite ($\text{Pb}_3(\text{CO}_3)_2(\text{OH})_2$) which has a higher solubility. Such a shift lead species from Pb (IV) to Pb (II) due to conversion from free chlorine to chloramines resulted in the case of Washington D.C system in 2004. Chlorine decay modeling by Vasconcelos et al., (1996) indicates zero order decay with the rate controlled by formation of CP rather than by the concentration of chlorine. Rossman et al., (1994) also reports that the rate coefficient for wall reaction was an order of magnitude greater than that of bulk decay. Studies by Frateur et al., (1999) and Digiano & Zhang (2005); report that chlorine is more reactive with iron CP than oxygen. Chlorine resulted in reduction in occurrence of hematite ($\alpha\text{-Fe}_2\text{O}_3$) and goethite ($\alpha\text{-FeOOH}$); both oxygen induced scales in the CP.

2.2 Electrochemical aspects of corrosion in drinking water

The transfer of electrons from the anodic areas to the cathodic areas in a metal is initiated by a potential difference between them, and generally arises due to surface imperfections, crystal structure scales and trace impurities. These factors lead to a difference in metallic activity which drives the electrochemical potential. This mechanism is valid for any exposed metal and is displayed in Equation 2.1.

$$E_{\text{cell}} = [0.059/z] \log ([\text{Me}(a^{z+}_2)] / ([\text{Me}(a^{z+}_1)]) \quad \text{Equation 2.1 Equilibrium}$$

(Potential of half cell)

where z = # of electrons transferred
 (a^{z+}_2) = Oxidized form of metal
 (a^{z+}_1) = Reduced form of metal

Equilibration is reached quickly if no other electron acceptor is present. However in portable water there are at least three dominant electron acceptors viz. dissolved oxygen, chlorine and hydrogen ion. These compete for the electrons accumulated on the cathode, depending on their relative electrode potentials and their activities. A complicating factor is the effect of pH on chlorine species and thus on its electrode potential

2.3 Localized corrosion

Crevice corrosion is a dangerous form of localized corrosion, which occurs as a result of the occluded cell that forms under a crevice on the metal surface. Common items susceptible are flanges, gaskets, disbonded linings, fasteners, lap joints, weld zones and surface deposits. Systems relying on passive surface films for corrosion resistance can be particularly vulnerable even in absence of pH change or chloride build up inside crevices. Pickering (2003) showed that crevice corrosion is caused in Iron/Steel by the IR Voltage drop which raises the local potential of the crevice area to cause it to actively corrode. Changes in local electrolyte composition as caused in pits can also breakdown passive films. The separation between anodic and cathodic areas is necessary for crevice corrosion to occur by IR drop mechanism; and this condition prevails naturally for flow through systems due to presence of oxidants in the bulk solution. This causes the potential at the outer surface i.e. out of crevice to be raised and if sufficient can passivate the bulk surfaces. Inside the crevice due to reduced mobility of oxidants the potential may well be in the active region of the metal promoting crevice corrosion. Additionally oxygen depletion in the crevice also can enhance loss of passivity of crevice. Boffardi

(1995) reports relative corrosion rates of the order of 0.15 mpy for fresh carbon steel surfaces after 30 days of exposure to drinking water of low corrosivity. The simplest form of a mechanistic model for localized corrosion is for pitting corrosion. The pitting potential is defined as the potential below which a metal surface remains passive and above which pits start to initiate or existing pits grow. One mechanism which explained pitting of Copper in neutral/alkaline solutions deals with formation of a local low pH in the pit relative to the bulk solution has been well accepted since 1971 (Piccinini et al.,). The local acidification is a result of the dissolution of metal at the pit bottom with subsequent hydrolysis of metal ions.

2.4 Corrosion indices

A number of corrosion indices have been developed that relate the water quality to the corrosion potential of iron pipes. The Langelier Index has a prominent historical role among these indices as a measure of the stability of water quality being introduced into iron distribution systems. A positive LI indicates that the water is saturated with respect to CaCO_3 . The predominant mechanism expected here is the deposition of a protective CaCO_3 scale that will prevent corrosion. A negative LI indicates that the water is unsaturated with respect to CaCO_3 . Such waters tend to remove the protective CaCO_3 scale and expose the metal surface of the pipes to further corrosion. The general practice is to increase pH by 0.2 – 1 units above pH_s to prevent corrosion in distribution systems. A simplified form of the Langelier Index has traditionally been used as shown in Equation 2.2.

$$LI = pH - (pK_2 + pK_{so} + pCa^{2+} + pHCO_3^-) \quad \text{Equation 2.2}$$

(Langelier Index)

where pK_2 = Negative log of equilibrium constant for bicarbonate dissociation
 pK_{so} = Negative log of equilibrium constant for $CaCO_3$ dissociation
 pCa = Negative log of molar calcium concentration
 $pHCO_3^-$ = Negative log of molar bicarbonate concentration

A number of other related corrosion indices have been developed by various researchers that incorporate the calcium carbonate solubility criteria to evaluate the stability of the source waters. The calcium carbonate precipitation potential (CCPP) is the amount of calcium carbonate that will precipitate or dissolve from solution as it comes to equilibrium with solid calcium carbonate. McCauley (1960) used a rearranged form of the calcium carbonate solubility expression, termed the Driving Force Index (DFI), to calculate the tendency to deposit calcium carbonate. The DFI was modified by Merrill and Sanks (1983) to include the effect of alkalinity and pH. A similar qualitative attempt at predicting calcium carbonate precipitation was proposed by Dye (1964) and termed the momentary excess (ME).

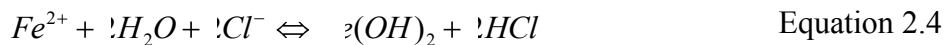
The drawbacks of the Langelier Index for predicting the stability of waters for corrosion control fueled the search for other water quality parameters that affected corrosion and iron release in distribution systems. One such measure is the Larson Ratio. Larson ratio is developed from the relative corrosive behavior of chlorides and sulfates to the protective properties of bicarbonate. The authors deduced that the corrosivity of air-saturated waters is dependent on the proportion of corrosive agents to the inhibitive agents and their concentrations (Larson and Skold 1958). Larson and Skold (1957) observed that calcium in the presence of alkalinity, regardless of pH or saturation index,

is an effective inhibitor of corrosion. The authors concluded that tubercles are formed when inhibitors to corrosion are present in insufficient concentration. However, unsaturated water exhibited generalized corrosion. The Larson Ratio (LR) is defined as shown in Equation 2.3. A LR above 0.5 is considered corrosive.

$$LR = \frac{[Cl^-] + [SO_4^{2-}]}{[HCO_3^-]} \quad \text{(Larson ratio)} \quad \text{Equation 2.3}$$

where [] = concentration in meq/L

Chlorides and sulfates were identified as major factors that increased the corrosion rate through interference with the formation of the protective calcite and siderite layers. Sulfates in particular may be involved in biological reactions with the indigenous microbial populations within the distribution system. In a slightly alkaline solution a simplified model for corrosion of iron may be given as shown in Equation 2.4. The resultant decrease in pH is localized in pits and can lead to further breakdown of the passive film on the metal surface. Other anions of strong acids, such as sulfates and nitrate, will also hydrate to acidic pH, but chloride is far more mobile in solution and more aggressive in both pitting and crevice corrosion.



(Fe corrosion in alkaline solutions)

Vatankhah et al., (1998) evaluated the electrochemical behavior of iron electrodes in the presence of bicarbonate solutions at different sulfate levels. The authors observed that in the presence of sulfate ions only, iron electrodes experience uniform corrosion and

sulfate ions were aggressive. However, in the presence of bicarbonate the sulfate ions became less aggressive and pitting-passivation behavior was observed. The authors recommended that a molar ratio of 10:1 of bicarbonate to sulfate results in a complete suppression of any localized attacks induced in the presence of sulfate ions. The authors explained that the main difference between the pitting behavior exhibited by chlorides and sulfates could be related to the ratio of their ionic radii (1:8). It was deduced that chloride ions are more mobile than sulfate ions. Another explanation is based on the nature of the corrosion products formed. The chloride corrosion products are highly soluble and therefore not protective. Sulfates react with iron forming relatively stable products and may compete with carbonates species. However, since the transient compounds have higher selectivity for carbonates, passivation occurs with the accumulation of carbonate species on the electrode.

Based on laboratory loop studies and field investigations, Pisigan and Singley (1987) observed that an increase in buffer capacity at constant alkalinity (100 mg/L as CaCO_3) in the pH range of 6.0-9.0 decreased the corrosion rate of mild steel. However, raising the buffer capacity by raising alkalinity was counterproductive due to a corresponding increase in ionic strength and conductivity. Increasing flow rates was observed to increase the corrosion rates due to increased supply of oxygen. The authors recommend buffer capacity as a better indicator of corrosion potential than alkalinity. They related corrosion rates to the ratio defined in Equation 2.5. The authors report that increasing the ratio causes a decrease in corrosion rate. Based on observations from field studies, the authors note that an elevated Total Dissolved Solids (TDS) or chloride content can lead to higher corrosion rates.

$$\frac{\beta}{\text{Cond}^{3/2}}$$

Equation 2.5

(Buffering capacity ratio)

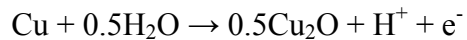
where β = Buffer capacity in M/L
Cond = Conductivity in $\mu\Omega/cm$

Increased total dissolved solids (TDS) cause an increase in the ionic strength of the waters. This can cause a change in the activities of the ionic species in the water. Another effect of increased TDS is increase in conductivity of the water which increases the corrosive current and facilitates electrochemical reactions. TDS may also effect the formation of protective films depending upon its nature. If TDS is present as chlorides and sulfates, it will cause increased corrosivity of iron. If the TDS is composed of bicarbonate and hardness ions the water tends to be non-corrosive towards iron (Schock, 1999). Singley (1981) conducted a survey of existing corrosion indices and concluded that all indices developed were based on certain simplifying assumptions that were applicable to the specific cases for which they were developed. Therefore, no single corrosion index is applicable universally. The author observes that based on the review of literature and experience; there are a number of water quality parameters that need to be considered in addition to calcium carbonate solubility, including calcium, magnesium, alkalinity, carbonate, carbon dioxide, pH, chlorides, sulfates, ionic strength, conductivity, total dissolved solids, color, hydrogen sulfide, buffer capacity, phosphate, silica, dissolved oxygen, chlorine and temperature. The author advises that the most useful form of corrosion index would consider all relevant factors for the water, but must be

designed in such a way that the protective mechanisms for a given water would predominate in the calculation of the index.

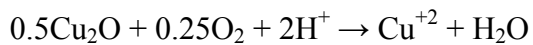
2.5 Copper corrosion

An electrochemical theory of uniform copper corrosion in aqueous was proposed by Ives and Rawson (1962). Copper oxidation leading to cuprite formation is driven by a series of reactions initiated at the metal surface and the half cell reaction for dissolution is displayed below in Equation 2.6. Electrons produced by this reaction are removed by migration of lattice defects through the cuprite film to the outer surface where the cathodic reaction consumes the electrons and allows corrosion to proceed. Copper release as a corrosion by product occurs via oxidation of cuprite usually with oxygen as displayed in Equation 2.7.



Equation 2.6

(Cu oxidation to Cuprite)



Equation 2.7

(Cuprite oxidation)

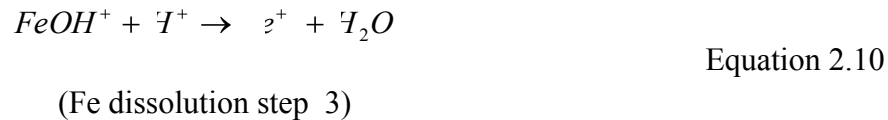
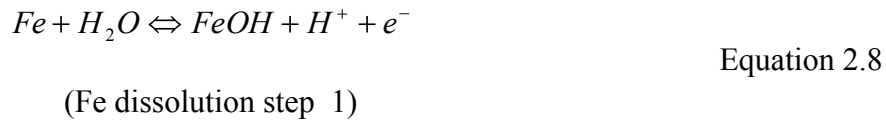
Edwards et al., (1994 b) evaluated the effect of water quality on copper corrosion rates with a specific emphasis on chloride, bicarbonate, sulfate and pH. In the presence of bicarbonate, copper corrosion undergoes a critical transition somewhere between pH 7.0 and 8.5. Scale formed at pH 7.0 catalyzes oxygen reduction and increases the over all corrosion rate. In contrast, oxygen reduction rates are unchanged at pH 8.5, but the anodic reaction (copper dissolution) is inhibited, passivating the copper surface. An inner

cubic scale layer present at pH 7.0 but absent at pH 8.5 might cause the transition, which is speculated to depend on bicarbonate concentration. Edwards et al., (1994 a) evaluated the effect of water quality on pitting corrosion of copper, and demonstrated that chloride was more aggressive than sulfate during short term experiments i.e. for freshly exposed surfaces. On the other hand long term effects which are important for copper plumbing are not well understood. The study concluded that chloride induces formation of a scale that passivated copper corrosion and pitting, whereas the scale formed in presence of sulfate promoted copper corrosion.

2.6 Iron corrosion

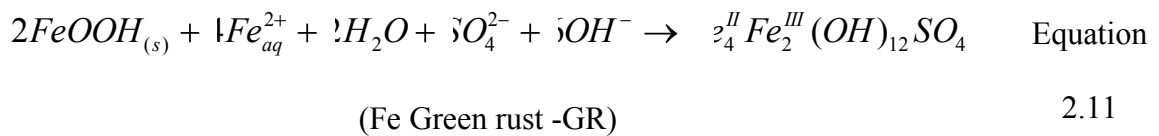
Control of iron release in drinking water distribution systems is complicated by the many potential iron sources (raw water, ferric coagulation for surface waters, iron pipe corrosion) and release mechanisms (corrosion product solubility and film release). Sarin et al., (2000) state that iron release bears no simple relation to the rate of iron corrosion, while Sander et al., (1997) emphasizes the need to distinguish between red water problems and corrosion rate and they suggest that corrosion-related water quality problems are mainly a function of the precipitation and dissolution properties of corrosion products formed. McNeill and Edwards (2001) concur with Sander et al., (1997) that red water quality problems do not depend primarily on the corrosion process, but on a large reservoir of corrosion product layers making it difficult to model scale behavior. It is however important to note that corrosion, an electrochemical thermodynamic process, ultimately supplies the initial source of corrosion related iron within the water supply system. The solubility of passive layers and film release

processes predominantly contribute to the total iron concentration causing red water problems. The widely accepted mechanism of iron dissolution is displayed below in Equation 2.8, Equation 2.9 and Equation 2.10.



Equation 2.9 displays the rate determining step (rds). Hence the concentration of ferrous ions in the solution does not influence the kinetics of dissolution. Several studies (Kuch 1988; Sander et al., 1997; Sarin et al., 2001; and Lin et al., 2001) have identified the following species as commonly found within the passive layers, goethite (α -FeOOH), lepidocrocite (γ -FeOOH), Magnetite (Fe_3O_4), Siderite ($FeCO_3$), ferric hydroxide ($Fe(OH)_3$), ferrous hydroxide ($Fe(OH)_2$), and calcium carbonate ($CaCO_3$). The contribution of the dissolved iron from the passive layers is controlled by the solubility of the solid species, available pipe surface area, flow velocity and the concentration gradient of ions between the pipe water and bulk liquid. Recent research on iron corrosion in chloride and sulfate environments has revealed the existence of green rusts that are unstable Fe(II)-Fe(III) hydroxyl salts that oxidize in the presence of oxygen. The crystal structure of green rusts is characterized as composed of a stacking of $Fe(OH)_2$ -like layers

carrying a positive charge due to the presence of Fe(III) and interlayers constituted of anions and water molecules. They are transient compounds between metallic iron and final corrosion products, and therefore may govern the mechanisms and kinetics of corrosion and passivation of iron in aqueous media. A number of green rusts like GR(Cl), GR(CO₃⁻²), GR(SO₃⁻²) and GR(SO₄⁻²) have been identified and a typical structure is shown in Equation 2.11 (Refait et al., 1998, 2003).

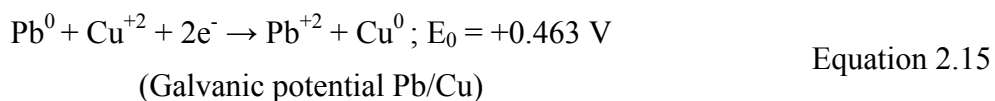
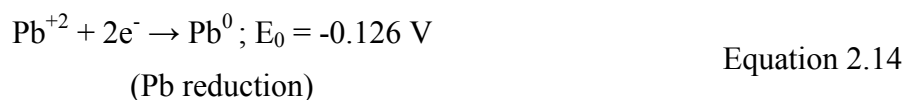
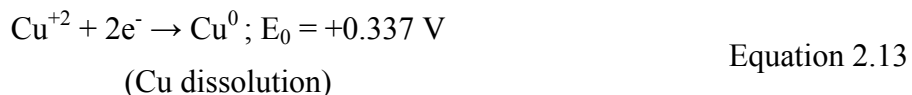


Green rusts differ significantly in their structure and composition and if green rusts are the controlling solid phase for iron solubility, they complicate the evaluation of corrosion byproduct release by thermodynamic considerations. At present, not enough literature exists to delineate the role of green rusts in corrosion prevention and scale formation. The morphology and stability of corrosion products are correlated with the linkages of a local structure which is fundamentally described by FeO₆ octahedral structural units Cornell & Schwertmann (2003). The structure is very complicated by these units are believed to be maintained even in the amorphous state of ferric hydroxide Fe(OH)₃, and the linkages of the local structure are likely to be influenced by cations and anions. Sarin et al., (2003) reported that siderite model explained the corrosion occurring for corroded unlined cast iron pipes; and GR(CO₃) was insensitive to the water quality variations in the study; hence did not control iron release.

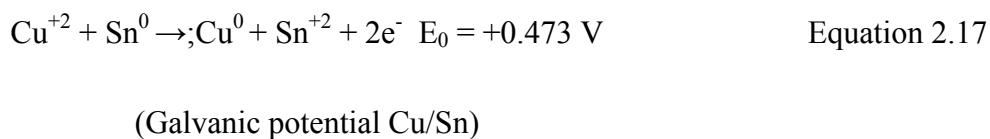
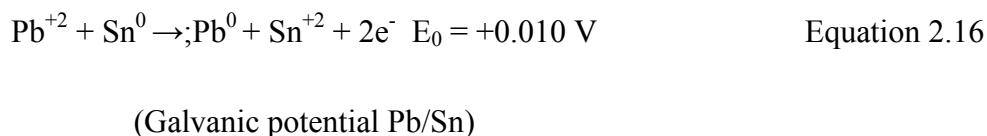
Volk et al., (2000) used a two-electrode linear polarization probe in a distribution main found that measurement of corrosion rates can be strongly influenced by the location of probe, the measuring device and/or flow or pressure conditions. The influence of temperature on many parameters including dissolved oxygen solubility, solution viscosity, diffusion rates, activity coefficients, enthalpies of reaction, compound solubility, oxidation rates, and biological activity was evaluated by McNeill and Edwards (2001). The authors recommended accurate monitoring for temperature for determining the rate of iron corrosion, the composition and properties of scale built up inside pipes, and aspects of corrosion by-product release.

2.7 Lead corrosion

Lead comes in contact with portable water via lead pipes, lead based solders used to join copper pipes, and brass and bronze fixtures. The Lead ban by the 1986 EPA amendments limit the lead content of solders, fluxes and pipes to 0.2 percent and the lead content of fixtures to 8.0 percent. For pure lead pipes and fixtures the primary mechanism of corrosion is due to a concentration cell on the surface. The reaction of water with lead ions released at the anode (Equation 2.12) leads to further complications due to the presence of either alkalinity as bicarbonate or inhibitors such as phosphates or silicates forming more complex insoluble products. For lead based solders the mechanism is the same i.e. galvanic corrosion, and is due to a direct contact between dissimilar metals. The lead copper couple half cell reactions are displayed in Equation 2.13 and Equation 2.14. The cell reaction is displayed in Equation 2.15.



The galvanic couples due to lead-tin solder (Equation 2.16) and tin-copper couple (Equation 2.17) also affects lead release. Both the lead-tin couple in the solder and the tin-copper couple result in dissolution of tin (a non regulated contaminant). The removal of tin from the solder exposes more lead to the water and may lead to the subsequent corrosion of lead or the physical release particulate lead (Gregory, 1990).



Lead in drinking water results mostly from corrosion of lead materials in the distribution system, and is generally not present in source waters. Significant sources of lead and copper in drinking water are lead solder pipe joints, lead service connections, brass fixtures, and copper pipes found in existing plumbing systems of homes. Lead is

anodic in distribution systems and produces Pb (II) and Pb (IV) ions, which form stable lead complexes in water. The most common oxidant for lead in drinking water is dissolved oxygen (DO). Primary lead corrosion products are Pb (II) species in most cases (AWWA 1996). The oxidized solid phases are primarily PbO, PbO₂, PbCO₃ and Pb₃(CO₃)₂(OH)₂. Other lead species that occur in drinking water are lead carbonate, hydroxyl, chloride or sulfate complexes, which affect the solubility of lead in water. The major Pb (II) complex in drinking water is PbCO₃⁰. PbCO_{3(s)} and Pb₃(CO₃)₂(OH)_{2(s)} are the primary solid phases in drinking water, but do not adequately passivate lead corrosion because of discontinuous formation. The discontinuous character of lead deposits is a probable reason for the persistent corrosion of new lead materials.

pH is the most important factor controlling lead release. Normally, pH is associated with alkalinity, but lead solubility is relatively more sensitive to pH than to alkalinity. Lead solubility decreases with increasing pH in alkalinity range common to drinking water. Optimum alkalinity is associated with pH, and the best combinations of alkalinity and pH have to be determined experimentally in each case. pH and alkalinity adjustment has been used in many cases to reduce lead level in drinking water. A Pb₃(OH)₂(CO₃)₂ thermodynamic model was developed by Schock (1980, 1989) and showed the response of the theoretical solubility curves for lead as a function of dissolved inorganic carbonate concentration and pH. The model agreed very well with the experimental data. Experiential models were developed from statistical analysis of actual data Haring (AWWA 1996). Hydraulic models were also developed based on the hydraulic properties of pipe and flow (Kuch and Wagner 1983). However, accurate prediction of lead release in water is difficult because of the variability of lead release,

which is caused by the release of particulate lead and to a lesser extent by the precision and accuracy associated with the low concentrations in relation to the EPA "Action Level". McNeill and Edwards (2004) reported that a significant fraction of the CP release from lead pipes and to a lesser degree from Copper pipes was found to be particulate ($>0.45 \mu\text{m}$) after a 8 hour stagnation for a variety of water qualities tested. The waters were ground, surface or blends with a wide range in parameters normally expected for drinking water sources. The occurrence of particulate and colloidal ($>0.1 \mu\text{m}$) species especially for Lead was also confirmed by utility tap water sampling. Higher alkalinity benefits were due almost exclusively to lower particulate release. Both ortho and Polyphosphates decreased particulate lead release. Scale analysis revealed hydrocerussite solids were dominant in low pH and alkalinity waters which had the most significant waters in terms of particulate Lead release. Zinc-ortho phosphate either had an insignificant effect with respect to orthophosphate alone or in some cases worsened CP release for both Lead and Copper. This was attributed to the release of particulates associated with a zinc-phosphate precipitate. The addition of Orthophosphate decreased dissolved copper levels and had little effect on particulate copper. Polyphosphates generally had a higher particulate fraction for Copper , and the authors speculate it to be due to formation of a less durable copper-phosphate solid.

2.8 Brief overview of corrosion inhibitor studies

A study by Volk et al., (2000) having low raw water phosphate levels ($<0.2 \text{ mg/l}$) and total phosphate concentrations after inhibitor dosage between 0.56 and 1.2 mg/l (average of 0.86 mg/l) found that iron corrosion was strongly related to water temperature

and/or other seasonal factors). Plant effluent corrosion rates were approximately 2.5 mpy at the beginning of the study (temperature $<13^{\circ}\text{C}$) and started to increase when temperature increased in May 1996, and remained between 5 and 7 mpy when water temperatures were $>20^{\circ}\text{C}$ (July to September 1996). Corrosion rates could vary up to 7 mpy, even when the plant was feeding a corrosion inhibitor (constant dose of 0.86 mg PO_4/L over the year). The corrosion rates were maintained below 3 mpy when phosphate dosages were slightly increased (between 1.5 and 2 PO_4/L) especially during warm periods. A seasonal corrosion control strategy was developed that would require slightly higher corrosion inhibitor concentrations during the summer and possibly lower dosages during winter months, rather than using a constant concentration over the entire year. There was no evidence of increased bacterial levels due to increased levels of phosphate used for corrosion control.

Similar seasonal variations in drinking water for iron corrosion have been observed for other systems, with one system in Virginia having corrosion rates as high as 9 mpy during the summer, and 2 mpy during the winter (LeChevallier et al., 1996). Orthophosphate is known to impact iron corrosion rates and increases in phosphate concentrations from 0.5 to 1 mg/l have been shown to reduce iron leaching by two-thirds (AWWARF, 1996). Benjamin et al., (1990) showed that 1 mg/L of phosphorus effectively reduced corrosion rates in Seattle water at pH 8. Zinc is often present in the composition of PO_4 -based corrosion inhibitor. It has been shown that zinc is effective at levels in the range of 0.1 ± 0.3 mg/L as P (AWWARF, 1996). It may form protective films on the interior of pipe. Zinc molecules are supposed to react with carbonates at the cathode and form deposits, while phosphates block the anodic sites. It was also reported

that bimetallic phosphates often performed better than orthophosphates for certain water types (AWWARF, 1996). The presence of zinc in ortho-phosphate solutions usually reduces the preconditioning period to establish a film within pipes. However, using products with low, or no, zinc content may be beneficial in circumstances where zinc creates problems with environmental regulations in wastewater or sludges. Therefore, maintaining zinc concentrations lower than 0.25 mg/L may provide a balance between corrosion control and prevention of pollution problems. Murray (1970) reported usage of zinc sulfamate and phosphate acids to control iron corrosion. A dosage of 1-3 mg/L of zinc passivated the surface of pipes with uniform deposition of zinc phosphate film and resulted in a 95 % reduction in iron levels to 0.04 mg/L.

The combination of ortho and poly phosphates may control copper corrosion better than orthophosphates alone (AWWARF, 1996). A survey conducted on 365 utilities showed that the effect of phosphate inhibitors on Copper/Lead was strongly dependent on plant effluent pH and alkalinity (Dodrill and Edwards, 1994). The use of phosphates reduced lead release by 20±90 % for very low alkalinity waters (<30 mg/L as CaCO₃). Corrosion inhibitors generally had an adverse effects on lead release for waters with higher alkalinity (>30 mg/L) and pH > 7.4. For copper, phosphate inhibitors decreased copper concentrations at pH < 7.8, while copper release could be adversely impacted in some waters with high pH (Dodrill and Edwards, 1994). The use of phosphate based corrosion inhibitors was found to be associated with lower coliform levels (LeChevallier et al., 1996). Lowther and Moser (1984) reported that the levels of coliforms decreased within a few weeks following the application of zinc orthophosphate in the Seymour, IN system. Other studies (Abernathy and Camper, 1997) performed

using iron annular reactors showed that the addition of zinc orthophosphate or polyphosphate reduced biofilm densities compared to a chlorinated reactor that contained no corrosion inhibitor. Similarly biofilm densities in iron annular reactors were reduced by 1.5 log when chloraminated water was supplemented with zinc-orthophosphate.

The WASA & CH2M HILL study (2004) found that pH ($\text{pH} > 8.5$) control for optimal corrosion control resulted in CCCP values of 60-80 mg/L and was not feasible due to the possibility of excessive Calcium Carbonate precipitation. WASA supplies drinking water which is conventionally treated surface water with coagulation, sedimentation, filtration and primary & secondary disinfection. Conversion from free chlorine to chloramines resulted in exceeding the LCR action level for Lead from July 2001 to June 2002 with corresponding 90th percentile values of 8 and 75 ppb. The study also identified secondary concerns with usage of phosphate inhibitors. Orthophosphate may not be viable due to pH swings in the distribution system, the required orthophosphate dose of 3mg/L may cause red water problems and pipe-loop testing to access red water potential was recommended. The study also reported the controlling solids from thermodynamic equilibrium considerations. For Lead the controlling solids in the pH range of 5-12 were identified as Cerussite (PbCO_3) and hydrocerussite ($\text{Pb}(\text{CO}_3)_2(\text{OH})_2$) and Hydroxypyromorphite ($\text{Pb}_5(\text{PO}_4)_3(\text{OH})$) is considered if orthophosphate is added. For copper the controlling solids in the pH range of 6-11 were identified as Malachite ($\text{Cu}_2(\text{OH})_2(\text{CO}_3)$), cupric hydroxide ($\text{Cu}(\text{OH})_2$), Tenorite (CuO) and cupric phosphate ($\text{Cu}_3(\text{PO}_4)_2 \cdot 2\text{H}_2\text{O}$). Orthophosphate use on a part of the distribution system was started by WASA in 2004.

A study by Lytle and Snoeyink (2002), reports that phosphates mask the effect of dissolved Iron in bench scale laboratory studies. Polyphosphates and orthophosphate to a lesser degree reduce apparent color and turbidity, decreased particle size, created amore negative zeta potential and increased Iron suspension stability. They suggest that following hydrolysis, oxidation and nucleation, orthophosphate adsorbed to Iron surfaces at an early stage of particle aggregation. The iron-phosphate bonds probably involve interaction of PO_4^{-3} with two Fe^{+3} ions to form relatively stable Fe- PO_4 -Fe linkages. The mechanism by which polyphosphates operate appeared to differ than that of orthophosphate. The data suggested that polyphosphates strongly interact with Iron colloids earlier than, near or at the point of nucleation.

Cohen et al., (2003) investigated full scale implementation of phosphate inhibitors using blended and zinc orthophosphates. In bench scale studies the blended ortho-polyphosphates produced CPs which were physically softer and less cohesive than zinc orthophosphates. However zinc orthophosphates were not used in full scale study which may be attributed to increased zinc levels for the wastewater treatment facilities. The study was carried out on pipes of diameter from 4 to 12 inches on an isolated part of a southern California district. Polyphosphates at varying doses were added to chloraminated finished water from 5 ground water plants and one surface water plant. The dose was dispensed at 1 mg/L per 1 mg/L of iron, manganese, all divalent metals, 200 mg/L of hardness (as CaCO_3); and a further 0.15-0.3 mg/L for a blend residual and corrosion control. Polyphosphate addition yielded almost immediate benefits with a short span in maintaining water quality. The flushing volume requirements declined to 10 % and within 3 years dropped to 5 % or less with respect to the initial requirement. Due to

the color sequestering ability of polyphosphates the number of customer complaints consistently dropped from an average of 35 per month to about 5 a month including a number of summer months with no complaints. Chlorine residual goal of 1 mg/L for the district improved from an average of 30 % of sampled sites to a minimum of 90 % after 6 months. The HPC levels decreased significantly but required almost 2 years to be consistently lower than 100 cfu/mL. The authors suspect that initially the polyphosphate dissolves the CPs –biofilm matrix and releases it in the bulk resulting in higher HPC levels.

As early as 1968, Schenk and Weber Jr. have investigated the effect of dissolved silica on iron corrosion. They reported that silica acts to catalyze the oxidation of ferrous ion, while it retards the hydrolysis of ferric ions. Dart and Foley (1970) report usage of sodium silicate at a dosage range of 2.5-6.5 (mg/L as SiO₂) and found that silicate stabilized iron best at elevated pH values. A pH of 7.5 appeared to be mid-way in the transition range towards more effective iron stabilization. Silica reacts with ferric ions to form complexes and was relatively unreactive with Ferrous ions. The mechanism proposed was dissolution of iron to ferric ions with rapid polymerization to giant molecular structure; which agglomerate to form commonly visible floc. Silica was effective only with reactions with ferric species i.e. before oxidation to ferrous structures. Dart and Foley (1972) report that the silica complex formed did not appear to be stable against further reaction with excess ferric ions, as evidenced by its breakdown on further additions of iron after complex formation. This imposes a requirement to exceed a critical silicate dose to control iron deposition.

Robinson et al., (1992) reported the ratio of SiO_2/Fe (mg/L) from 11-34, for 5 Canadian utilities having approximately hardness of 200-300 mg/L (as CaCO_3). Previous laboratory studies by the authors evaluated the ratio SiO_2/Fe (mg/L) to 6.5 in hardness free model ground water. This suggests that higher silicate doses are needed for higher hardness levels. The treated waters also showed an increase in color and turbidity over a 5 day period after silicate addition. The authors concluded that sequestering of iron occurs for a limited period. More complaints from consumer whose homes were on dead end mains were observed, and the authors point out this temporal nature of sequestering for utilities in the study having systems having detention times longer than 1.4 to 3.5 days.

A combination of sodium silicate and sodium hydroxide was investigated (Schock et al., 2005) for groundwater source to meet LCR compliance. An initial dose of 25-30 mg/L elevated the pH from 6.3 to 7.1 and immediately resulted in 55 % reduction in Lead levels and 87 % reduction in Copper levels. The water had low alkalinity (34-51 mg/L as CaCO_3), low pH (6.1 to 6.3), a high TOC (13-18 mg/L as C), low calcium (7 -9.7 mg/L as Ca) and background levels of Silicate from 13-15 mg/L. (as SiO_2). The low pH resulted only in some reduction of copper for phosphate inhibitors. Elevated lead levels were observed for phosphate and attributed to sequestering of polyphosphate and ineffectiveness of orthophosphate at low pH.

2.9 Corrosion monitoring studies in drinking water

Corrosion monitoring only in environments similar to drinking water is presented. A study by Norton and LeChevallier (1997) reports corrosion rates from 0.5 to 6.1 mpy

and 1.2 to 11.4 mpy in two distribution systems. The corrosion rate exhibited a close relationship with temperature and lagged by a month or two with maximum and minimum temperatures. The corrosion rate from plant effluent dropped from a range of 4.9-5.6 mpy to 1.3-1.4 mpy after increasing Zinc orthophosphate levels from 0.5 to 2.0 (mg/L as P). Subsequent increase in the distribution system resulted in a sustained corrosion rate below 4.0 mpy with no coliforms detection. They also report that by closely monitoring daily corrosion rates using on-line monitoring equipment the operating expenses could be decreased by optimizing corrosion inhibitor feed rates.

A study by Reffass et al., (2005) identified iron carbonate (FeCO_3) as the corrosion product at potential above breakdown potential. The authors also reported that Iron carbonate is subsequently oxidized by dissolved oxygen into hydroxycarbonate green rust $\text{GR}(\text{CO}_3^{2-})$ and is commonly found in the rust covering water pipes. According to the authors this green rust (GR) belongs to a class of divalent-trivalent ionic minerals; which are characterized by a crystal structure consisting of stacking of $\text{Fe}(\text{OH})_2$ - like layers carrying a positive charge and interlayers of anions and water molecules. Several GRs are known the most common being composed of chlorides, carbonates and sulfates. The other Fe(II)-Fe(III) compound is magnetite, the oxide Fe_3O_4 characterized by a spinel structure similar to that of a passive film. In most conditions magnetite is the thermodynamically stable phase whereas GRs are metastable. $\text{GR}(\text{CO}_3^{2-})$ is reported (Drissi et al., 1995) to have a molecular formula of $\text{Fe}_4^{\text{II}}\text{Fe}_2^{\text{III}}(\text{OH})_{12}\text{CO}_3 \cdot 2\text{H}_2\text{O}$ and an average oxidation number of +7/3 and ΔG°_f of -4076 (KJ/mole). The key role of iron carbonate i.e. Siderite in high alkalinity waters has been reported by Taylor et al., (2005) and hence for drinking water systems $\text{GR}(\text{CO}_3^{2-})$ is a possible controlling solid.

The morphology and stability of corrosion products are correlated with the linkages of a local structure which is fundamentally described by FeO₆ octahedral structural units (R.M Cornell & U Schwertmann, 2003). The structure is very complicated by these units are believed to be maintained even in the amorphous state of ferric hydroxide Fe(OH)₃, and the linkages of the local structure are likely to be influenced by cations and anions. Sarin et al., (2003) reports that siderite model explained the corrosion occurring for corroded unlined cast iron pipes and GR(CO₃) was insensitive to the water quality variations in the study; hence did not control iron release.

According to Abiola and Oforika (2002) the activation energy due to chemical adsorption (>80kJmol⁻¹) is considerably larger than due to physical adsorption (<80kJmol⁻¹). The surface coverage (θ) as shown in Equation 2.18 was calculated by these authors and used in adsorption isotherms to fit the data. The parameter of interest chosen is weight loss or corrosion rate or polarization resistance or corrosion current density (Fouda et al., 2005). Inhibitor coverage has been quantified (Gasparac, 2000) and attempts were made to fit these θ values to various isotherms including Frumkin, Langmuir, Temkin, and Freundlich. Gasparac (2000) reported the best fit was for Freundlich isotherm for ΔG° values from -13 to -17 kJ/mol which suggested physisorption of inhibitor on the surface. They also suggested that chemisorption requires a standard free energy of adsorption on the order 100 kJ/mol.

$$\text{Surface coverage } \theta = 1 - R_i/R$$

(Surface coverage of an Inhibitor)

Equation 2.18

where R_i = the value of parameter of interest in presence of inhibitor
 R = the value without inhibitor.

A study by Boyle Engineering and M.J Schiff & Associates (Duranceau et al., 2004) investigated the application of electrochemical corrosion monitoring using the electrochemical noise (ECN) method. The average water quality and corrosion rates from this study are presented in Table 2.1. ECN monitoring was conducted at four utilities along with some water quality sampling. The study concluded that ECN can be used to derive practical information for assessment of corrosion susceptibility of metals and the type of corrosion process. A quote from the report reads, “the usefulness of this type of testing is demonstrated in this project by the conclusion that for some conditions, ‘inhibition’ increases the corrosion rate”. Inhibition herein was referred to as addition of the corrosion inhibitor ZOP at 1 mg/L as P.

Table 2.1 ECNCR and water quality from other EN studies

Water Quality Parameter	Sarasota	IRWD-#1	IRWD-#2	LVVWD # 2	PCU # 2
pH	7.82	7.92	7.92	7.61	7.74
Hardness (mg/L as CaCO ₃)	129	204	204	255	226
Calcium (mg/L as CaCO ₃)	44	121	121	141	199
Alkalinity (mg/L as CaCO ₃)	117	94	94	162	202
TDS (mg/L)	593	455	455	293	378
Sodium (mg/L)	150	65	65	6	14
Sulfate (mg/L)	288	154	154	44	21
Chloride (mg/L)	28	69	69	8	12
Dissolved Oxygen (mg/L)	7.2	7.8	7.8	7.3	0.7
Temperature (°C)	27.1	22.6	22.6	23.5	23.9
Influent P (mg/L)	0.33	0.33	0.33	0.33	0.33
LSI	-0.24	0.26	0.26	0.26	0.54
Fe corrosion -control(mpy)	14.7	8.0	4.0	6.5	3.5
Fe corrosion-Inhibitor (mpy)	14.9	7.5	6.0	1.7	2.3
Cu corrosion -control(mpy)	1.4	-	3.0	1.7	2.5
Cu corrosion-Inhibitor (mpy)	0.7	-	1.0	1.6	2.3
Pb solder corrosion -control(mpy)	0.4	0.4	-	0.5	2.3
Pb solder corrosion-Inhibitor (mpy)	0.7	0.3	-	25.9	1.7

Sarasota = City of Sarasota, Fla.
IRWD = Irvine Ranch Water District, Calif.
LVVWD = Las Vegas Valley Water District, Nev.
PCU = Pinellas County Utilities, Fla.
Inhibitor = 1 ppm ZOP as PO₄

Benjamin et al. (1996) observed that iron release from corroded pipes often bears no simple relationship to the corrosion rate. Even though the metal surface is covered with scale, corrosion may occur and may directly affect metal release. The scale break up due to thermal expansion and stress or shear by flow or chemical interactions with oxidants as chlorine or oxygen result in metal release being rather unpredictable. Further more passivation and subsequent breakdown of passive scale at localized corrosion spots may result in low corrosion rates but yield high metal release or vice-versa. In stagnant

water depletion of oxidants due to consumption by metal reactions can result in metal release (Sarin et al., 2004). The authors report that for Iron dissolved oxygen is beneficial in that it oxidizes the ferrous ions at the pipe wall and forms a precipitate of Fe(III) and reduces scale porosity. However when ferrous ions in bulk water are oxidized to Fe(III) they are likely to be carried out to the consumers tap as red water release.

Jones Edmunds & Associates (JE & A, 2004) conducted a corrosion inhibitor screening evaluation using EN techniques. Four poly-orthophosphate formulations were tested one at a time at various doses (0.4 to 1.2 mg/L as P) for a period of 28 to 31 days. The test apparatus comprised two parallel flow through pipe loops and EN data was monitored with two identical sets of probes. The flow was intermittent with 2-3 hours of flow (total 9 hrs/day) and one 6 hour stagnant period. The source water was a blend of Ground, Surface and Desalinized water. The calcium ranged from 150-210 (mg/L as CaCO₃), Sulfate from 50-150 (mg/L), alkalinity at or above 100 (mg/L as CaCO₃) and ph from 7.1-8. Parameters found to be approximately constant for this study were Chlorides at 40 (mg/L), Dissolved Oxygen at 8 (mg/L), temperature at 22°C, total Chlorine at 3.8 (mg/L) and the background orthophosphate consistently below 0.05 (mg/L). The study examined the correlation coefficient between water quality and Noise resistance and made recommendations on a qualitative basis. All inhibitors showed evidence of reduced localized corrosion for Iron, mitigating in Iron corrosion with increase in alkalinity and calcium, decrease in sulfate, dissolved oxygen, chlorine residual and chlorides. Copper corrosion was increased by higher alkalinity and mitigated by decrease in sulfate while Lead corrosion was mitigated by decrease in sulfate and chlorides. Passivity has been related to the formation of a duplex structure Cu₂O/CuO, Cu~OH₂. It is believed that at

pH higher than 7.0 copper forms a passivation duplex layer. Brusic et al., (1991) showed that a stable oxide of copper can be formed at a pH higher than 7.0. At pH 7.0 dissolution of Cu_2O begins and becomes significant at pH below pH 5 where the formation of stable surface oxide is not possible. The authors also displayed evidence that the overall corrosion process is controlled by the diffusion of copper ions in the oxide film. Similar results are reported by Vukmirovic et al., (2003). The authors report that influence of oxygen reduction reaction kinetics was not detected over the entire pH range from 3 to 12. This indicates that the conductivity of this layer was high enough as to not impede the mass transport limited rate of oxygen reduction. The results lead to the conclusion that the diffusion limited current density for oxygen reduction via a four-electron mechanism in a stagnant electrolyte was about $20\text{-}30 \text{ mA cm}^2$ which corresponds to a 9.22 mpy corrosion rate. Hence it is expected that oxygen diffusion may not be the rate limiting step for Copper corrosion in drinking water environment.

A laboratory study by Tan et al., (1996) provided evidence that the trend of Electrochemical Noise (EN) effectively followed inhibitor film formation and destruction process. The authors state that EN is a valid technique for continuous monitoring of inhibitor film performance and evaluation of inhibitor film persistency. They also confirmed the strong correlation between EN and linear polarization resistance (LPR) or the sum of charge transfer resistance and inhibitor film resistance. This may prove advantageous for EN over LPR since film resistance effects can be a serious limitation in case of oxide/inhibitor films.

2.10 Literature on Electrochemical-Noise

The potential for application of electrochemical noise (ECN) to yield corrosion rates can be inferred from available literature (Chen & Bogaerts 1995, Eden D.A 1998, Holcomb et al., 2002, NACE 1993, R.A Cottis 2000 and Tan et al., 1996). ECN has a relatively smooth appearance for general i.e. uniform corrosion. When pits begin to form on the metal surface or initiate, occasional sharp increases and decreases in the amplitude of both the potential and current noise data occur. The electrochemical noise technique can differentiate general from localized corrosion and provide estimates of corrosion rates without external perturbation of the corroding system. Each type of corrosion (for example general corrosion, pitting corrosion, crevice corrosion, and stress corrosion cracking) will have a characteristic “fingerprint” or “signature” in the signal noise. This “fingerprint” can be used to identify the type and severity of corrosion that is occurring. Electrochemical noise arising from general corrosion has a relatively smooth, Gaussian, distribution, with little or no skew, since the anodic and cathodic processes are relatively uniformly distributed across the metal surface. Localized attack is not uniform and in the short term will show symptoms of a skewed distribution. Similarly the kurtosis may be used to identify periods of pitting. By comparison during general corrosion the kurtosis value is relatively low. The estimated error of Skew is $(6/N)^{1/2}$ while the estimated error of Kurtosis $(24/N)^{1/2}$ where N is the data points during the monitoring event. Table 2.2 presents guidelines from a study (Holcomb et al., 2002) for correlating skew and kurtosis values to corrosion types.

Table 2.2 Guidelines for corrosion types with EN skew and kurtosis

Corrosion Mechanism	Potential		Current	
	Skew	Kurtosis	Skew	Kurtosis
General	<±1	<3	<±1	<3
Pitting	<-2	>>3	>±2	>>3
Transgranular SCC	+4	20	-4	20
Intergranular SCC # 1	-6.6	18 to 114	1.5 to 3.2	6.4 to 15.6
Intergranular SCC # 2	-2 to -6	5 to 45	3 to 6	10 to 60

3 MATERIAL AND METHODS

3.1 Existing facilities

The pilot distribution system (PDS) and two pilot treatment systems used in the implementation of this project were designed and built by UCF and TBW-MG personnel in the previous project, “Effects on Blending on Distribution System Water Quality” (Taylor et al., 2005). The previous project is sometimes referred to as Tampa Bay Water 1 (TBW I) and this current project, which is the continuation of the previous TCP, is sometimes referred to as Tampa Bay Water 2 (TBW II). The PDS was designed to allow flexibility to study water quality changes resulting from blends of significantly different source waters in old distribution pipe systems. The feed water blends represented the typical water chemistry likely to be experienced by TBW member governments. The pipes used in the PDS traditionally received conventionally treated groundwater. Both the physical systems and pipe geometries selected represent typical scenarios experienced in a real distribution system. Pictures of these facilities are shown in Figure 3.1, Figure 3.2, and Figure 3.3. These facilities were unique and offered a highly capable research environment for evaluating and possibly anticipating water quality problems in distribution systems.



Figure 3.1 Tanker truck for surface water hauling and surface water storage tanks



Figure 3.2 Water production area and laboratory, storage, pilot RO and EN trailers



Figure 3.3 Pilot distribution systems and coupon cradles

The PDSs are composed of 18 different distribution lines. Lines 1 to 14 are hybrid lines that contain segments of four different materials: PVC, unlined cast iron, lined cast iron, and galvanized steel pipes. Lines 15 to 18 contain multiple segments of each of the single material. The PDS was constructed of aged pipes that were obtained from existing utility distribution

systems to represent the pipe materials used in the TBW Member Government's distribution systems. The PDS has been maintained with a feed of 100% GW since completion of field activity for TBW I in the summer of 2005. Introduction of a blend of GW, SW, and RO was initiated in December 2005. Prior to introduction of the blend, field monitoring was resumed in the fall of 2005 to verify uniformity between the PDS effluent for all PDS lines. As learned during the equilibration phase from TBW I, apparent color is a useful parameter for definition of the attainment of an equilibrated condition in the PDS and was used for this purpose. The project was divided into 4 phases; each of three months duration. The blend used during each phase was different to evaluate the effect of water quality. Similar blends were used during phases I and III to evaluate the effect of seasonal conditions on the PDS.

3.1.1 PDS components

The pilot distribution systems were identified sequentially (PDS01 to PDS18). The pilot distribution lines were operated to maintain a two-day hydraulic residence time (HRT). Standpipes were located at the beginning and end of each PDS. The standpipes were made from translucent plastic pipe that were 60 inches (1.5 m) long and had a diameter of 4 inches (0.1 m). The retention time in the PDS feed standpipe was 3.1 hours because of the low velocities associated with the two-day HRTs. To avoid bacterial growth, the standpipes were wrapped in a non-transparent material to eliminate direct light exposure and cleaned regularly with a plastic brush and a 0.1% solution of sodium hypochlorite. The sodium hypochlorite solution was allowed a 4-hour contact time in the standpipes. All pilot distribution systems were constructed with a sampling port after each pipe segment to allow an assessment of water quality changes associated with each pipe material. PDS 1 to 14 were composed of four materials, laid out sequentially as:

- Approximately 20 feet (6.1 m) of 6-inch (0.15 m) diameter polyvinylchloride (PVC) pipe,
- Approximately 20 feet (6.1 m) of 6-inch (0.15 m) diameter lined cast iron (LCI) pipe,
- Approximately 12 feet (3.7 m) of 6-inch (0.15 m) diameter unlined cast iron (UCI) pipe,
- Approximately 40 feet (12.2 m) of 2-inch (0.05 m) diameter galvanized steel (G) pipe

PDS 15 to 18 were composed of a single material each as follows:

- PDS15: Eight reaches of approximately 12 feet (6.1 m) of 6-inch (0.15 m) diameter cast iron each,
- PDS16: Four pipe reaches of approximately 20 feet (6.1 m) of 6-inch (0.15 m) diameter lined cast iron plus 10 feet (3.0 m) of 6-inch (0.15 m) lined cast iron,
- PDS17: Five pipe reaches of approximately 20 feet (6.1 m) of 6-inch (0.15 m) diameter PVC each,
- PDS18: Eight pipe reaches totaling 135 feet (41.1 m) of 2-inch (0.05 m) diameter galvanized steel pipe.

The surface water was obtained from the TBW regional surface water treatment plant. The surface water was stored in two 7000 gallon (26.5 m³) storage tanks before being transferred to the finished water tank. The large process area used to prepare the finished waters and was covered by 4400 ft² (409 m²) of 6 inches (0.15 m) cement pad and hurricane rated roof. The trailers shown in Figure 3.2 contained a reverse osmosis pilot plant, an electro-noise monitoring facility, a storage facility, and a field laboratory.

Figure 3.4 shows the influent standpipes which allowed direct input from the finished storage and inhibitor tanks. Peristaltic pumps were used to control the flow of water and inhibitors to the PDS as well as the flow to the cradles. The inhibitors tanks and the pumps used

to feed the PDS and the cradles are shown in Figure 3.5. The pilot distribution system was followed by coupon cradles. The cradles were four inch (0.1 m) PVC pipes that housed six-inch (0.15 m) PVC pipes, which had been cut in half and supported pipe coupons for surface characterization and microbiological studies. Finally, the majority of the PDS effluent was directed to a corrosion shed which contained eighteen loops of copper pipes and lead coupons, shown in Figure 3.6. The rest of the PDS effluent was sent to the electrochemical noise trailer to feed the Nadles (noise cradles), shown in Figure 3.7, which contained iron, copper, and lead electrodes and coupons.



Figure 3.4 Influent standpipes



Figure 3.5 Inhibitor tanks and feed pumps

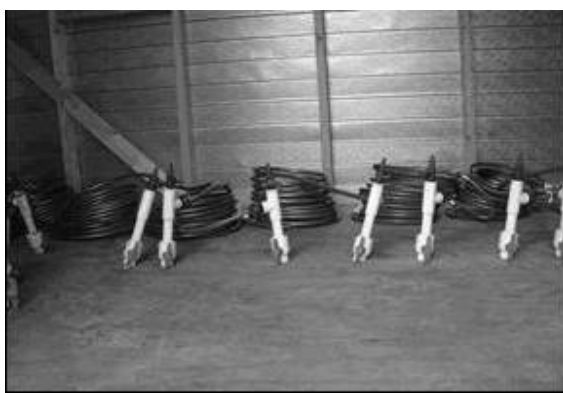


Figure 3.6 Copper loops with lead coupons



Figure 3.7 Electrochemical Noise Trailer

3.1.2 Blends of finished waters used in TBW II

Three different waters were used as source waters to be blended and fed to the PDS: conventionally treated groundwater (GW), enhanced CSF treated surface water (SW) and desalinated water by reverse osmosis (RO). The surface water was actual finished surface water from the Regional Surface Water Treatment Facility that was transported to the project site and the groundwater and desalinated water were obtained from the pilot water treatment systems at the project site. At the end of each three month period the blend composition was changed as shown in Table 3.1. All PDSs received the same blend composition for a three month period or phase. The description of finished source waters and the finished water treatment goals for the project are presented in Table 3.2 and Table 3.3 respectively. The PDS lines were flushed at an interval of two weeks. The flushing event achieved a velocity of 1 ft/s (0.3 m/s) for several minutes. This duration was selected to pass three pipe volumes of flush water through the hybrid lines. The nominal length of the hybrid lines is only 100 feet (30.5 m), thus the normal system velocities are very small. The objective of the flushing exercise is periodic removal of excessive films by hydraulic scour that may otherwise accumulate on the pipe interior during the nearly stagnant conditions associated with the 2-day HRT. The influent and effluent standpipes were cleaned at the same frequency to remove biological growths. The PDS sampling activity was undertaken at the beginning of the week. PDS effluent samples were not collected until at least 60 hours had elapsed after a flushing event in order to provide the desired two day HRT prior to sample collection.

Table 3.1 Blend ratios of GW, SW and RO used in TBW II

Phase	Time Period	% GW	%SW	%RO
I	Feb-May 2006	62	27	11
II	May-Aug 2006	27	62	11
III	Aug-Nov 2006	62	27	11
IV	Nov 2006-Feb 2007	40	40	20

Table 3.2 Finished source water descriptions

Source Water	Source	System Description
GW	Groundwater	Ground water source. Treatment by aeration, disinfection by free chlorine with a residual of 5 mg/L after a 5 minute contact time. 5.0 mg/L chloramine residual.
SW	Surface water	TBW treatment plant: Treatment by ferric sulfate coagulation, flocculation, settling, filtration, disinfection by ozonation and chloramination. Project site: adjustment of chloramine residual to 5.0 chloramine residual.
RO	Groundwater	Treatment by membrane reverse osmosis, aeration, disinfection by free chlorine with a residual of 5 mg/L after a 5 minute contact time. 5.0 mg/L chloramine residual.

Table 3.3 Pilot plant finished water treatment goals

Parameter	Standard	Target
pH units	7.4 min.	0.2 above pH _s
Alkalinity (mg/L as CaCO ₃)	40 min	50 min
Calcium (mg/L as CaCO ₃)	50 min, 250 max	60 mg/L
Total Chlorine (mg/L Cl ₂)		5 mg/L
Na (mg/L)	80 max	<80
Cl (mg/L)	100 max	<100
Sulfate & Chloride Sum.	3.8 meq/L max	<3.8 meq/L
TDS (mg/L)	500 max	<500
Fe (mg/L)	0.15 max	<0.15
Color (CPU)	15 max	<15
TOC (mg/L)	3.6 max avg./6.5 max	<3.6
Ammonia (mg/L as N)	1 max	<0.5
Turbidity (NTU)	At filter 0.3 max/ 0.1 (95%), 0.25(100%) Finished 1 max avg.	<0.2 <0.3

3.2 Corrosion inhibitors

The four types of inhibitors selected for project use were: orthophosphates (OP), blended ortho and polyphosphates (BOP), zinc orthophosphate (ZOP), and silicates (SiO₂). The target doses of the inhibitors were defined as: 0.5, 1.0, and 2.0 mg/L as P for the phosphorus-based inhibitors and 10, 20, and 40 mg/L as SiO₂ above the background concentration for the silicate-based inhibitor. After 1 month of operation, the doses of the silicate inhibitor had to be changed to 3, 6, and 12 mg/L because the 20 and 40 mg/L doses were causing CaCO₃ within the PDS. The variation of water quality and inhibitors by PDS is shown in Table 3.4. The dose utilized were selected by combining information of recommended doses from the inhibitor manufacturers specific for the blends of GW, SW, and RO used in the project as well as a survey of utilities that use the same types of inhibitors. However, the methods used by the manufacturers and utilities appeared to be based on experience and were qualitative rather than quantitative. This variation of independent variables provided an evaluation of inhibitor, dose, and season in a varying water

quality environment for control of color, turbidity and total iron release, residual maintenance, biofilm stability, and bulk water biostability.

The stock solutions of the corrosion inhibitors were diluted in a 40 gallon (151 m³) tank prepared twice a week, and the feed rates of the diluted inhibitor solution were calibrated to deliver the low, medium, and high inhibitor target concentration. The water used during the flushes was also dosed with the required type and amount of inhibitor to mimic the operating conditions of the respective PDS. The diluted inhibitor tanks were cleaned every week and maintained with a free chlorine residual enough to minimize bacteriological growth.

Table 3.4 Variations of water quality, inhibitor and dose by project phase

Ind. Var.	Water Quality 1													
	Phase I	PDS 1	P 2	P 3	P 4	P 5	P 6	P 7	P 8	P 9	P 10*	P 11*	P 12*	P 13
Inhibitor	BOP	BOP	BOP	OP	OP	OP	ZOP	ZOP	ZOP	Si	Si	Si	pH _s	pH _s + 0.3
Dose (mg/L)	0.5 - P	1.0 - P	2.0 - P	0.5 - P	1.0 - P	2.0 - P	0.5 - P	1.0 - P	2.0 - P	3 -SiO ₂	6 - SiO ₂	12 - SiO ₂	0	0
Ind. Var.	Water Quality 2													
	Phase II	P 1	P 2	P 3	P 4	P 5	P 6	P 7	P 8	P 9	P 10	P 11	P 12	P 13
Inhibitor	BOP	BOP	BOP	OP	OP	OP	ZOP	ZOP	ZOP	Si	Si	Si	pH _s	pH _s + 0.3
Dose (mg/L)	0.5 - P	1.0 - P	2.0 - P	0.5 - P	1.0 - P	2.0 - P	0.5 - P	1.0 - P	2.0 - P	3 SiO ₂	6 SiO ₂	12 SiO ₂	0	0
Ind. Var.	Water Quality 3													
	Phase IV	P 1	P 2	P 3	P 4	P 5	P 6	P 7	P 8	P 9	P 10	P 11	P 12	P 13
Inhibitor	BOP	BOP	BOP	OP	OP	OP	ZOP	ZOP	ZOP	Si	Si	Si	pH _s	pH _s + 0.3
Dose (mg/L)	0.5 - P	1.0 - P	2.0 - P	0.5 - P	1.0 - P	2.0 - P	0.5 - P	1.0 - P	2.0 - P	3 SiO ₂	6 SiO ₂	12 SiO ₂	0	0

*Original doses of 10, 20 and 40 mg/L were changed to reported doses after 3 weeks.
Phase III was also fed water Quality 1.*

The relevant properties of each inhibitor used during the project are shown in Table 3.5. The selected blended orthophosphate (BOP) product is called Sodium Polyphosphate SK-7641 (Stiles-Kem/Met-Pro Corporation, Waukegan, Ill.). Manufacturer claimed that when produced the BOP product contained approximately 40% orthophosphate and 60% polyphosphate. However, monitoring of BOP dose administered during operation indicated a 60-80% orthophosphate. Periodic determination of the actual ratio was conducted to administer the correct dose of the product. The ortho-phosphate inhibitor was Inhibit-All WSF-36 (SPER Chemical Corporation, Clearwater, Fla.). The zinc orthophosphate inhibitor was CP630 (Sweetwater Technologies, Temecula, Calif.). It is made by dissolving zinc sulfate into phosphoric acid solution in a 1:5 Zinc to PO₄ ratio. The silica inhibitor, product name N, was a sodium silicate solution (PQ Corporation, Valley Forge, Pa.).

Table 3.5 Inhibitor product properties

Parameter	BOP	OP	ZOP	SiO ₂
Percent Active Product	36%	36%	44%	37.50%
Bulk Density (lbs/gal)	11.5	11.25	10.8	11.6
Specific Gravity (at 72°F)	1.3	1.35	1.45	1.39
pH 1% solution (at 72°F)	6.3-6.6	5.1-5.4	<1	11.3
Recommended Dose (mg/L)	1-2 as P	1-4 as P	2-3 as P	4-12 as SiO ₂
Recommended pH Range	6.0-8.5	6.8-7.8	7-8	N/A
Solubility in water (g/g H ₂ O)	60/100	N/A	N/A	Miscible
Shelf Life (months)	6	None	6	None
Storage Limitation	Indoors	None	None	None

N/A = Not available

lbs/gal = 0.12 g/mL

3.3 Data collection and quality assurance/control

The general water quality varied in sets of four, as there are four phases to the project. The feed water quality was similar for all PDSs except for pH, inhibitor type and concentration and sometimes alkalinity. Parameters such as free and total chlorine, free ammonia, ortho-phosphorus and silica were monitored at least 3 times a week, and more if necessary. Weekly analyses were completed in the field laboratory and samples were also brought back to UCF laboratory for analysis. The monitoring frequency is shown in Table 3.6. Quality assurance and quality control of both the laboratory and field determinations of water quality parameters was established by duplicating analyses of at least 10% of the samples. Where appropriate standards were available, 10% of the samples were spiked with known concentrations of the parameter being analyzed and the recovery measured. Blind duplicates and spikes were also used to determine the accuracy of measurements. Dynamic control charts were used to determine whether the results were acceptable.

Table 3.6 PDS Influent and effluent monitoring frequency

Parameter	Location	Method	Frequency in phase I		Frequency in phase II, III & IV			
			PDS 1-14		PDS 1-12		PDS 13 /14	
			Inf	Eff	Inf	Eff	Inf	Eff
Alkalinity	Field lab	titration	W	W	BW	BW	W	W
Ammonia	Field lab	NH ₃ probe	W	W	BW	BW	W	W
Chlorine, Free	Field lab	spectrophotometer	W	W	W	W	W	W
Chlorine, Total	Field lab	spectrophotometer	W	W	W	W	W	W
Color, Apparent	Field lab	spectrophotometer	W	W	BW	BW	W	W
Conductivity	Field lab	Conduct probe	W	W	BW	BW	W	W
Nitrite-N	Field lab	spectrophotometer	no	W	no	W	no	W
ORP	Field lab	Redox probe	W	W	BW	BW	W	W
Oxygen, Dissolved	Field lab	DO probe	W	W	W	W	W	W
pH	Field lab	pH probe	W	W	W	W	W	W
Phosphorus, Ortho	Field lab	spectrophotometer	3/W	3/W	3/W	3/W	3/W	3/W
Silica	Field lab	spectrophotometer	3/W	3/W	3/W	3/W	3/W	3/W
TDS	Field lab	TDS probe	W	W	BW	BW	W	W
Temperature	Field lab	probe	W	W	W	W	W	W
Turbidity	Field lab	turbidimeter	W	W	W	W	W	W
UV-254	Field lab	spectrophotometer	W	W	W	W	W	W
Aluminum	UCF lab	ICP	W	W	BW	BW	W	W
Calcium	UCF lab	ICP	W	W	BW	BW	W	W
Chloride	UCF lab	IC	W	W	BW	BW	W	W
Copper, Dissolved	UCF lab	ICP	no	W	no	BW	N/A	W
Copper, Total	UCF lab	ICP	no	W	no	BW	N/A	W
Iron, Dissolved	UCF lab	ICP	W	W	BW	BW	W	W
Iron, Total	UCF lab	ICP	W	W	BW	BW	W	W
Lead, Dissolved	UCF lab	ICP	no	W	no	BW	No	W
Lead, Total	UCF lab	ICP	no	W	no	BW	no	W
Magnesium	UCF lab	ICP	W	W	BW	BW	W	W
NPDOC	UCF lab	spectrophotometer	W	W	BW	BW	W	W
Phosphorus, Total	UCF lab	ICP	W	W	W	W	W	W
Silica	UCF lab	ICP	W	W	W	W	W	W
Sodium	UCF lab	ICP	W	W	BW	BW	W	W
Sulfate	UCF lab	IC	W	W	BW	BW	W	W
TKN	UCF lab	Digestion	Q	Q	Q	Q	Q	Q
Zinc, Dissolved	UCF lab	ICP	W	W	BW	BW	W	W
Zinc, Total	UCF lab	ICP	W	W	BW	BW	W	W
AOC	UCF lab		Q	Q	Q	Q	Q	Q
HPC, bulk	UCF lab		W	W	W	W	W	W

<i>3/W</i>	=	<i>three times a week</i>
<i>W</i>	=	<i>once a week</i>
<i>BW</i>	=	<i>every two weeks</i>
<i>Q</i>	=	<i>quarterly, four times a year</i>
<i>N/A</i>	=	<i>Not available</i>
<i>lbs/gal</i>	=	<i>0.12 g/mL</i>

3.4 EN monitoring

Water from each PDS exited via the effluent standpipe to the copper loops in the corrosion shed on the North end of the site. Water was also withdrawn from the 14 effluent standpipes for PDSs 1 through 14 and pumped via 1/8th inch (0.125 inch) diameter flexible PVC tubing to the Noise Trailers into the individual flush tanks for each of the 14 respective Nadles. This ensured that the water quality for both; the copper loops in the corrosion shed and for the Nadles; which housed the probes for EN monitoring as well as the corrosion coupons for surface characterization was the same. The probes were placed with the more noble metal i.e. (Cu>Fe>Pb) upstream to minimize any galvanic corrosion due to any particulate release and subsequent deposition on the downstream metal. Copper is nobler to Iron which is nobler to Lead; a noble metal requires a higher Electrochemical Potential i.e. driving force for corrosion to occur. Figure 3.8 displays an inside view of the EN Trailer. The Nadles were flushed with the water from the flush tank at an average velocity of 1 ft/s and then corrosion data was collected continuously for at least 6 hour standing period to simulate conditions applicable as per Lead and Copper Rule [40 CFR 141.86(b)2] There is no outer limit on standing time. The EN monitoring equipment is commercially called ‘Smart CET’ and is made by Honeywell Intercorr international, Houston TX.



Figure 3.8 The Nadles layout with the probes connected

3.4.1 EN equipment- SmartCET system

The SmartCET corrosion monitoring system is displayed in Figure 3.9 and comprised of the following components:

1. Corrosion probe (Figure 3.10), one per SmartCET device. Each probe housed 3 electrodes of the same metal either Copper, Carbon Steel (Iron) or Lead-Tin.
2. Probe cable, one per SmartCET device. The cable was 15-foot length, with 6-pin connector to connect the probe to the SmartCET device. Also provided per device is 15-foot flying lead for power & communications.
3. SmartCET device, one per probe.
4. Medium for transfer of data between monitoring instrument and computer. A hardwire connection using Belden 9328 specification cable updates data from the CET to the computer once every 430 seconds.

5. Power supply 110V/60 Hz. The system power/communications interface was supplied with 6-foot mains power cord.

User interface Field CETTM software was used to transfer 'raw' data to provide calculated user data. The interface to the computer was through a regular COM port. The software allowed the user to create and store data from each probe into a separate DAT extension file which was converted to ASCII file format i.e. Microsoft Excel format and was used for data analysis. New electrodes before inserting in the Nadles are shown in Figure 3.11.

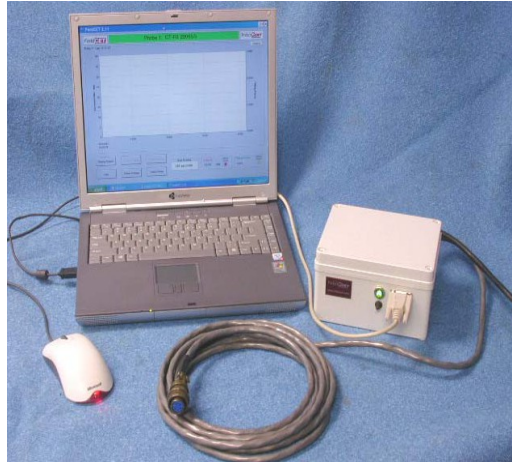


Figure 3.9 SmartCET system and electrodes

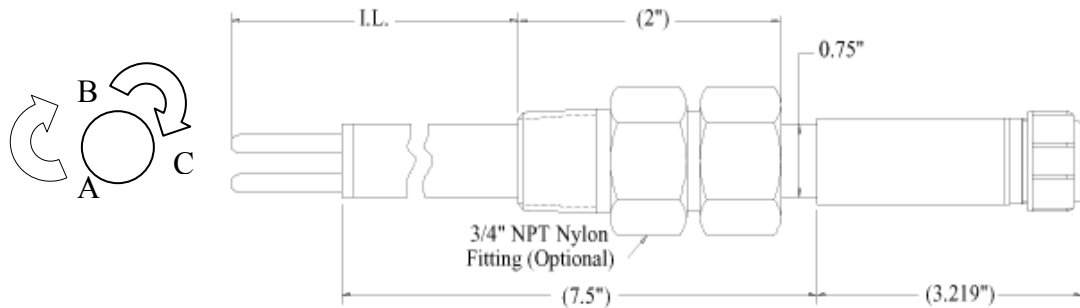


Figure 3.10 Schematic of electrodes

Note: The assembly consists of a glass epoxy probe with a 3/4" NPT nylon compression fitting for insertion into the system. The studs for mounting the electrodes and the six-pin connector are held in place by the epoxy fill material. The maximum insertion length (I.L.) is 6.75" when the compression fitting is used and 8.75" when the fitting is not used. Temperature Rating - w/ nylon compression fitting - 150° F / 65° C, Pressure Rating - 100 PSI / 7 Ba, and Mounting - 3/4" NPT Pipe Plug

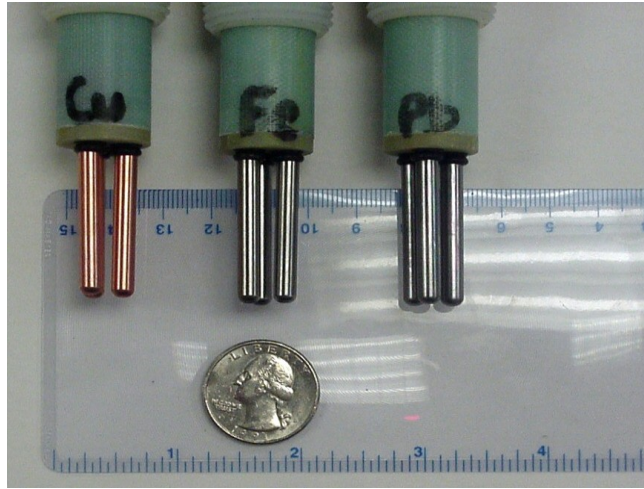


Figure 3.11 Electrode probes detail

All electrodes had an area of 4.67 cm²; the electrodes were numbered clockwise from A through C, with location of a marked by a black line (sharpie) on the probe body. Table 3.7 displays the numbering scheme to identify each individual electrode. It must be noted that the anodic and cathodic areas keep changing irrespective of electrode during an electrochemical process. Figure 3.12 displays the probe connection details in the Nadles.

Table 3.7 Numbering of electrodes

Probe #	Electrode ID	Element	Atomic Weight	# electrons *	Density (gm/cm ³)
01-14	A,B,C	Cu	63.54	2	8.89
15-28	A,B,C	Fe	55.46	2	7.84
29-42	A,B,C	Pb/Sn	162.95	2	7.86

of electrons transferred in electrochemical reaction for corrosion.



Figure 3.12 Probe connection details

Monitoring was continuous which comprised of 430 s of cycle time of which 300 s was for EN, 100 s for LPR and harmonic distortion analysis (HDA which used time lagged AC impedance) and 30 s for the solution resistance. A typical output is displayed below in Table 3.8 with the parameter description in Table 3.9. Each of the Fe, Cu and Pb probes has three electrodes (A, B, and C). There were three probes (for example #'s 01, 14, and 29) in each Nadle, which allowed simultaneous monitoring of Cu, Fe and Pb corrosion data and was collected by the CET. There was only one CET, so the CET connection was switched manually every 6 hours or so, to allow collection of corrosion data from all Nadles.

Table 3.8 Typical output from Electrochemical Noise Monitoring (Iron)

Parameter	Value	Unit
LPRCR	0.155	mpy
HMCR	0.112	mpy
ECNCR	0.385	mpy
PF	0.047	-
B	0.014	Volts
Ba	0.069	Volts/decade
Bc	0.065	Volts/decade
PSKW	-17.8	-
PKRT	391	-
ISKW	-9.7	-
IKRT	154	-
RSOL	7095	ohms

Table 3.9 Output parameters from EN monitoring

1	LPRCR	It is the Linear Polarization Resistance corrosion rate.
2	HMCR	It is the Harmonic Distortion Analysis corrosion rate.
3	ECNCR	It is the Electrochemical Noise corrosion rate.
4	PF	The Pitting Factor is evaluated from Electrochemical noise measurements.
5	<i>B</i>	It is the Stern Geary constant evaluated from the Harmonic Distortion Analysis.
6	<i>Ba</i>	It is the anodic tafel slope.
7	<i>Bc</i>	It is the cathodic tafel slope.
8	PSKW	Skew of potential.
9	PKRT	It is the kurtosis of the potential.
10	ISKW	Skew of current.
11	IKRT	It is the kurtosis of the current.
12	RSOL (<i>R_s</i>)	It is the solution resistance.

3.5 Theory of measurement of EN parameters

The corrosion rates from linear polarization resistance (LPR), the harmonic distortion analysis (HDA), and the electrochemical noise (ECN) were abbreviated as LPRCR, HMCR, and ECNCR, respectively and are reported in units of mils/yr, mpy (1 mpy = 0.0254 mm/yr). All three methods employ Ohm's law as the basis of corrosion

rate determination. Ohms law is shown in Equation 3.1. LPR applies a small direct current (DC) voltage across the electrodes, measures the current passing through the electrodes, and evaluates the resistance (R) as shown in Equation 3.1. HDA applies a small alternating current (AC) voltage over a range of frequencies, measures the current response at each frequency, and evaluates the impedance (Z) as shown in Equation 3.2. With LPR, the resistance R, is independent of the applied voltage. However, with HDA, the impedance, Z, depends on the frequency of applied voltage. The relationship between impedance, Z, and the applied voltage frequency within HDA is analyzed to determine both the anodic Tafel slope B_a and the cathodic Tafel slope B_c . The Stern-Geary coefficient (B), is then computed from the anodic and cathodic Tafel slopes. This coefficient, B, is then used to compute the HMCR as shown in Equation 3.3 and for LPRCR the computed R is analogous to R_p .

$$V = I.R \quad \text{Equation 3.1}$$

$$V = I.Z \quad \text{Equation 3.2}$$

$$I_{corr} = \frac{B}{R_p} \quad \text{Equation 3.3}$$

where V = potential across the electrodes (volts)
 I = current through the electrodes (amperes)
 R = resistance of the electrodes (ohms).

In electrochemical measurements, the total measured resistance for an applied voltage is the sum of resistance in the solution and at the electrode surfaces. The solution resistance (RSOL) relates to the conductivity of solution, whereas the polarization resistance (R_p) relates to the resistance caused by polarization at the electrode surfaces. The true electrode resistance, R_p , is calculated by subtracting RSOL from the total

measured resistance. RSOL is determined during measurement of HDA by evaluating the changes in impedance with changes in the frequency and amplitude of the voltage. Unlike LPR and HDA, the electrochemical noise (ECN) technique does not apply a DC or AC voltage to the electrodes, but rather, it monitors the variability of the naturally occurring voltage and current fluctuations caused by reactions on the electrode surfaces. This information is used to calculate the noise resistance R_N as shown in Equation 3.4. The ECN technique uses R_N to calculate the corrosion current, I_{corr} using Equation 3.5. In contrast, LPR and HDA use R or R_p respectively to calculate the corrosion current, as shown previously in Equation 3.3. For all three techniques, once I_{corr} is calculated, Equation 3.6 is used to convert the corrosion current density to the corrosion rate.

$$R_N = \frac{\sigma_v}{\sigma_i} \quad \text{Equation 3.4}$$

$$I_{corr} = \frac{B}{R_N} \quad \text{Equation 3.5}$$

$$CR = \frac{A I_{corr}}{z F \rho} = \frac{K I_{corr} \cdot A}{z \cdot \rho} \quad \text{Equation 3.6}$$

where σ_E = standard deviation of potential
 σ_i = standard deviation of current
 CR = corrosion rate of LPRCR or HMCR or ECNCR (mpy)
 A = atomic weight of the metal
 I_{corr} = corrosion current density (Amperes/cm²)
 z = number of electrons transferred per atom of metal corroded
 F = faraday's constant=96,500 coulombs/equivalent
 ρ = density of the metal (g/cm³)
 K = 1.288x10⁵ constant for conversion of units.

In addition the standard deviation, skew, and kurtosis for both voltage and current can be used as EN parameters which indicate the stability of corrosion process.

Equations for each of these statistical parameters are shown in Equation 3.7, Equation 3.8 and Equation 3.9 respectively. The pitting factor, (PF), is shown in Equation 3.10.

$$\sigma = \frac{\sum_1^n (Y_i - \bar{Y})^2}{(n - 1)} \quad \text{Equation 3.7}$$

$$Skew = \frac{\sum_1^n (Y_i - \bar{Y})^3}{(n - 1)\sigma} \quad \text{Equation 3.8}$$

$$Kurtosis = \frac{\sum_1^n (Y_i - \bar{Y})^4}{(n - 1)\sigma^2} \quad \text{Equation 3.9}$$

$$PF = \frac{\sigma}{(I_{corrHDA})} \quad \text{Equation 3.10}$$

where σ = standard deviation
 \bar{Y} = mean
 σ_i = standard deviation of corrosion current density from ECNCR
 I_{corr} = mean corrosion current density from HMCR

3.6 References

1. Abernathy C. G. and Camper A. K. (1997) Interactions between pipe materials, disinfectants, corrosion inhibitors, organics and distribution biofilms. In Proceedings of AWWA WQTC, Denver, CO (9-12 November).
2. Al-Mazeedi H.A.A and R.A Cottis.2004. A practical evaluation of electrochemical noise parameters as indicators of corrosion type. *Electrochimica Acta.*(49)2787-2793.
3. AwwaRF.1996. Internal corrosion of water distribution systems. AWWARF-DVGW-TZW cooperative research report, Denver, Colorado.
4. AwwaRF. Cruse H, Von Franque O and Pomeroy R. D. 1985. Corrosion of copper in portable water systems. Internal corrosion of water distribution systems. Denver Colorado.
5. Benjamin M. M., Reiber S., Ferguson J. F., Van der Werff E. A. and Miller M. W. 1990. Chemistry of corrosion inhibitors in potable water. AWWA Research Foundation Report, Denver, Colorado.
6. Boffardi. Bennett P Water treatments. 1995. Chapter 77, pp704. Corrosion tests and standards: application and interpretation. Robert Baboaiian (Editor). ASTM manual series MNL 20, PCN 28-020095-27. ISBN 0-8031-2058-3
7. Boxall J.B, A.J Saul and P.J Skipworth. 2004. Modeling for hydraulic capacity. *Jour AWWA* 96(4):161-169.
8. Brusic V., M. A. Frishe, B. N. Eldidge, F. P. Novak, F. B. Kaufman, B. M. Rush, and G. S. Frankel, *Journal of Electrochem. Soc.*, 138, 2253 -1991.
9. Cantor Abigail F, David Denig-Chakroff, Richard R Vela, Mark G Oleinik and Daniel L Lynch. 2000. Use of polyphosphates in corrosion control. *Jour AWWA* February(2000):95-102.
10. Cantor Abigail F, Jae K Park and Prasit Vaiyavatjamai. 2003. Effect of chlorine on corrosion in drinking water systems. *Jour AWWA* 95(5):112-123.
11. Cao C. 1996. On Electrochemical techniques for interface inhibitor research. *Corrosion Science.* 38(12) 2073-2082.
12. Cappeln F, N.J Bjerrum and I.M Petrushina. 2005. Electrochemical noise measurements of steel corrosion in the molten NaCl-K₂SO₄ system.. *Jour Electrochem. Soc.* 152(7)B228-B235.
13. Chen J.F and W.F Bogaerts. 1995. The physical meaning of noise resistance. *Corrosion Science.* 37(11):1839-1842.
14. Cohen Koby, Abernathy G. Calvin and Hill P Christopher.2003. Distribution systems. Corrosion control aids residuals. AWWA. *Opflow.* 29(1)3-6.
15. Cornell R M and Udo Schwertmann. 2003. The Iron oxides: Structure, properties, reactions, occurrences and uses. Wiley –VCH, Weinheim. ISBN 3-527-29669-7
16. Cottis R.A. 2000. Simulation of electrochemical noise due to metastable pitting. *JCSE-Jour of corrosion science and engineering.*(3)paper 4.
17. Cottis, R.A. 2000. Simulation of Electrochemical Noise due to Metastable Pitting. *Journal of Corrosion science and Engineering (Online Journal).* Vol 3(Paper4). <http://www.jcse.org/>

18. Cruse H & Pomeroy. 1974. Corrosion of copper pipes. Jour AWWA 67(8):479.
19. Dart F James and Paul D Foley. 1970. Preventing iron deposition with sodium silicate. Jour AWWA October(1970):663-668.
20. Dart F James and Paul D Foley. 1972. Silicate as Fe, Mn deposition preventative in distribution systems. Jour AWWA April(1972):244-249.
21. Dart F. James and Foley D. Paul. 1970. Preventing iron deposition with sodium silicate. Jour AWWA. Oct 1970. pp 244-249.
22. Dart F. James and Foley D. Paul. 1972. Silicate as Fe, Mn deposition preventative in distribution systems. Jour AWWA. April 1972. pp 663-668.
23. Digiano A. Francis and Zhang Weidong. 2005. Pipe section reactor to evaluate chlorine-wall reaction. Jour AWWA. 97(1)74-85.
24. Dodrill D. M. and Edwards M. 1994. A general frame work for corrosion control. In Proceedings of AWWA Water Quality Technology Conference, San Francisco CA (6-10 November).
25. Dodrill Donna M and Marc Edwards. 1995. Corrosion control on the basis of utility experience. Jour AWWA July(1995):74-85.
26. Dolterly P E.. D.C.A. Moore. W.M. Cox. J.L. Dawson. 1990. An Application of Advanced Electrochemical Monitoring to Corrosion of Heat Exchanging Tubes. Proc. Environmental Degradation of Materials in Nuclear Power Systems -Water Reactors, Jekyll Island. Georgia, ed. D. Cubrecrotti (Houston, TX: NACE, 1990), 13-65.
27. Drissi S.H, Ph. Refait M Abdelmoula, J M.R Genin. 1995. Corrosion Science 37:2025.
28. Duranceau Steven J, Dan Townley and Graham E.C Bell. 2004. Optimizing corrosion control in water distribution systems. AwwaRF (American Water Works Association Research Foundation). Denver Colorado. ISBN 1-58321-326-0.
29. Duranceau, S.J., D. Townley, and G.E.C. Bell. 2004. *Optimizing Corrosion Control in Water Distribution Systems*. Denver, Colo.: AwwaRF.
30. Dye, J.F. 1964. Review of Anticorrosion Water Treatment. Jour. AWWA, 56(4): 457-465.
31. Eden D.A 1998. Electrochemical Noise –The first two octaves. Paper No 386 in Corrosion/98. NACE International.
32. Edwards Marc, J.F Ferguson and S.H Reiber. 1994 a. The pitting corrosion of copper. Jour AWWA, 86(7):74-90.
33. Edwards Marc, Laurie S McNeill, Thomas R Holm and Michael C Lawrence. 2001. Role of phosphate inhibitors in mitigating lead and copper corrosion. Denver Colorado. ISBN 1-58321-086-5.
34. Edwards Marc, Meyer Travis and Rehring John. 1994 b. Effect of selected anions on copper corrosion rates. Jour AWWA, December (1994)73-81.
35. Edwards Marc, Sara Jacobs and Donna Dodrill. 1999. Desktop guidance for mitigating Pb and Cu corrosion by-products. Jour AWWA. 91(5):66-77.
36. Farshad Fred F and Thomas C Pesacreta. 2003. Coated pipe interior surface roughness as measured by three scanning probe instruments. Anti-corrosion methods and materials. 50(1)6-16.

37. Fouada A.S., A.M. El Desoky and A.A.El Serawy. Corrosion Science and Engineering 7. 2005. Some Hydrazide Derivatives as Inhibitors for The Corrosion of Zinc in Sodium Hydroxide Solution.
38. Frankel G.S. Localized corrosion of metals; A review of the rate controlling factors in initiation and growth. Fontana Corrosion center. Ohio State University, Columbus Ohio.
39. Frankel G.S. Pitting corrosion of metals; A summary of the critical factors. Fontana Corrosion center. Ohio State University, Columbus Ohio.
40. Frateur I et al. 1999. Free chlorine consumption induced by cast-iron corrosion in drinking water distribution system. Water resources. 33(12)1781.
41. Galvele Jose R. Transport process and the mechanisms of pitting of metals. Fontana Corrosion center. Ohio State University, Columbus Ohio. Reprinted from the Jour Electrochem. Soc. 123(4) April 1976.
42. Gasparac R, C. R. Martin, and E. Stupnis ek-Lisaca. 2000. In Situ Studies of Imidazole and Its Derivatives as Copper Corrosion Inhibitors. I. Activation Energies and Thermodynamics of Adsorption. Journal of The Electrochemical Society, 147 (2) 548-551
43. Gonzalez-Nunez M.A and J Uruchurtu-Chavarin.2003. R/S fractal analysis of electrochemical noise signals of three organic coating samples under corrosion conditions. JCSE-Jour of Corrosion science and engineering.(6)paper C117.
44. Gregory R. 1990. Galvanic corrosion of Lead solder in copper pipework. Jour IWEM. 4:4.
45. Gustavo E Lagos, Claudia A Cudrado and M Victoria Letelier. 2001. Aging of copper pipes by drinking water. Jour AWWA, November (2001)94-103
46. Holcomb G.R and Bernard S. Covino, Jr. and David Eden. State-of-the-Art Review of Electrochemical Noise Sensors – White paper for U.S Department of energy. 2002 DOE/ARC-TR-03-0002.
47. Hozalski Raymond M, Elizabeth Esbri-Amador and Che Fe Chen. 2005. Comparison of stannous chloride and phosphate for lead corrosion control. Jour AWWA. 97(3):89-103.
48. <http://www2.umist.ac.uk/corrosion/JCSE/Volume7/Default.html> ISSN 1466-8858
49. Ives D. J and Rawson A. E. 1962. Copper Corrosion I Thermodynamic aspects. Jour Electrochem. Soc., 109 (6):447.
50. Ives D. J and Rawson A. E. 1962. Copper Corrosion II Kinetic studies. Jour Electrochem. Soc., 109 (6):452.
51. Ives D. J and Rawson A. E. 1962. Copper Corrosion III Electrochemical theory of general corrosion. Jour Electrochem. Soc., 109 (6):458.
52. Ives D. J and Rawson A. E. 1962. Copper Corrosion IV The effect of saline additions. Jour Electrochem. Soc., 109 (6):462.
53. Jones Edmunds & Associates, Boyle Engineering Corporation and MJ Schiff & Associates. 2004. Pinellas county utilities water blending studies. Corrosion inhibitor screening evaluation.
54. K. Abiiola, N.C. Oforika, Corrosion Science and Engineering 3. 2002. <http://www2.umist.ac.uk/corrosion/JCSE/Volume3/Paper21/v3p21.htm> ISSN 1466-8858

55. Kuch, A. 1988. Investigations of The Reduction and Re-oxidation Kinetics of Iron (III) Oxide Scales Formed in Waters. *Corrosion Science.*, 28(3):221-231.
56. Kuch, A., and I. Wagner. 1983. A Mass Transfer Model to Describe Lead Concentration in Drinking Water. *Water Res.*, 17(10):1303-1307.
57. Larson, T.E., and R.V. Skold. 1957. Corrosion and Tuberculation of Cast Iron. *Jour. AWWA*, 49(10):1294-1302.
58. LeChevallier M. W., Shaw N. and Smith D. B. (1996) Factors limiting microbial growth in the distribution system: full scale experiments. AWWA Research Foundation Report. Denver, CO.
59. Lin, J., M. Ellaway, and R. Adrien. 2001. Study of Corrosion Material Accumulated on The Inner Wall of Steel Water Pipe. *Corrosion Science.*, 43(11):2065-2081.
60. Lowther E. D. and Moser R. H. 1984. Detecting and eliminating coliform regrowth. In Proceedings of AWWA Water Quality Technology Conference, Denver, CO. Rompre.
61. Lytle A Darren and Snoeyink L Vernon. 2002. Effect of ortho-and polyphosphates on the properties of iron particles and suspensions. *Jour AWWA* 94(10):87-98.
62. Lytle Darren A and Vernon L Snoeyink. 2002. Effect of ortho-and polyphosphates on the properties of iron particles and suspensions. *Jour AWWA* 94(10):87-98.
63. McIntyre P. and A.D. Mercer. eds. 1994. Corrosion and Related Aspects of Materials for Potable Water Supplies. London, U.K., Maney Publishing.
64. McNeill Laurie S and Marc Edwards.2001. Iron pipe corrosion in distribution systems. *Jour AWWA*, July (2001)88-100.
65. McNeill Laurie S and Marc Edwards.2004. Importance of Pb and Cu particulate species for corrosion control. *Jour Environ Engg ASCE*, Feb (2004)136-144.
66. Merrill, D.T. and R.L. Sanks. 1978. Corrosion control by deposition of CaCO₃ films: A practical approach for plant operators. *Jour. AWWA*. 70(1):12-18.
67. Meszaros L, G Meszaros, A Pirnat and B Lengyel. 1996. An experimental study of iron corrosion in sulfuric acid solution containing inhibitors by noise measurement. *Jour Electrochem. Soc.* 143(11)3597-3599.
68. Murray Bruce W..1970. a corrosion inhibitor process for domestic water. *Jour AWWA*. Oct 1970. pp659-662.
69. Murray W Bruce. 1970. A corrosion inhibitor process for domestic water. *Jour AWWA* October(1970):659-662.
70. NACE 1976. Passivity and its breakdown on Iron and Iron base alloys. Library of congress catalog number 76-5317. (Houston. TX: NACE. 1976).
71. NACE 1993. A Legal. Electrochemical Noise as the Basis of Corrosion Monitoring. 12th International Corrosion Congress, vol. 3A (Houston. TX: NACE. 1993), 1410.
72. Norton Cheryl D. and Mark W. LeChevallier.1997. Chlorination: Its effect on distribution system water quality. *Jour AWWA*. 89(7): 66-77.
73. Piccinini R, M Marek, A.J.E Pourbaix and R.F Hoffman. 1971. Localized Corrosion, NACE Houston TX. Pp. 79-183.

74. Pickering H.W. 2003. Jour electrochemical society. 150:K1
75. Prevostet Michele, Annie Rompre, Helene baribeau, Josee Coallier and Pierre Lafrance.1997. Service lines: their effect on microbiological quality. Jour AWWA 89(7):78-91.
76. Refait, Ph., J.B. Memet, C. Bon, R. Sabot, and J.M. R.. Genin. 2003. Formation of the Fe(II)-Fe(III) Hydroxysulfate Green Rust During the Marine Corrosion of Steel. *Corrosion Science*.. 45(4):833-845.
77. Refait, Ph., M. Abdelmoula, and J.M. R. Genin. 1998. Mechanisms of Formation and Structure of Green Rust one in Aqueous Corrosion of Iron in the Presence of Chloride Ions. *Corrosion Science*., 40(9):1547-1560.
78. Reffass M, R sabot, C Savall, M Jeannin, J Creus and Ph. Refait. 2005. Localized corrosion of carbon steel in NaHCO₃/NaCl electrolytes: role of Fe(II)-containing compounds. *Corrosion Science* 48:709-726
79. Riber S. 1989. Copper plumbing surfaces: An Electrochemical study. Jour AWWA, 81(7):114
80. Robinson R. Bruce, Reed D Gregory and Frazier Brett. 1992. Iron and manganese sequestration facilities using sodium silicate. Jour AWWA Feb 1992. 77-82.
81. Rossman L.A, Clark R.M and Grayman W.M.1994. Modeling chlorine residuals in drinking water distribution systems. Jour environmental Engineering. ASCE. 120(4)803.
82. Russel L Porter and J.F Ferguson. 1995. Improved monitoring of corrosion process. Jour AWWA, November (1995):85-95.
83. Sander, A., B. Berghult, A.E. Broo, E.L. Johansson, and T. Hedberg. 1996. Iron Corrosion in Drinking Water Distribution Systems - The Effect of pH, Calcium and Hydrogen Carbonate. *Corrosion Science*., 38(3): 443-455.
84. Sarin Pankaj, Jonathan A. Clement, Vernon L Snoeyink and Waltraud M Kriven. Iron release from corroded, unlined cast iron pipe.2003. Jour AWWA. 95(11):85-96.
85. Sarin, P., V.L. Snoeyink, D A Lytle and W.M. Kriven.. 2004. Iron Corrosion Scales: Model for scale growth, iron release, and colored water formation. Jour Environmental engg. ASCE. April (2004) :2364-371.
86. Sarin, P., V.L. Snoeyink, J. Bebee, W.M. Kriven, and J.A. Clement. 2001. Physico-chemical Characteristics of Corrosion Scales in Old Iron Pipes. *Water Res.*, 35(12):2961-2969.
87. Sathiyarayanan S and G Venkatachari. 2004. evaluation of corrosion inhibitors by harmonic analysis. JCSE-Jour of Corrosion science and engineering.(7)Preprint 13.
88. Schenk E. John and Weber Jr.Walter J. 1968. Chemical interactions of dissolved silica with iron (II) and (III). Jour AWWA. Feb 1968. pp199-210.
89. Schenk John E and Walter J Weber Jr. 1968. Chemical Interactions of dissolved silica with iron (II) and (III). Jour AWWA February(1968):199-211.
90. Schock Michael R, Darren A Lytle, Anne M Sandvig, Jonathan Clement and Stephen M Harmon. 2005. Replacing Polyphosphate with Silicate to solve lead, copper and source water iron problems.Jour AWWA, 97(11):84-93.

91. Schock Michael R., Jerry Holldber, Thomas R Lovejoy and Jerry Lowry. 2002. California's first aeration plants for corrosion control. *Jour AWWA*, 94(3):88-100.
92. Schock, M.R. 1989. Understanding Corrosion Control Strategies for Lead. *Jour. AWWA*. 81(7):88-100.
93. Singley J.Edward. 1994. Electrochemical nature of lead contamination. *Jour AWWA*, 86(7):91-96.
94. Singley, J.E. 1981. The Search for a Corrosion Index. *Jour. AWWA*, 73(11):578-582.
95. Tan Y.J, Bailey S and Kinsell B. 1996. The monitoring of the formation and destruction of corrosion inhibitor films using electrochemical noise analysis (ENA). *Corrosion science*. 38(10)1681-1695.
96. Taylor J.S, J.D Dietz, A.A Randall, S.K Hong, C.D Norris, L.A Mulford, J.M Arevalo, S. Imran, M Le Puil, I Mutoti, J Tang, W. Xiao, C. Cullen, R. Heaviside, A. Mehta, M. Patel, F. Vasquez and D. Webb. University of Central Florida. Effects of blending on distribution system water quality. 2005. *AwwaRF*, Denver, Colorado.
97. Taylor, J.S., J.D. Dietz, A.A. Randall, C.D. Norris, A. Alshehri, J. Arevalo, X. Guan, P. Lintereur, D. MacNevin, E. Stone, R. Vaidya, B. Zhao, S. Glatthorn and A. Shekhar. 2007. Control of distribution system water quality in a changing water quality environment using inhibitors. Draft final report submitted to AWWA Research Foundation Denver CO and Tampa Bay Water. (TBW II report)
98. Taylor, J.S., J.D. Dietz, A.A. Randall, S.K. Hong, C.D. Norris, L.A. Mulford, J.M. Arevalo, S. Imran, M. Le Puil, S. Liu, I. Mutoti, J. Tang, W. Xiao, C. Cullen, R. Heaviside, A. Mehta, M. Patel, F. Vasquez, and D. Webb. 2005. Effects of Blending on Distribution System Water Quality. AWWA Research Foundation Denver CO and Tampa Bay Water. (TBW I report).
99. USEPA 1979. National secondary drinking water regulations. Final Rule. *Federal Register*, 44:140:42195(July 19, 1979)
100. USEPA 1991. Lead and Copper. Final Rule. *Federal Register*, 56:110:26460(June 7, 1991)
101. Vasconcelos JJ. Et al. 1996. Characterization and modeling of chlorine decay in distribution systems. *AwwaRF and AWWA*, Denver.
102. Vasquez Ferdinand A, Robert Heaviside, Jason Tang and James S Taylor. 2006. Effect of free chlorine and chloramines on lead release in a distribution system. *Jour AWWA* 98(2):144-154.
103. Vatankhah, G., M. Drogowska, and H. Menard. 1998. Electrodeposition of Iron in Sodium Sulfate and Sodium Bicarbonate Solutions at pH 8. *Jour. of App. Electrochem.*, 28(2):173-183.
104. Volk Christian, Esther Dundore, John Schiermann and Mark LeChevallier. 2000. Practical Evaluation of Iron Corrosion Control in a Drinking Water Distribution System. *Water resources*, 34(6):1967-1974.

105. Vukmirovic M. B., N.Vasiljevic,a, N. Dimitrov, and K. Sieradzka.2003. Diffusion-Limited Current Density of Oxygen Reduction on Copper Journal of The Electrochemical Society, 150 (1). B10-B15.
106. Washington Aqueduct and Sewer Authority (WASA) and CH2M HILL. Desktop corrosion control study. 2004. prepared for US EPA Region III.
107. Wharton J.A and R.J.K Wood. 2004. Influence of flow conditions on the corrosion of AISI 304L stainless steel. Elsevier science direct (256)525-536.
108. Zerfaoui M, H Oudda, B Hammouti, S Kertit and M Benkassour. 2004. Inhibition of corrosion of iron in citric acid media by amino acids. Progress in Organic Coatings 51:134-138.

4 CORRELATING COPPER RELEASE WITH ELECTROCHEMICAL CORROSION MONITORING IN DRINKING WATER

ABSTRACT

Electrochemical corrosion monitoring (EN) was used to monitor corrosion and predict copper (Cu) release in a pilot-scale test facility operated for a one-year period. Data was collected from fourteen Cu corrosion loops and fourteen EN probes with Cu electrodes with and without phosphate and silicate inhibitors at varying doses. EN models were developed that found the Linear Polarization Rate (LPR) and Electrochemical Noise (ECN) described Cu release as well as chemical models, which indicated both localized and general corrosion mechanisms were active. The actual data and the EN model found that Cu release was highest for pH controls and was reduced by all inhibitors investigated. The ranked order of inhibition was BOP>OP>ZOP>Si>>pH. EN monitoring is significantly faster and less labor intensive relative to traditional water quality monitoring techniques, and provided a good fit to total and dissolved Cu release with a R^2 of 0.72 and 0.68, respectively.

4.1 Introduction

Preventing corrosion is one of the more important tasks facing the drinking water community. The Lead and Copper Rule (LCR) has mandated corrosion control to reduce human exposure to waterborne lead (Pb) and copper (Cu), the result of the gradual deterioration of distribution system metal surfaces by chemical action, commonly induced by electrochemical processes (SDWA, 1991). Monitoring corrosion rates using

methods that take advantage of electrochemical processes are typically fast compared to alternatives of weight loss coupons, electrical resistance probes, or direct inspection by visual, ultrasonic, or nuclear means (Duranceau et al., 2004). However, correlating corrosion rate monitoring information to metal release concentration, although highly desirable, is not yet fully understood. This article demonstrates the use of EN parameters that can be correlated to concentration and hence be used to estimate Cu release for a wide variety of distributed water qualities.

4.2 Background

Tampa Bay Water (TBW) manages drinking water resources for six member governments (MGs) on the west coast of central Florida: the cities of New Port Richey, St. Petersburg, and Tampa, and Hillsborough, Pasco, and Pinellas counties. TBW serves nearly two million consumers at a 250 MGD average daily demand. This region, like most of Florida, has historically utilized groundwater for its drinking water supply; however, adverse environmental impacts have mandated that alternatives (non-groundwater sources such as desalinated seawater and treated surface water) be used for future supply. TBW manages two alternative supplies: a 66 MGD ($2.5 \times 10^5 \text{ m}^3$ per day) surface water treatment facility, which utilizes enhanced coagulation, ozone, and biological filtration; and a 25 MGD ($9.5 \times 10^4 \text{ m}^3/\text{day}$) desalination plant. Finished water from these facilities are blended with finished groundwater and distributed to the MGs through a large regional transmission system, which runs through the three-county area. Blends of the various resources depend on the location of delivery and supply availability. The impact of new source waters and their blends on water quality changes

were evaluated (Taylor et al., 2005) under a tailored collaboration project (TCP) conducted by the University of Central Florida (UCF) and funded by TBW and AwwaRF. This TCP called TBW I identified the most significant controlling parameters within the variation of water quality expected in the MG distribution systems as alkalinity, sulfates and chlorides. The models developed in TBW I predicted violations in excess of the 1.30 mg/L total copper (TCu) action level specified by the LCR (Lead and Copper Rule) for high alkalinity waters i.e. for blends with high percentage of ground water.

4.3 TBW II study

In this follow up one-year TCP called TBW II, the effect of corrosion inhibitors to mitigate adverse impacts in distribution systems that receive blended finished waters produced from ground, surface and saline sources was investigated. This TCP had the objective of investigating the best available inhibitors for maintaining acceptable water quality in the TBW and member government (MG) distribution systems. Corrosion inhibitors offer an opportunity for scale control because they bond directly with the elemental metal or scale on the pipe surface, forming a barrier between the interior pipe surface and the bulk water. The film formed by such inhibitors will only be dependent on the surface active agent that is added to finished water's. Additionally the pipe scale film will not be dependent on alkalinity, sulfates, chlorides or any other of the water quality parameters that will vary seasonally in the regional finished water. To conduct the inhibitor study, four different corrosion inhibitors were selected and added to the PDS system: blended ortho-phosphate (BOP), ortho-phosphate (OP), zinc ortho-phosphate

(ZOP), and silicate. Each phosphate based inhibitor was studied at three doses: 0.5, 1, and 2 mg/L as P for all the phosphate type inhibitors. The silicate inhibitor was applied as 3, 6, and 12 mg/L as SiO₂. The mechanism of phosphate inhibitors is believed to be due to formation of Cu₃(PO₄)₂ or similar film which inhibits the electrochemical process causing corrosion (Reiber, 1989; Schock et al., 1995). Although phosphate inhibitors have been widely used there is no universal agreement on their role in Cu corrosion or how they actually work (Edwards et al., 2001). In some studies certain inhibitors aggravate corrosion and have been demonstrated to increase Cu release (Cantor et al., 2000; Edwards et al., 2002); particularly for waters with high alkalinity and hardness with neutral pH a mixture of ortho/polyphosphate may increase Cu release. A recent study (Qiu and Dvorak, 2004) is in agreement with the previous studies in that orthophosphate had a stronger effect than polyphosphate on reducing Cu release for high alkalinity and hardness waters at neutral pH.

4.4 Literature on copper corrosion rates

The random variations in potential (volts) and current (amperes) during a corrosion process are termed as noise (Cottis & Turgoose, 1999). EN is based on the theory that different kinds of noise can give important information about corrosion processes. EN generally consists of low frequency (<1 Hz) and amplitude (0.1 μV-10mV and 1 nA/cm² to 10 μA/cm²) signals spontaneously generated by electrochemical reactions on corroding or other surfaces. EN has been used to monitor Cu corrosion in industrial process systems (Monticelli et al., 1999), simulated drinking water (Zang et al., 2002; Edwards et al., 1996 & 1994; Feng et al., 1996 a & b; Royuela & Otero, 1993;

Drogowska et al., 1992), and more recently in full scale systems (Duranceau et al., 2004). These studies report a corrosion rate for Cu from 0.084 mpy to 0.139 mpy for a pH of about 7.5-8.5. These studies indicate an adverse effect of low pH and most studies indicate an adverse effect of high alkalinity and chlorides. Adverse effect of alkalinity for Cu release is sensitive to pH and Cu release increases with alkalinity particularly as pH decreases (Taylor et al., 2005; Edwards et al., 1996 & 1994). Chlorides and sulfates have been shown to have opposing effects on corrosion rates of aged Cu surfaces (Edwards et al., 1994), in that chlorides tend to decrease where as sulfates tend to increase Cu corrosion rates. The author's (Edwards et al., 1994) report that aging resulted in a decrease in the anodic reaction rate in the presence of higher chlorides at a pH of 8.5; and both anodic and cathodic reactions were increased (catalyzed) by sulfates at a pH of 7. Bicarbonate ions increased Cu corrosion rates upon aging at a pH of 7.0, but passivated the Cu surface at a pH of 8.5. These studies identify the water quality effects on Cu corrosion and release; however a complete comprehensive understanding of relationship between corrosion rate and Cu release in presence of inhibitors in a varying water quality is lacking. Moreover corrosion rates may not always correlate directly to metal release, and one study (Edwards et al., 1996) states that only about 3 percent of Cu that was corroded was actually released to solution; approximately 97 percent of the corroded Cu must have been incorporated into scale formed on the pipe surface. Hence correlating corrosion rates to Cu release is complex and understood poorly at best. A summary of water quality and corrosion rates from these studies along with results from this study is shown in Table 4.1.

Table 4.1 Summary of water quality and corrosion rates for copper from various studies

Water/Study	pH	Cl (mg/L)	SO ₄ (mg/L)	Ca (CaCO ₃ mg/L)	Alkalinity (CaCO ₃ mg/L)	Corrosion rate (mpy)	Method
Blends of GW, SW & RO. (Taylor et al. 2007) This study	7.9	47	72	202	163	0.112 to 0.224	LPR
	7.9	59	112	105	109	0.068 to 0.123	
	7.9	64	73	206	154	0.01 to 0.28	
	7.8	56	84	168	127	0.133 to 0.017	
Various utilities (Duranceau et al. 2004)	7.8	28	288	44	117	0.7 to 1.4	ECN
	7.9	69	154	121	94	1 to 3	
	7.6	8	44	141	162	1.6 to 1.7	
	7.7	12	21	199	202	2.3 to 2.5	
Simulated tap. (Monticelli et al. 1999)	5.5	300	760	300	300	2.976	LPR
	7.0	300	760	300	300	0.214	
	8.4	300	760	300	300	0.084	
Simulated tap. (Edwards et al. 1996)	7.2	6	6	25	12-18	0.139 *	LPR
Simulated tap. (Feng et al. 1996 a & b)	7.6	65	40	50	30	0.102 *	LPR
Simulated tap. (Edwards et al. 1996)	6.5	14	24	-	30	0.911 *	LPR
	9.2	14	24	-	30	0.069 *	
	6.5	14	24	-	30	10.323 ^a	
	9.2	14	24	-	30	4.557 ^a	
Simulated tap. (Edwards et al. 1994)	5.5	71	192	-	200	1.07-3.20 *	LPR
	7.0	71	192	-	200	<2.58 *	
	8.5	71	192	-	200	<0.311 ^a	
	10.0	71	192	-	200	<0.25 ^a	
Simulated tap. (Royuela & Otero 1993)	7.9	50	100	93	117	0.069 *	LPR
	7.8	4	7	40	48	0.045 *	
	8.4	414	140	256	200	0.132 *	
	8.0	50	104	216	155	0.072 *	

*denotes the corrosion current density ($\mu\text{A}/\text{cm}^2$) was converted to corrosion rate (mpy)

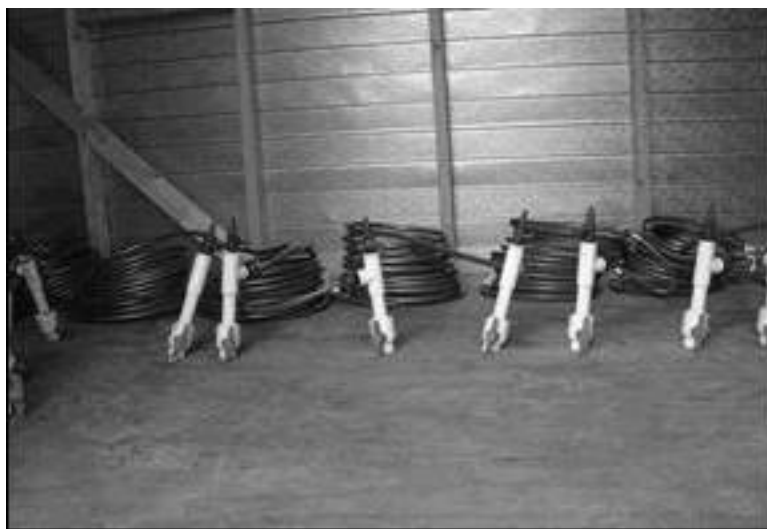
^adenotes corrosion rate in presence of 5 mg/L sulfides

4.5 Materials and methods

The field facility was constructed in 2001 and consisted of pilot distribution systems (PDSs), copper loops, cradles and treatment processes to obtain finished waters.

To maintain integrity of the system finished ground water (GW) was fed to the PDSs and copper loops when the facility was not used after TBW I and before start of this study. The PDSs were constructed of aged pipes that were obtained from existing utility distribution systems to represent the pipe materials used in the TBW Member Government's distribution systems. A complete description of PDSs is given elsewhere (Taylor et al., 2005).

The effluent from the PDSs was split in two parts; one part was dedicated to the copper corrosion loops shown in Photograph 4.1, which were housed inside a shed. The other part was directed to the EN Trailer which housed the Nadles which had Cu probes for EN monitoring. The EN trailer housed PVC pipes of 4 inch inside diameter with tees to house the EN probes; since these pipes house the Electrochemical noise monitoring cradles these are termed as Nadles and shown in Photograph 4.2. The corrosion loop consisted of 30 feet (9.1 m) copper tubing with a diameter of 1.6 cm (5/8 inch), which could hold approximately 1.8 L of water. All other fittings and materials were PVC or other plastic polymers. The corrosion loops were flushed with 2 gallons (7.6 L) of water every morning. The effluent of the copper loops was monitored regularly for copper and lead concentrations.



Photograph 4.1 Copper corrosion loops

The sampling followed the conditions applicable as per the Lead and Copper Rule (U.S. EPA 1991). Samples were usually taken weekly with extra samples taken when needed for specific purposes. To sample the copper loops, a first draw 1 liter sample was collected after six hours of water stagnation, shaken to mix completely, and then 125 ml of it was used for metal measurements. The Nadles housed both the EN probes and corrosion coupons for Fe, Cu and Pb/Sn (50:50), with the coupons placed downstream of the EN probes.

Photograph 4.2 shows the connection of a typical EN probe in a Nadle. The probes were placed with the more noble metal upstream i.e. (Cu>Fe>Pb) to minimize any galvanic corrosion due to possible particulate release and subsequent deposition on the downstream metal. The Nadles were flushed daily and before each monitoring event with 5 pipe volumes of water at an average velocity of 1 ft/s (0.3 m/s).



Photograph 4.2 EN probe connection in Nadle

4.5.1 Operation

This project was divided into four phases; each of three months duration, that started in February 2006. All PDSs received the same blend composition for a three month period (or phase). At the end of each three month period the blend composition was changed. The average water quality of the blends is shown by phase in Table 4.2. Finished ground water (GW), surface water (SW) and desalinated water (RO) were blended in different ratios to achieve the desired water quality. GW was high in alkalinity and total hardness and low in sulfates and chlorides. SW was high in sulfate and low in alkalinity and chlorides where as RO was high in chlorides and low in alkalinity and sulfates. Similar blends were used during phases I and III to evaluate the effect of seasonal conditions on the PDS consisted of a high percentage of GW and low percentage of SW and RO. Phase II consisted of a high percentage of SW and low percentage of GW & RO; where as Phase IV had a high percentage of RO and low percentage of GW and

SW. The individual sources were chloraminated to produce a residual of approximately 4.5 to 5.0 mg/L, and additions were made to the blend to maintain the desired combined monochloramine residual of about 5 mg/L. The target doses of the inhibitors were defined as: 0.5, 1.0, and 2.0 mg/L as P for the phosphorus-based inhibitors and 10, 20, and 40 mg/L as SiO₂ above the background concentration for the silicate-based inhibitor. After 1 month of operation, the doses of the silicate inhibitor had to be changed to 3, 6, and 12 mg/L because the 20 and 40 mg/L doses were causing CaCO₃ precipitation within the PDS. The equipment connection to the EN probes was switched manually between the Nadles every 6 hours to allow data collection from all Nadles.

Table 4.2 TBW II Water quality by phase

Parameter	Project Minimum	Project Maximum	Phase I	Phase II	Phase III	Phase IV
Alkalinity (mg/L as CaCO ₃)	84	175	163	109	154	127
Calcium (mg/L as CaCO ₃)	54	220	202	105	206	168
Dissolved Oxygen (mg/L)	6.6	10.9	8.7	8	8	9.1
Chloride (mg/L)	35	123	47	59	65	56
pH	7.4	9.1	7.9	7.9	7.9	7.8
Silica (mg/L)	4	65.0*	10.9	5.1	10.2	6.4
Sulfate (mg/L)	52	119	72	112	74	85
Sodium (mg/L)	5	53.3	7	36.7	39.5	32
TDS (mg/L)	338	436	365	388	413	378
Temperature (°C)	10.4	29.7	21.2	25.5	24.7	19.6
Total Phosphorus (mg/L as P)	0	3.36*	0.2	0	0	0.1
UV-254 (cm ⁻¹)	0.007	0.105	0.071	0.069	0.077	0.063
Zinc (mg/L)	0.001	0.793	0.031	0.023	0.04	0.037

4.5.2 Electrochemical corrosion rate measurement

Corrosion data was collected continuously for at least a 6 hour standing period to correlate with samples taken for Cu release from the corrosion loops. Each Cu probe had three electrodes. All Cu electrodes had an area of 4.67 cm^2 (0.72 in^2) each, atomic weight of 63.54 and a density of 8.89 g/cm^3 . Electrodes were numbered sequentially as A, B, and C on the probe body for identification. EN monitoring was conducted using commercially available equipment¹ which monitored corrosion rates continuously, with cycles of 430 seconds. Each cycle of 430 seconds was divided into parts with 300 seconds for electrochemical noise (ECN), 100 seconds for linear polarization resistance (LPR), and 30 seconds for harmonic distortion analysis (HDA). The parameters obtained from EN monitoring output are displayed in Table 4.3. The corrosion rates from these three techniques are abbreviated as ECNCR, LPRCR and HMCR respectively and are reported in units of mils/yr, mpy ($1 \text{ mpy} = 0.0254 \text{ mm/yr}$).

Cu electrodes from all 14 PDSs were exposed to varying blends for the project duration of one year and subsequently examined by Scanning Electron Microscope (SEM) and Energy Dispersive Spectroscopy (EDS) for surface characterization of chemical scales. SEM visually magnifies the physical structure of the scale surface for identification of the morphology of the corrosion products. EDS identifies the elemental composition of the surface layer.

Table 4.3 Output parameters from electrochemical noise monitoring

Symbol	Parameter name	mpy
LPRCR	Linear Polarization Resistance Corrosion Rate	mpy
HMCR	Harmonic Distortion Analysis Corrosion Rate	mpy
ECNCR	Electrochemical Noise Corrosion Rate	mpy
PF	Pitting Factor- evaluated from electrochemical noise & harmonic distortion analysis	-
B	Stearn Geary constant -evaluated from the Harmonic Distortion Analysis	Volts
Ba	Anodic tafel slope	Volts/decade
Bc	Cathodic tafel slope	Volts/decade
PSKW	Skew of potential	-
PKRT	Kurtosis of the potential	-
ISKW	Skew of current	-
IKRT	Kurtosis of the current	-
RSOL	Solution resistance	ohms

4.5.3 Quality assurance & control

Samples were collected and analyzed in the field and at the UCF laboratory. Quality assurance and quality control of both the laboratory and field determinations of water quality parameters was established by duplicating analyses of at least 10% of the samples. Blind duplicates and spikes were also used to determine the accuracy of measurements. Dynamic control charts were used to determine whether the results were acceptable. A comprehensive overview of quality control procedures, analytical results and supplementary discussion of associated PDS sampling events and process sampling events over the duration of this entire project is given elsewhere (Taylor et al., 2007). A brief discussion of comparison of Cu corrosion rates from literature with similar water quality with the values obtained from this study is presented herein. This serves to offer a

qualitative measure of accuracy of EN measurements made in this study (TBW II). LPR corrosion rates from TBW II shown in Table 4.1 ranged from 0.01 to 0.28 mpy which were obtained for varying water quality dosed with various phosphate and silicate inhibitors and pH controls. These are compatible with the corrosion rates from other studies (Edwards et al., 1994 and Royuela & Otero, 1993) with similar water quality also shown in Table 4.1.

4.6 Results and discussion

4.6.1 Copper release by inhibitor and phase :

Variation of water quality was achieved by blending finished GW, SW and RO as shown in Table 4.2. Phase I & III water quality was typical of high GW blends, and had high alkalinity, low chloride and low sulfate. Phase II had a higher SW and hence sulfate were relatively higher, and alkalinity and chlorides were lower. The Phase IV blend had a relative higher fraction of RO finished water, which had relatively higher chlorides, lower sulfates and moderate alkalinity. The actual variation in phase water quality was 84 mg/L-175 mg/L as CaCO₃ alkalinity, 35.4 mg/L to 122.9 mg/L Cl and 136 mg/L-252 mg/L as CaCO₃ total hardness. Maximum Cu release was observed in the pH_s PDS. All other corrosion control strategies: pH_{s+0.3}, BOP, OP and ZOP at 0.5, 1.0 and 2.0 mg/L as P and SiO₂ at 3.0, 6.0 or 12 mg/L as SiO₂ mitigated dissolved (DCu) and total (TCu) copper release in all phases. Unless otherwise noted, data is reported as weekly averages for each PDS by phase over one year, which produced 715 observations.

Figure 4.1 shows a box plot of TCu release on the y axis against PDS on the x axis by phase. The boxes are bounded by the 25th to 75th percentile of released TCu. The

whiskers are one inter-quartile range above and below the box and thus bound a total spread of 3 times the inter-quartile range. Hence the whiskers represent a total three deviations of the inter-quartile range. Data outside the whiskers represented by individual points shown in black are potential outliers if the data is assumed to be normally distributed. The median Cu release is shown by the top of the shaded area within the box. Figure 4.1 provides a quick way of assessing TCu release by inhibitor type, dose and phase. As shown in Figure 4.1, maximum TCu release occurred in PDS 13 (pH_s) the data suggests that the 1.3 mg/L action level for Cu would be exceeded unless a phosphate or silica based inhibitor was used. Copper release was reduced most effectively by phosphate based inhibitors and somewhat less effectively with increasing dose. The benefit of BOP against OP was significant for mitigating TCu release in this study. For the medium to high alkalinity waters at pH around 8.0 used in this study, BOP was found to do equally well and at times better than OP. The order of released copper by inhibitor was $\text{BOP} < \text{OP} < \text{ZOP} < \text{Si} < \text{pH}_{s+0.3} < \text{pH}_s$ in every phase (for the water qualities tested) and for the total project.

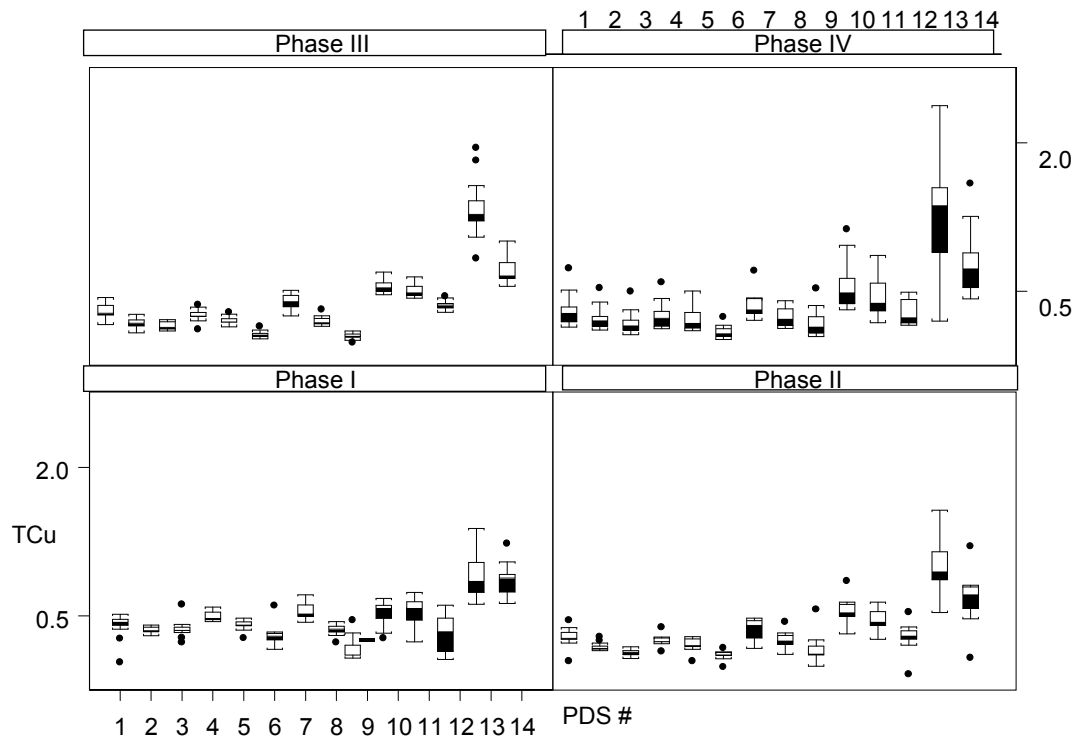


Figure 4.1 Total copper release by PDS and phase.

4.6.2 Observations by photographs and SEM/EDS

Digital images were taken of all Cu electrodes after exposure to blended waters for one year. An orange to dark brown scale was on the electrodes, which also had, numerous blue-green spots on the surface scale except those exposed to 2 mg P/L ZOP.

Photograph 4.3 (left) shows a typical blue-green scale on an OP electrode seen as spots mostly in the centre of the electrodes, while (right) the ZOP electrodes at highest dose of 2 mg P/L, these (ZOP at 2 mg P/L) were the only ones without any spots of blue green scale. Occurrence of such blue green scales was reported (Lytle and Payne, 2004) with Type I cold water pitting for well waters (high alkalinity) with a high sulfate to chloride ratio. The authors (Lytle and Payne, 2004) had identified Brochantite [$\text{Cu}_4(\text{OH})$

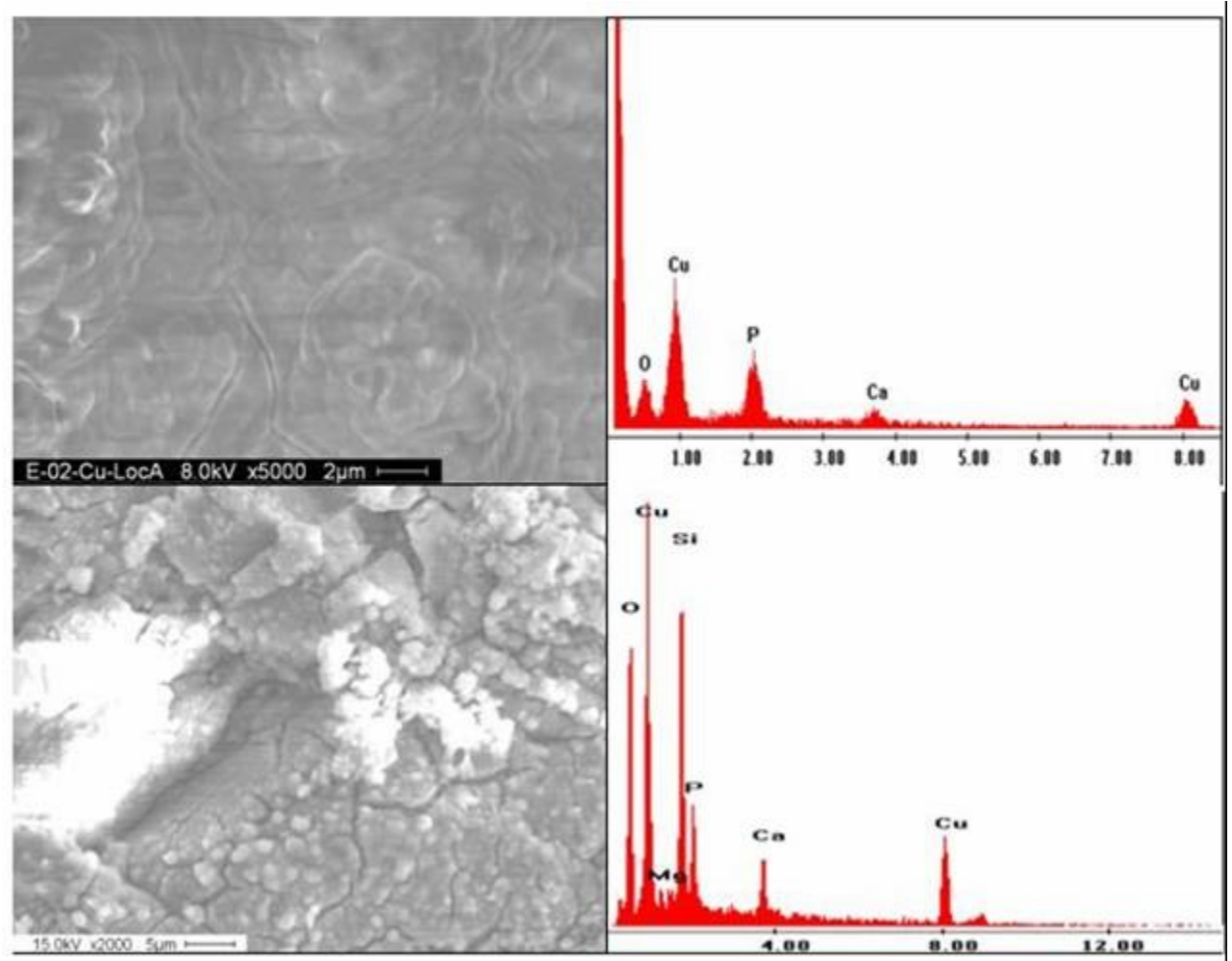
SO_4] and Ponsjakite $[Cu_4(OH)_6SO_4 \cdot nH_2O]$ as the blue-green scales, which were also observed in this work. The mean SO_4/Cl ratio for this data was 1.35 and ranged from 0.53 to 2.22. Evidence of pits mostly in the centre of the blue green scales was also consistently observed with the scales covering the pit in most cases.



Photograph 4.3 Copper electrodes, left OP (1 mg P/L) and right ZOP (2 mg P/L).

The SEM for EN electrodes showed presence of Cu and O with irregular occurrence of Ca and C. The P or Si content of the scales increased with respective dose. The blue green spots are shown in the upper half of Photograph 4.4 and consisted of stacked layers of rounded scale that were analyzed by EDAX and found to consist of Cu, P, Ca and O. The general scale is shown in the bottom half of Photograph 4.4 and appears bright due to the SEM induced charge. EDAX revealed an abundance of lighter elements as O, Si and Ca as shown in the bottom half of Photograph 4.4. Chloride was also detected in some areas. The medium and high doses of electrodes exposed to the P and Si inhibitors had numerous patches wherein the scales appeared harder and crystalline.

EDAX (not shown) showed a higher % of Ca (from 30-60 %) along with P or Si. Thus P at doses of 1 mg/L and above or Si at doses of 6 mg/L SiO₂ appeared to change the scale composition to predominantly to Ca, O, P, Si on a Cu (20-40 %) surface.



Photograph 4.4 SEM & EDAX of electrode exposed to BOP at 1 mg /L of P

For the pH controls EDAX (not shown) revealed the surface composition was higher in Cu (85 %) with significantly less O (6 %) and Ca (4 %) and minor amounts of Si, Cl etc. pH elevation to pHs+0.3 reduced the Cu to about 70 % and increased the O (12

%), Ca (8 %) and Si (6 %) compared to pHs. Hence the data indicate that naturally occurring Si mitigated Cu release. This is consistent with the finding in TBW I (Taylor et al., 2005) wherein an empirical regression model for copper release had negative exponent for Si, and the authors emphasized that Si acted as a natural inhibitor.

The occurrence of blue water has long been recognized and reported previously (Edwards et al., 2000), and a recent study (Letelier et al., 2007) reports the blue-green corrosion products originating from precipitation of Cu compounds as Malachite $[\text{CuCO}_3\text{Cu}(\text{OH})_2]$, Chrysocolla $[(\text{Cu},\text{Al})_2\text{H}_2\text{Si}_2\text{O}_5(\text{OH})_4 \cdot n\text{H}_2\text{O}]$ and Dioptase $[\text{CuSiO}_2(\text{OH})_2]$. The authors (Likelier et al., 2007) concluded that such precipitation can occur even at Cu release as low as 0.2 mg/L. In this work, the presence of blue-green spots on all but one electrode (2 mg P/L ZOP) suggested formation of carbonates and hydrated silicates on the Cu surface. EDAX found P and Si on all electrodes exposed to P and Si inhibition, and the relative fractions increased with respective inhibitor dose. Copper release was inhibited by both P & Si although the chemical compound on the surface was not identified by SEM/EDAX.

4.6.3 Water quality correlations with EN

Confounding of EN parameters was evaluated by regression analysis in order to develop metal release models. No confounding effects were found as the highest correlation (Pearson's R^2) coefficient was 0.292, (LPRCR_{Cu} versus HMCR_{Cu}). The one EN parameter found to be well correlated with water quality was pitting factor (PF) for Cu denoted as PF_{Cu} . The correlation of PF_{Cu} with alkalinity, chlorides, sulfate and temperature was poor at best (Pearson's $R^2 < 0.29$). PF is a ratio of standard deviation of

the ECN instantaneous current over the HDA mean current and hence a high PF_{Cu} represents either a widely varying corrosion rate with a low mean corrosion rate or actual pitting along with a general corrosion rate that is significantly different than zero.

Although PF_{Cu} correlated with water quality, it did not directly correlate well with Cu release. Larson's ratio was modified to include temperature and is shown as Larson's ratio one including temperature effect (LR1T) in Equation 4.1. The data and linear regression of $\log(PF_{Cu})$ versus LR1T is shown in Figure 4.2 for all data. The R^2 is 0.37; however, the p value < 0.001 and $F = 281.8$, which show the trend of the data is statistically significant. This shows that a slight change in LR1T would change PF_{Cu} values considerably since it is on a \log (base 10) scale in Figure 4.2.

$$LR1T = \frac{([SO_4^-] + [Cl^-])}{[HCO_3^-]} \times \frac{Temp}{25} \quad \text{Equation 4.1 LR1T1}$$

where $[]$ = concentration (meq/L)
 LR1T = Larson's ratio one including temperature effect
 Temp = Temperature ($^{\circ}C$)

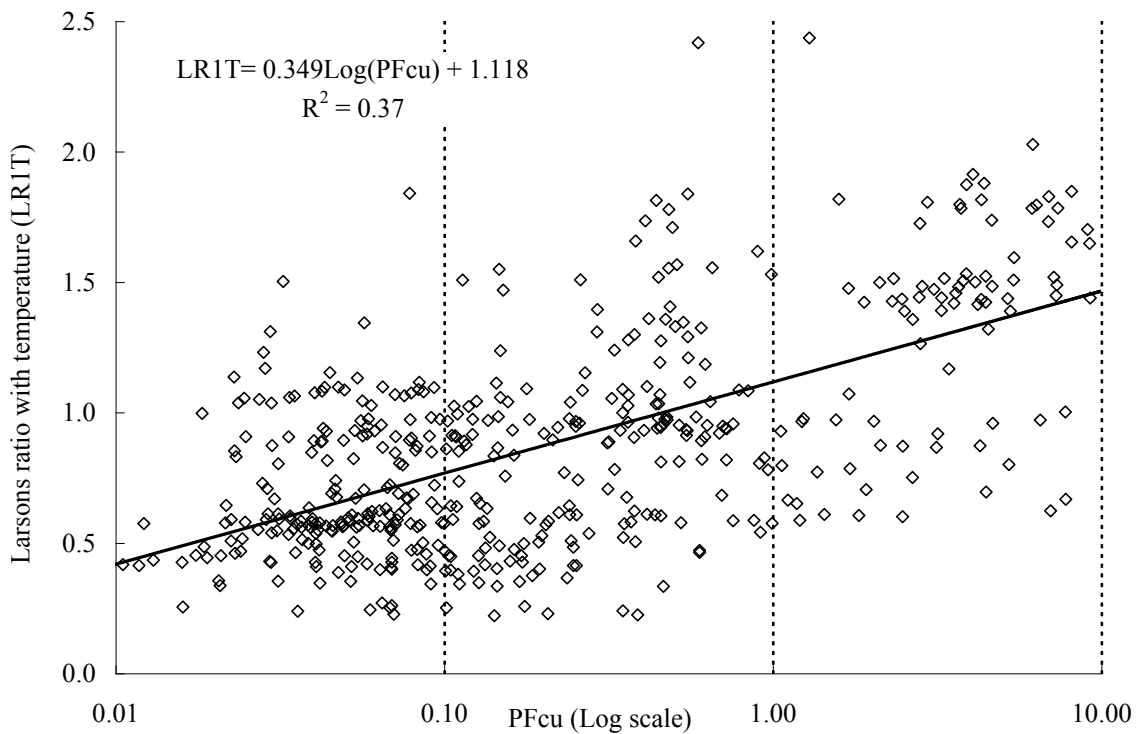


Figure 4.2 PF_{Cu} vs. LRIT for TBW II data

Dissolved oxygen (D.O.) and chlorine residual are oxidants in drinking water. The influent D.O. to the PDSs in this study varied from 6.6 to 10.9 (mg/L), while the PDSs effluent D.O. which was directed to the Cu corrosion loops varied from 4.1 to 10.7. Hence D.O. was not considered to be low or rate limiting for copper release and Cu release was independent of D.O. or chloramine dose or residual for this work. Cu release may have been kinetically limited and not reached equilibrium in the 6 hour stagnation period prior to sampling. From a total of 715 weekly data points for influent chloramine residual from all PDSs, 41 values were from 1.7 to 3.5 mg/L with remaining values from 3.5 to 7 mg/L as Cl_2 . Only two values of PF_{Cu} (0.64, 0.98) exceeded 0.5 in the low residual range where half of the values exceeded 1.0 in the upper residual range. A $PF \ll 1$ is considered to be an indication of a more or less constant general corrosion rate where

as PF consistently approaching one may indicate actual pitting or a widely varying general corrosion (Cottis & Turgoose, 1999; Eden, 1994). PF for all metals monitored was evaluated as per Equation 4.2 and thus both general corrosion and localized corrosion effects are incorporated as PF_{Cu} . Note that PF is not limited to unity since it is the ratio of standard deviation of naturally occurring current to the mean corrosion current from applied alternating current during HDA. The correlation of PF_{Cu} with LR1T and influent chlorine is significant as both parameters were correlated to bulk water quality and can be used to estimate metal release.

$$PF = \frac{\sigma}{(I_{corrHDA})} \quad \text{Equation 4.2 PF}$$

where σ_i = standard deviation of corrosion current density from ECNCR
 $I_{corrHDA}$ = mean corrosion current density from HMCR

4.6.4 Statistical model development

Regression models were developed using EN parameters to predict both total and dissolved copper release. The models used dummy variables to segregate the effect of inhibitor dose by inhibitor type. The effects of the EN parameters and temperature were included in the model without regard to inhibitor type. Models using all 12 EN parameters did not converge. Subsequent modeling attempts using reduced sets of EN parameters eventually produced a model based on LPRCR, HMCR, HMCR and PF. The general form of the EN power model with dummy variables for inhibitor type is shown in Equation 4.3. The remaining 8 EN parameters were added one at a time and are represented by EN^{ai} in Equation 4.3, where EN represents either B, B_a, B_c, PSKW, PKRT, ISKW, IKRT or RSOL. The same approach was used to develop models for both

total and dissolved forms of iron, copper and lead. The dummy variables shown in Equation 4.3 represent the effects of influent concentrations of total phosphate or silicate. The temperature used for all EN models was the average temperature in the flush tanks which supplied water to the EN trailer. The resulting models for total and dissolved copper have the dummy variables abbreviated as DV for convenience, and are shown in Equation 4.4.

$$\begin{aligned}
 Me = & (LPRCR_{Me}^{a1} \times HMCR_{Me}^{a2} \times ECNRCR_{Me}^{a3} \times PF_{Me}^{a4} \times EN_{Me}^{ai}) \\
 & \times (a \times BOP \times TP^f + b \times OP \times TP^g + c \times ZOP \times TP^h \times Zn^i + d \times Si \times SiO_2^j \\
 & + e \times pH_s) \times Temp^o
 \end{aligned}
 \tag{Equation 4.3}$$

(EN model variables)

where	<i>Me</i>	= Cu, mg/L
	<i>a1</i>	= <i>LPRCR_{Me}</i> exponent
	<i>a2</i>	= <i>HMCR_{Me}</i> exponent
	<i>a3</i>	= <i>ECNRCR_{Me}</i> exponent
	<i>a4</i>	= <i>PF_{Me}</i> exponent
	<i>EN_{Me}^{ai}</i>	= One of the terms associated with exponents <i>a5</i> , <i>a6</i> , <i>a7</i> , <i>a8</i> , <i>a9</i> , <i>a10</i> , <i>a11</i> or <i>a12</i>
	<i>a5</i>	= <i>B_{Me}</i> exponent
	<i>a6</i>	= <i>Ba_{Me}</i> exponent
	<i>a7</i>	= <i>Bc_{Me}</i> exponent
	<i>a8</i>	= <i>PSKW_{Me}</i> exponent
	<i>a9</i>	= <i>PKRT_{Me}</i> exponent
	<i>a10</i>	= <i>ISKW_{Me}</i> exponent
	<i>a11</i>	= <i>IKRT_{Me}</i> exponent
	<i>a12</i>	= <i>RSOL_{Me}</i> exponent
	<i>BOP</i>	= BOP inhibitor dummy variable (0, 1)
	<i>OP</i>	= OP inhibitor dummy variable (0, 1)
	<i>ZOP</i>	= ZOP inhibitor dummy variable (0, 1)
	<i>Si</i>	= Silica inhibitor dummy variable (0, 1)
	<i>pH_s</i>	= pH control dummy variable (0, 1)
	<i>TP</i>	= total phosphorus, mg/L
	<i>Zn</i>	= zinc, mg/L
	<i>SiO₂</i>	= silica, mg/L as SiO ₂
	<i>Temp</i>	= Temperature, °C
	<i>a</i>	= BOP dummy variable coefficient
	<i>b</i>	= OP dummy variable coefficient
	<i>c</i>	= ZOP dummy variable coefficient
	<i>d</i>	= Silica dummy variable coefficient
	<i>e</i>	= pH control dummy variable coefficient
	<i>f</i>	= TP exponent associated with BOP dummy variable
	<i>g</i>	= TP exponent associated with OP dummy variable
	<i>h</i>	= TP exponent associated with ZOP dummy variable
	<i>i</i>	= Zn exponent associated with ZOP dummy variable

$$\begin{aligned}
 j &= \text{SiO}_2 \text{ exponent associated with Silica dummy variable} \\
 o &= \text{Temperature exponent} \\
 DV &= (\alpha \times \beta OP \times P^f + \gamma \times \delta P \times P^g + \epsilon \times \zeta OP \times P^h \times \eta^i \\
 &+ \theta \times \iota \times \kappa \times \lambda O_2^j + \rho \times \sigma H_s) \times \tau emp^o
 \end{aligned}
 \tag{Equation 4.4}$$

(Dummy Variables)

where σ_i = standard deviation of corrosion current density from ECNCR
 I_{corrHDA} = mean corrosion current density from HMCR

4.6.5 EN empirical model for copper concentration

The statistically significant ($p < 0.05$) empirical EN models developed for total and dissolved Cu release (TCu & DCu respectively) in this study are shown in Table 4.4. A 3-parameter model based on $LPRCR_{Cu}$, $ECNCR_{Cu}$ and $PKRT_{Cu}$ for TCu release was developed, which has a 0.71 R^2 . Models with either of these parameters do equally well as seen by the very similar R^2 from Table 4.4. LPRCR quantifies general (uniform) corrosion but is inapplicable for localized corrosion while ECNCR is capable of detecting localized (pitting) corrosion. Numerous reactions are expected to occur on a metal surface in drinking water environment. Metal scale formation, oxygen consumption, hydrogen generation, chlorine reduction, biological oxidation and oxidation of metals are examples of reactions that change surface potential (voltage) and result in current flow. This total current flow is measured as ECNCR and hence is not a direct measurement of metal release. Hence ECNCR can over estimate the actual corrosion rate of metal dissolution because ECNCR represents the total current activity on a metal surface. Hence a combination of these two methods obtained by retaining both $LPRCR_{Cu}$ and $ECNCR_{Cu}$ in the regression model was used to provide robust estimate of Cu release. Robust herein implies that the model is likely to account for the effect of general and localized corrosion more accurately than the models using either parameter alone. The

best fit EN model for TCu release shown in bold font in Table 4.4 is presented in its full form in Equation 4.5.

Table 4.4 Copper release EN models

Model	R ²	S.E (mg/L)	Model p value	Parameter** of highest p value	p value**
TCu=(LPRCR _{Cu} ^{a1} *ECNCR _{Cu} ^{a3} * PKRT _{Cu} ^{a9})*DV	0.71	0.18	<1e-4	PKRT _{Cu}	0.002
TCu=(LPRCR _{Cu} ^{a1})*DV	0.71	0.18	<1e-4	LPRCR _{Cu}	<0.0001
TCu=(ECNCR _{Cu} ^{a3})*DV	0.71	0.18	<1e-4	ECNCR _{Cu}	<0.0001
TCu=(PKRT _{Cu} ^{a9})*DV	0.69	0.19	<1e-4	PKRT _{Cu}	<0.0001
TCu=(LPRCR_{Cu}^{a1}*ECNCR_{Cu}^{a3})*DV	0.72	0.18	<1e-4	ECNCR_{Cu}	<0.0001
DCu=(LPRCR_{Cu}^{a1}*ECNCR_{Cu}^{a3})*DV	0.68	0.17	<1e-4	ECNCR_{Cu}	0.002

where * represents multiplication

DV= Dummy Variable terms shown in (2).

S.E is the standard error of prediction.

Bold font indicates model evaluated as the best fit

$$\begin{aligned}
 TCu = & LPRCR_{Cu}^{0.028} \times ECNCR_{Cu}^{0.031} \times 0.510 \times BOP \times TP^{-.116} \\
 & + .476 \times OP \times TP^{-.281} + .471 \times ZOP \times TP^{-.232} \times Zn^{-.048} \\
 & + .960 \times Si \times SiO_2^{-.324} + .505 \times pH_s \times Temp^{-.063}
 \end{aligned}
 \tag{Equation 4.5}$$

(TCu EN model)

where

- TCu = total copper, mg/L
- LPRCR_{Cu} = Corrosion rate from linear polarization for copper (mpy)
- ECNCR_{Cu} = Corrosion rate from electrochemical noise for copper (mpy)
- BOP = BOP inhibitor (0, 1)
- OP = OP inhibitor (0, 1)
- ZOP = ZOP inhibitor (0, 1)
- Si = Silica inhibitor (0, 1)
- pH_s = pH control (0, 1)
- TP = total phosphorus, mg/L as P
- Zn = zinc, mg/L
- SiO₂ = silica, mg/L as SiO₂
- Temp = Temperature, °C

A water quality (WQ) model for TCu release was developed from TBW II study (Taylor et al., 2007) and is presented in Equation 4.6. Alkalinity in Equation 4.6 is represented as Alk (mg/l CaCO₃) and chlorides as Cl (mg/L) and pH is in standard units of $-\text{Log}(\text{H}^+)$; the rest of terms in Equation 4.6 are explained before in (5). The EN model shown in Equation 4.5 indicates that TCu release will increase as LPRCR_{Cu} and ECNCR_{Cu} increase. This model also suggests an increase in phosphate, zinc or silicate from any inhibitor will decrease TCu release as the model exponents for TP, Zn and SiO₂ are negative, which is the same for the WQ Cu release model shown in Equation 4.6. The R² of TCu model by EN shown in Equation 4.5 and by WQ shown in Equation 4.6; were 0.72 and 0.76 respectively. Both models had a similar standard error (S.E) of prediction of 0.18 mg/L. Hence the EN model does equally well as the WQ model.

$$TCu = 6.13BOP \times P^{-.174} + 1.76OP \times P^{-.328} + 5.24ZOP \times P^{-.205} \times Zn^{-.069} + 10.9Si \times SiO_2^{-.214} + 6.7pH_s \times pH^{-.48} \times Alk^{0.569} \times T^{0.394} \quad \text{Equation 4.6}$$

(TCu WQ model)

The temperature exponent for EN model was -0.063, and indicates that Cu release will vary slightly with temperature, but that higher temperature will decrease TCu release. A change in temperature from 10°C to 30°C which was the range in this study would change the temperature effect by the ratio $(30/10)^{-0.063}$ i.e. by 0.93 and decrease the model predicted TCu release at 30°C compared to the release at 10°C by 7 % which is not very significant. Figure 4.3 shows the fit of the TCu model predictions with the actual observations for all phases. A line is indicated on the plot that would represent perfect

agreement between the model predictions and the actual data. The model tends to have a good fit for low Cu concentrations and fits modestly at the higher concentrations of Cu. The model also shows that Cu release is highest for pH control and that the inhibitors evaluated reduced TCu release.

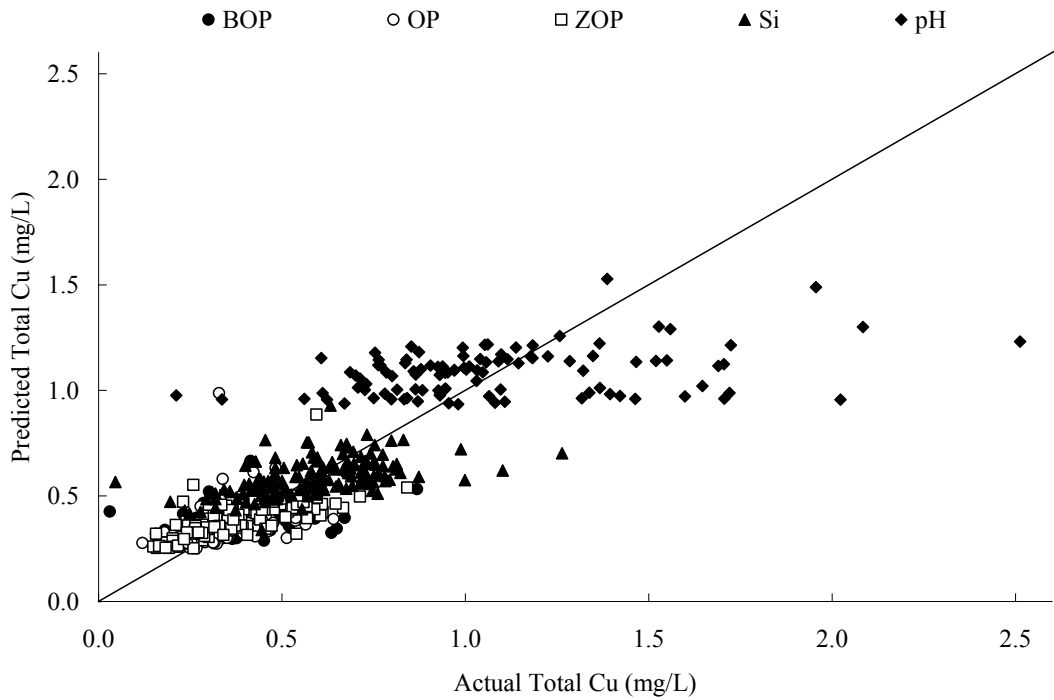


Figure 4.3 EN model predicted versus actual total copper concentration

Similar EN model development was conducted for DCu and the best fit models are also shown in bold font in Table 4.4. The best fit model selected for DCu has the same form as the model selected for TCu release and has both LPRCRCu and ECNCRcu. The observations for DCu release model with inhibitor type or dose are similar to that of the TCu release model. The temperature exponent indicates that higher temperature will lower DCu release; however, Cu release is not practically sensitive to temperature. A change in temperature from 10°C to 30°C would decrease the model

predicted DCu release by 3% which is practically insignificant. The best fit EN model for DCu release in its full form is presented in Equation 4.7 and achieves a reasonable fit between the predictions and the observations. A water quality (WQ) model for DCu release was developed from TBW II study (Taylor et al., 2007) and is presented in Equation 4.8. The R² of DCu model by EN shown in Equation 4.7 and by WQ shown in Equation 4.8; were 0.72 and 0.68 respectively. Both models had a similar standard error (S.E) of prediction of 0.17 mg/L. Hence the EN model does equally well as the WQ model for DCu.

$$\begin{aligned}
 DCu = & (LPRCR_{Cu}^{0.026} * ECNCR_{Cu}^{0.027}) \times 0.406 \times BOP \times TP^{-.107} \\
 & + 1.372 \times OP \times TP^{-.293} + 1.386 \times ZOP \times TP^{-.242} \times Zn^{-.021} \\
 & + .528 \times Si \times SiO_2^{-.320} + .181 \times pH_s \times Temp^{-.028}
 \end{aligned}
 \tag{Equation 4.7}$$

(DCu EN model)

$$\begin{aligned}
 DCu = & 0.302BOP \times P^{-.140} + 1.281OP \times P^{-.338} \\
 & + 1.276ZOP \times P^{-.217} \times Zn^{-.038} + .20Si \times SiO_2^{-.285} + 1.831pH_s \\
 & \times H^{-.48} Alk^{0.713} \times T^{0.421}
 \end{aligned}
 \tag{Equation 4.8}$$

(DCu WQ model)

where DCu = Dissolved copper, mg/L

The EN models provided a reasonable to both TCu and DCu release. A statistical evaluation of EN parameters was done with a view to evaluate the likely difference in behavior of Cu surfaces exposed to pH controls and inhibitors. Likely difference in behavior herein means anodic or cathodic reaction rates or surface film resistance etc. From the available EN data the parameters which can potentially yield such information are I_{corr}, B, B_a and B_c. These represent the corrosion current density, Stearn-Geary

constant, and the anodic and cathodic tafel slopes respectively. Electrochemical corrosion measurements result in corrosion current density values which can be directly correlated to a corrosion rate using the Stern-Geary equation. The corrosion rate (CR) is related to I_{corr} as shown in Equation 4.9. Since the EN models using $LPRCR_{Cu}$ and $ECNCR_{Cu}$ were statistically significant, I_{corr} is expected to show significant differences by inhibitor type and dose. The Stern-Geary constant (B) is derived from ohms law and is related to I_{corr} as shown in Equation 4.10. Hence normalized for the electrode area, I_{corr} increases linearly with B and decreases linearly with R_p , the polarization resistance. Note that Equation 4.10 is a result of application of ohm's law in which voltage is equal to current times resistance, and herein B is equal to I_{corr} times R_p .

$$CR = \frac{K.A}{zF\rho} I_{corr} \quad \text{Equation 4.9}$$

(Corrosion rate)

where CR = corrosion rate; $LPRCR$ or $HMCR$ or $ECNCR$ (mpy)
 A = atomic weight of the metal
 I_{corr} = corrosion current density (Amperes/cm²)
 z = number of electrons transferred per atom of metal corroded
 F = faraday's constant=96,500 coulombs/equivalent
 ρ = density of the metal (g/cm³)
 K = 1.288x10⁵ constant for conversion of units.

$$I_{corr} = \frac{B}{R_p} \quad \text{Equation 4.10}$$

where B = Stern-Geary constant, (Volts)
 I_{corr} = corrosion current density (Amperes/cm²)
 a = area of the electrode (cm²)
 R_p = resistance of the electrodes (ohms).

The stern-geary constant further is derived from the combination of anodic (B_a) and cathodic (B_c) tafel slopes as shown in Equation 4.11. Tafel slopes represent the slope of the linear response between $\text{Log}(I_{corr})$ and potential E (volts) for uniform corrosion. B_a

represents metal dissolution reaction rate and B_c represents the cathodic reaction rate. An increase in either of the tafel slopes reduces B and hence also reduces I_{corr} . For the numerous simultaneous anodic and cathodic reactions which are expected to occur in drinking water the tafel slopes represent the overall effect of these reactions considered simultaneously. If corrosion bears a direct relationship with Cu release then a lowest possible I_{corr} is desired. Hence as large as possible values are desired for B_a , B_c and R_p while as small as possible values are desired for B . Note the relationships presented above are valid only for uniform corrosion and not for localized corrosion.

$$B = \frac{B_a \cdot B_c}{(B_a + B_c)} \quad \text{Equation 4.11}$$

The comparison of B , B_a and B_c of each corrosion control strategy i.e. inhibitor addition either showed no significant difference in values or the difference was inconsistently observed. Inconsistency is referred to as observing the Stearn-Geary (B) of an inhibitor dosed PDS smaller than that of pH_s for some phases but not all phases. Out of 12 comparisons for B only 4 were significantly smaller than that for pH_s and were observed for 0.5 and 2.0 mg P/L BOP, 2.0 mg P/L OP, and 0.5 mg P/L ZOP. Out of 12 comparisons each for B_a and B_c 4 were actually significantly smaller than that for pH_s and were observed for 2.0 mg P/L BOP, 1.0 mg P/L OP, 0.5 and 2.0 mg P/L ZOP. Comparisons of I_{corr} from all other PDSs with that of pH_s revealed that the latter had a consistent higher I_{corr} , which was statistically significant. Table 4.5 presents the average I_{corr} from both LPRCR and ECNCR of all but pH_s PDS. The average I_{corr} from pH_s for LPRCR was 0.158 and for ECNCR was 35.9 $\mu\text{A}/\text{cm}^2$. Since the data was not normally

distributed an ANOVA on ranks was used for all comparison with pH_s. The test used was Wilcoxon signed rank test. The Wilcoxon test statistic W is computed by ranking all the differences before and after the treatment based on their absolute value, then attaching the signs of the difference to the corresponding ranks. The signed ranks are summed and compared. If the absolute value of W is "large", then there was a treatment effect (i.e., the ranks tend to have the same sign, so there is a statistically significant difference before and after the treatment).

Table 4.5 Corrosion current density (I_{corr}) comparison from LPR for Cu

PDS #	I_{corr} (LPRCR) of PDS	I_{corr} (ECNCR) of PDS 13	LPRCR < LPRCR PDS 13 p<0.05	ECNCR < ECNCR PDS 13 p<0.05
1	0.062	21.5	Y	Y
2	0.035	4.3	Y	Y
3	0.007	11.1	Y	Y
4	0.075	89.5	Y	N*
5	0.048	14.0	Y	Y
6	0.033	4.2	Y	Y
7	0.030	1.8	Y	Y
8	0.012	1.0	Y	Y
9	0.011	49.8	Y	N*
10	0.084	1.8	Y	Y
11	0.061	3.0	Y	Y
12	0.022	4.7	Y	Y
14	0.005	0.9	Y	Y

LPRCR I_{corr} values for all PDSs were consistently lower than that from pH_s. The values also decreased consistently with increasing dose i.e. I_{corr} decreased from PDS 1 to 3 for BOP, 4 to 6 for OP, 7 to 9 for ZOP and 10 to 12 for Si. The comparisons were statistically significant at 95 % confidence. Similar comparison of I_{corr} from ECNCR showed I_{corr} of all but 0.5 mg P/L OP (PDS 4) and 2.0 mg P/L ZOP (PDS 9) was less than

that of I_{corr} of pH_s . The I_{corr} (ECNCR) from these two PDSs was statistically greater than from pH_s . These comparisons show that I_{corr} correlates with Cu release where as no correlation was observed for tafel slopes or Stearn-Geary constant. Hence redox reaction rates for corrosion inhibitors were demonstrated not be significantly different than that for pH_s . In reference to Equation 4.10 this implies that the polarization resistance R_p consistently increased with inhibitor dose and correlated with Cu release for all inhibitors. Therefore inhibitor action is through the formation of some scale or film which increases the overall resistance for Cu for both corrosion and actual corrosion product release.

4.6.6 Advantages of EN in estimating copper release.

EN parameters can be used in the same way as water quality parameters as they are descriptive of general redox water quality. The data presented herein suggests that EN works well for estimating Cu release for a wide variety of water quality and corrosion inhibitor types and gave similar results as the water quality models developed from this study. Cu release in real systems is expected to be correlated with EN since this data was obtained at a pilot field facility which incorporated the effects of temperature variation, season variation in finished blends of GW, SW and RO, and influent water quality variations as chlorine residual, inhibitor dose etc. The short time frames of measurement of EN parameters over traditional water quality monitoring makes EN advantageous due to reduced time and labor, and offers timely corrosion monitoring and proactive actions at remote locations throughout the distribution system.

4.7 Conclusions

- EN like water quality is a global measurement, and measures the corrosion current which represents electron transfers due to all oxidation reactions on a metal surface, without regard to whether metal is released to the water or incorporated in an oxidized scale. However as water quality has been related to copper release, EN can also be related as well to copper release and used to proactively minimize copper violations of the Lead and Copper Rule.
- EN monitoring is significantly faster and less labor intensive relative to traditional water quality monitoring. Cu corrosion was found to manifest itself from both general and localized corrosion. However, general corrosion was more important for dissolved copper release, which was the predominant form in this study.
- EN regression models using $LPRCR_{Cu}$ and $ECNCR_{Cu}$ and influent inhibitor dose provided a reasonable fit to total (TCu) and dissolved (DCu) copper release with a R^2 of 0.72 and 0.68 respectively. The EN models without inhibitor dose had a similar R^2 (0.67 for total and 0.65 for dissolved) which suggests that EN correlated with Cu release and EN parameters were sensitive to inhibitor type but not to inhibitor dose. PF_{Cu} was the only EN parameter which consistently correlated with water quality. Water quality parameters considered in this study included alkalinity, chlorides, sulfate, influent chloramine residual and temperature. Temperature effects on TCu and DCu release were negligible for this study.

4.8 Recommendations

- EN monitoring should be used in actual distribution systems to verify and manage metal release. Monitoring periods of a few weeks may be sufficient to establish a baseline for correlation between EN and Cu release.
- The use of EN at field scale to measure corrosion parameters and correlate with Cu release must be undertaken to encompass a wider range of water quality parameters than used in this study. This would include low (<80 as CaCO₃) and high (>175) alkalinity waters, low pH (<7.4) waters, waters not at equilibrium with CaCO₃ (pH<pH_s), use of lower doses of phosphates (<0.5 mg/L P) and the effect of water velocity on both monitoring of Cu corrosion rates and their correlation with Cu release. This would help in extending application of EN monitoring which is a real-time, remote access technology to proactively identify the potential of adverse Cu release.

4.9 Acknowledgements

The University of Central Florida (UCF) and UCF project team wish to express their sincere gratitude to Tampa Bay Water (TBW); Hillsborough County, Fla.; Pasco County, Fla.; Pinellas County, Fla.; City of New Port Richey, Fla.; City of St. Petersburg, Fla.; and City of Tampa, Fla. which are the Member Governments of TBW and the American Water Works Association Research Foundation (AwwaRF) for their support and funding for this project. Special thanks to, Robert M. Powell the Pinellas County, Fla. Director of Laboratory and Pick Tally the Pinellas County, Fla. Director of Utilities for their support and grant for EN research; Christine Owen the Water Quality Assurance

Officer for TBW and also the TCP project coordinator for her endless support and coordination of all UCF project related activities; Roy Martinez the AwwaRF Project Officer for his continuous support and assistance in proposing, conducting and reporting and all other activities associated with the project, members of the project advisory committee (PAC) notably Jonathan Clement PhD, P.E. Black Veatch Engineers, Koby Cohen, VP Quality Assurance Suburban Water Systems and Bruce Johnson, Assistant Director of Utilities, Tucson AZ. This paper is dedicated to the late Dennis A. Marshall, who passed away in June 2007. Dennis was a dedicated Pinellas county Fla. employee who significantly contributed to the implementation of both TBW projects

4.10 References

1. Cottis .R and Turgoose .S, 1999. Electrochemical impedance and noise. NACE international. Corrosion testing made easy. ISBN 1-57590-093-9.
2. Drogowska M, Brossard L and Ménard H. 1992. Copper Dissolution in NaHCO_3 and $\text{NaHCO}_3 + \text{NaCl}$ aqueous solutions at pH 8. J. Electrochem. Soc. 139(1).
3. Duranceau, S.J., D. Townley, and G.E.C. Bell. 2004. Optimizing Corrosion Control in Water Distribution Systems. Denver, Colo. American Water Works Association Research Foundation (AwwaRF).
4. Eden D.A 1994. Comments on: Electrochemical noise analysis of iron exposed to NaCl solutions of different conductivity. Journal of Electrochemical Society. 141(5), 1402-1404.
5. Edwards M, Himdi L and Gladewell D. 2002. Phosphate inhibition of soluble corrosion-byproduct release. Corrosion science. 44(5), 1057.
6. Edwards M, McNeill L.S, Holm T.R and Lawrence M.C. 2001. Role of phosphate inhibitors in mitigating lead and copper corrosion. American Water Works Association (AWWA) and AWWA Research Foundation, Denver CO.
7. Edwards M, Jacobs S and Taylor R. 2000. The blue water phenomenon. American Water Works Association Journal. 92(7), 72-82.
8. Edwards M, Schock M. Rand Meyer T.E. 1996. Alkalinity, pH, and copper corrosion by-product release. American Water Works Association Journal. 88(3), 81-94.
9. Edwards M, Meyer T. and Rehring J. 1994. Effect of selected anions on copper corrosion rates. American Water Works Association Journal. 86(12), 73-81.

10. Feng Y, Teo W.K, Siow K.S, Tan K.L and Hsieh A.K. 1996 a. The corrosion behaviour of copper in neutral tap water. Part I: Corrosion mechanisms. *Corrosion science*. 38(3), 369-385.
11. Feng Y, Teo W.K, Siow K.S, Tan K.L and Hsieh A.K. 1996 b. The corrosion behaviour of copper in neutral tap water. Part II: Determination of corrosion rates. *Corrosion science*. 38(3), 387-395.
12. Letelier M.V, Lagos G.E and Reyes A. 2007. Chemical characterization of blue stains in domestic fixtures in contact with drinking water. *Environmental monitoring assessment*. DOI 10.1007/s10661-007-9836-6. Springer science.
13. Lytle D.A and Payne J.M. 2004. U.S Environmental Protection Agency, ORD, NRMRL, WSWRD, TTEB. Cincinnati Ohio-45268. Non-Uniform copper corrosion: Research update. Installation, condition assessment, and reliability of service lines, connections and fittings. AWWA Research Foundation, Denver CO. #2927 project meeting.
14. Monticelli C, Fonsati M, Meszaros G, and Trabanelia G. 1999. Copper corrosion in industrial waters a multimethod analysis. *Journal of the Electrochemical Society*. 146(4) 1386-1391.
15. Qiu J and Dvorak B.I. 2004. The impact of phosphate treatment on copper corrosion in two Nebraska public water supply systems. *Proceeding of 2004 AWWA WQTC*, San Antonio TX.
16. Riber S. 1989. Copper plumbing surfaces: An electrochemical study. *American Water Works Association Journal*. 81(7), 114-122.
17. Royuela J.J and Otero E. 1993. The assessment of short term data on pipe corrosion in drinking water-II Copper. *Corrosion Science*. 34(10) 1595-1606.
18. SDWA (Safe Drinking Water Act), 1991. 40 CFR 141 & 142. *Fed. Reg.*, 56:110, June 7. ERIC Clearinghouse, Columbus, Ohio.
19. Taylor, J.S., J.D. Dietz, A.A. Randall, C.D. Norris, A. Alshehri, J. Arevalo, X. Guan, P. Lintereur, D. MacNevin, E. Stone, R. Vaidya, B. Zhao, S. Glatthorn and A. Shekhar. 2007. Control of distribution system water quality in a changing water quality environment using inhibitors. Draft final report submitted to AWWA Research Foundation Denver CO and Tampa Bay Water. (TBW II report)
20. Taylor, J.S., J.D. Dietz, A.A. Randall, S.K. Hong, C.D. Norris, L.A. Mulford, J.M. Arevalo, S. Imran, M. Le Puil, S. Liu, I. Mutoti, J. Tang, W. Xiao, C. Cullen, R. Heaviside, A. Mehta, M. Patel, F. Vasquez, and D. Webb. 2005. Effects of Blending on Distribution System Water Quality. AWWA Research Foundation Denver CO and Tampa Bay Water. (TBW I report)
21. Zhang X, Pehkonen S, Kocherginsky N and Ellis G.A. 2002. Copper corrosion in mildly alkaline water with the disinfectant monochloramine. *Corrosion Science*. 44(11) 2507-2528

¹ SmartCET is the commercial name of the EN equipment used to monitor corrosion parameters in this study. SmartCET is made by InterCorr international, Houston Texas 77014.

5 MODELING TRANSIENT Cu RELEASE IN DRINKING WATER

ABSTRACT

The corrosion rates from electrochemical corrosion monitoring (EN) were correlated with Copper (Cu) release in a changing water quality environment in a one year pilot study. Transient Cu release models were developed from actual metal release and time called as water quality (WQ) models; and from EN parameters and time called as EN models. A first order kinetic rate incorporating temperature effect gave the best fit for WQ models and $LPRCR_{Cu}$ and time gave the best-fit for the EN models. Both models predicted a response time of about 90 days to reach a concentration of about 62 to 82 % of the steady state concentration; however the EN models were found to provide a better fit. Utilities can use EN due to its rapid response and less labor relative to traditional water quality monitoring to identify and mitigate adverse Cu release due to water quality changes.

5.1 Introduction

5.1.1 Background

The impacts of new source waters and their blends on water quality changes were evaluated (Taylor et al., 2005) under a tailored collaboration project (TCP) conducted by the University of Central Florida (UCF) and funded by TBW and AwwaRF. This TCP called TBW I identified the most significant controlling parameters within the variation

of water quality expected in the MG distribution systems as alkalinity, sulfates and chlorides. In this follow up one-year TCP called TBW II, the effect of corrosion inhibitors to mitigate adverse impacts in distribution systems that receive blended finished waters produced from ground, surface and saline sources was investigated. This TCP had the objective of investigating the best available inhibitors for maintaining acceptable water quality in the Tampa Bay Water (TBW) and member government (MG) distribution systems. Four different corrosion inhibitors were selected and added to the PDS system: blended ortho-phosphate (BOP), ortho-phosphate (OP), zinc ortho-phosphate (ZOP), and silicate (Si). Each phosphate based inhibitor was studied at three doses: 0.5, 1, and 2 mg/L as P for all the phosphate type inhibitors. The silicate inhibitor was applied as 3, 6, and 12 mg/L as SiO₂.

5.1.2 Literature on transient Cu release

The random variations in potential (volts) and current (amperes) during a corrosion process are termed as noise (Cottis & Turgoose, 1999). EN is based on the theory that different kinds of noise can give important information about corrosion processes. EN generally consists of low frequency (<1 Hz) and amplitude (0.1μV-10mV and 1 nA/cm² to 10μA/cm²) signals spontaneously generated by electrochemical reactions on corroding or other surfaces. Copper corrosion has been correlated with water quality in drinking water environment using simulated tap/drinking water (Edwards et al., 2002, 2001, 2000) and in full scale systems recently by Qiu and Dvorak (2004). EN has been used to monitor Cu corrosion in industrial process systems (Monticelli et al., 1999), simulated drinking water (Zang et al., 2002; Edwards et al., 1996 & 1994; Feng et al.,

1996 a & b; Royuela & Otero, 1993; Drogowska et al., 1992; Riber 1989), and more recently in full scale systems (Duranceau et al., 2004). However, relatively few or no studies have been conducted to understand transition from one steady state to another steady state.

Taylor et al., (2005) presented transient Cu models developed from the TBW I study. The models indicated that Cu release during water quality changes i.e. transient release could be fitted with a first order exponential model with metal release increasing or decreasing exponentially with time. The first order decay rate constant (k) for waters without inhibitors for TCu was 0.071 day^{-1} . The time to achieve 95 % of the steady-state concentration following a steady water quality change for Tcu was 42 days.

The rate limiting process controlling the corrosion rate of copper is the diffusion of copper ions through the oxide film given the different water quality conditions under which corrosion film development can occur in real distribution systems (Feng et al., 1996). In an effort to evaluate the short-term response (60 minutes) of chlorides and sulfates on aged copper specimens, Stone et al., (1987) found that, both increased copper corrosion and the effect of chlorides was greater than that of sulfates. The authors also showed that the corrosion rate of aged copper specimens decreased by approximately 55% as pH increased from 6 to 8 and increased by 50% with the increase in temperature from 10°C to 25°C . However, Broo, Berghult and Hedberg (1998) reported that chloride ions greatly affect the kinetics of corrosion process by retarding the oxidation of Cu (I) in natural waters (lowering corrosion rates) and can be helpful on a long-term basis.

Using coupon tests the authors found that total copper release in a drinking water environment was kinetically controlled and that the total copper released depended on

water quality. Pisigan and Singley (1987) stated that “For waters with sufficient buffering capacity the addition of chemicals for boosting alkalinity may reduce corrosion as enhanced corrosion of copper may result due to the increased ionic strength and conductivity”. However, two studies performed by Pisigan and Singley (1987) reported bicarbonate had little or no effect on initial rates of copper corrosion. Adverse effect of alkalinity for copper release is sensitive to pH and copper release increases with alkalinity as pH decreases (Taylor et al., 2005; Edwards et al., 1996 & 1994).

Chlorides and sulfates have been shown to have opposing effects on corrosion rates of aged copper surfaces (Edwards et al., 1994), in that chlorides tend to decrease where as sulfates tend to increase copper corrosion rates. The author’s report that aging resulted in a decrease in anodic reaction rate in the presence of higher chlorides at a pH of 8.5; and both anodic and cathodic reactions were increased (catalyzed) by sulfates at a pH of 7. Bicarbonate ions increased corrosion rates upon aging at a pH of 7.0, but passivated the copper surface at a pH of 8.5.

5.2 Materials and methods

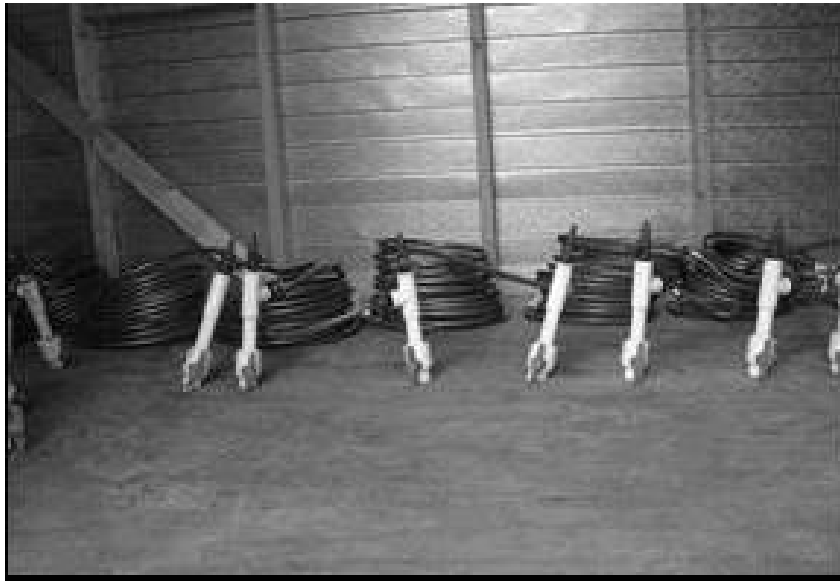
5.2.1 Field facility

The facility was built in 2001 and consists of pilot distribution systems (PDSs), copper loops, cradles and treatment processes to obtain finished waters. To maintain integrity of the system, finished GW was fed to the PDSs and copper loops when the facility was not used after TBW I and before start of this study. The PDSs were constructed of aged pipes that were obtained from existing utility distribution systems to

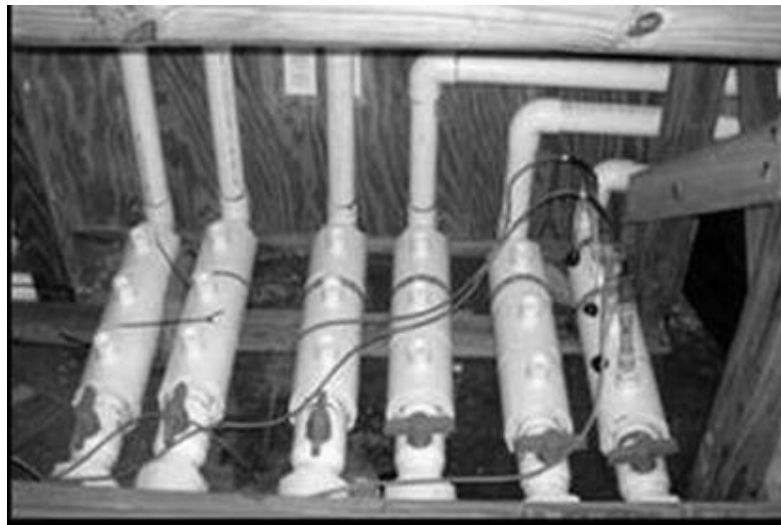
represent the pipe materials used in the TBW Member Government's distribution systems. A complete description of PDSs is given elsewhere (Taylor et al., 2005).

The effluent from the PDSs was split in two parts; one part was directed to the copper corrosion loops shown in Photograph 5.1 which were housed inside a shed. The other part was directed to the Electrochemical Noise Trailer. The Cu EN probes and corrosion coupons were housed in 4 inch diameter PVC pipes that were located in the EN trailer. These PVC pipes were referred to as Nadles. EN probes were used to monitor corrosion rates of Fe, Cu & Pb-Sn. The probes were placed with the more noble metal upstream (Cu>Fe>Pb-Sn) to minimize any galvanic corrosion from particulate release and subsequent deposition on the downstream metal. The corrosion loop consisted of 30 feet (9.1 m) copper tubing with a diameter of 1.6 cm (5/8 inch), which could hold approximately 1.8 L of water. All other fittings and materials were PVC or other plastic polymers. The electrodes and coupons in Nadles were new where as the copper corrosion loops were old in that they have been continuously wetted since 2001.

Photograph 5.2 shows the connection of a typical EN probe in a Nadle. The probes were placed with the more noble metal upstream i.e. (Cu>Fe>Pb) to minimize any galvanic corrosion due to possible particulate release and subsequent deposition on the downstream metal. All coupons and electrodes were of grade CDA 110 ETP for Cu (UNS # C11000) obtained directly from a manufacturer.¹



Photograph 5.1 Copper corrosion loops



Photograph 5.2 EN probe connection in Nadle

5.2.2 Electrochemical corrosion rate measurement

Corrosion data was collected continuously for at least a 6 hour standing period to correlate with samples taken for Cu from the corrosion loops. Each EN probe had three

Cu electrodes. All electrodes had an area of 4.67 cm^2 (0.72 in^2) each, atomic weight of 63.54 and a density of 8.89 g/cm^3 . Electrodes were numbered sequentially as A, B, and C on the probe body for identification. EN monitoring was conducted using commercially available equipment² which monitored corrosion rates continuously, with cycles of 430 seconds. Within each cycle 300 seconds were used for electrochemical noise (ECN), 100 seconds for linear polarization resistance (LPR), and 30 seconds for harmonic distortion analysis (HDA). The corrosion rates from these three techniques are abbreviated as ECNCR, LPRCR and HMCR respectively and are reported in units of mils/yr, mpy (1 mpy = 0.0254 mm/yr).

5.2.3 Operation

This project was divided into 4 phases; each of three months duration started from February 2006. All PDSs received the same blend composition for a three month period or phase. At the end of each three month period the blend composition was changed. The average water quality of the blends is shown by phase in Table 5.1 and average inhibitor doses used by PDS and phase are shown in Table 5.2. Similar blends were used during phases I and III to evaluate the effect of seasonal conditions on the PDS. The individual sources were chloraminated to produce a residual of approximately 4.5 to 5.0 mg/L, and additions were made to the blend to maintain the desired combined monochloramine residual of about 5 mg/L. The target doses of the inhibitors were defined as: 0.5, 1.0, and 2.0 mg/L as P for the phosphorus-based inhibitors and 10, 20, and 40 mg/L as SiO_2 above the background concentration for the silicate-based inhibitor. After 1 month of operation,

the doses of the silicate inhibitor had to be changed to 3, 6, and 12 mg/L because the 20 and 40 mg/L doses were causing CaCO₃ precipitation within the PDS.

Table 5.1 TBW II Water quality by phase

Parameter	Project Minimum	Project Maximum	Phase I	Phase II	Phase III	Phase IV
Alkalinity (mg/L as CaCO ₃)	84	175	163	109	154	127
Calcium (mg/L as CaCO ₃)	54	220	202	105	206	168
Dissolved Oxygen (mg/L)	6.6	10.9	8.7	8	8	9.1
Chloride (mg/L)	35	123	47	59	65	56
pH	7.4	9.1	7.9	7.9	7.9	7.8
Silica (mg/L)	4	65.0*	10.9	5.1	10.2	6.4
Sulfate (mg/L)	52	119	72	112	74	85
Sodium (mg/L)	5	53	7	37	40	32
TDS (mg/L)	338	436	365	388	413	378
Temperature (°C)	10.4	29.7	21.2	25.5	24.7	19.6
Total Phosphorus (mg/L as P)	0	3.36*	0.2	0	0	0.1
UV-254 (cm ⁻¹)	0.007	0.105	0.071	0.069	0.077	0.063
Zinc (mg/L)	0.001	0.793	0.031	0.023	0.04	0.037

* denotes due to inhibitor addition
Average values for each Phase shown

Table 5.2 TBW II Average inhibitor doses

Inhibitor	BOP	BOP	BOP	OP	OP	OP	ZOP	ZOP	ZOP	Si*	Si*	Si*
PDS #	1	2	3	4	5	6	7	8	9	10	11	12
Phase I Dose	0.58	1.08	1.82	0.5	1	1.8	0.65	0.99	1.76	2.81	6.33	11.66
Phase II Dose	0.57	1	1.95	0.6	0.9	1.9	0.54	0.89	1.77	2.69	6.57	12.06
Phase III Dose	0.49	0.9	1.73	0.5	1	1.9	0.49	0.88	1.82	2.79	6.54	12.05
Phase IV Dose	0.68	1.31	2.66	0.5	0.8	1.7	0.46	0.88	1.58	2.95	6.79	11.39

The corrosion loops were flushed with 2 gallons (7.6 L) of water every morning. The effluent of the copper loops was monitored regularly for Cu release. The sampling followed the conditions applicable as per the Lead and Copper Rule (U.S. EPA 1991). Samples were usually taken weekly with extra samples taken when needed for specific purposes. To sample the copper loops, a first draw 1 liter sample was collected after six hours of water stagnation, shaken to mix completely, and then 125 ml of it was used for metal measurements. The Nadles were flushed daily and before each monitoring event with 5 pipe volumes of water at an average velocity of 1 ft/s (0.3 m/s). The equipment connection to the EN probes was switched manually between the Nadles twice a day to obtain data from all 14 Nadles in a week. EN monitoring was conducted typically for 6 hours and 18 hours in two different Nadles per day to complete all 14 Nadles in a week. This EN data was averaged and paired with weekly water quality data taken by grab samples.

5.2.4 Quality assurance & control

Samples were collected and analyzed in the field and at the UCF laboratory. Quality assurance and quality control of both the laboratory and field determinations of water quality parameters was established by duplicating analyses of at least 10% of the samples. Blind duplicates and spikes were also used to determine the accuracy of measurements. Dynamic control charts were used to determine whether the results were acceptable. A comprehensive overview of quality control procedures, analytical results and supplementary discussion of associated PDS sampling events and process sampling events over the duration of this entire project is given elsewhere (Taylor et al., 2007).

5.3 Results and discussion

5.3.1 Corrosion rates with stagnation time

The influent D.O to the PDSs in this study was high and varied from 6.6 to 10.9 (mg/L), while the PDSs effluent D.O which was directed to the Cu corrosion loops varied from 4.1 to 10.7. Hence D.O was not considered to be low or rate limiting for copper release. Cu release did not show a direct relationship with either the D.O levels or with the PDS influent chlorine dose (chloramine). This is attributed to the sampling method of 6 hour stagnations; where in the copper release is kinetically limited and does not achieve the equilibrium concentration with bulk water.

Cu corrosion rate data was sorted by PDS and Phase. Average values of each of the corrosion rates viz. LPRCR, HMCR and ECNCR were evaluated for Cu for each individual PDS for each monitoring event (total 715) over the year. These average values were cumulative averages by stagnation time, thus a 2 hour stagnation time uses first 2

hours of corrosion rate where as 3 hour also includes the third hour in addition to the first two hours. Data was generally available for a 6 hour or 18 hour stagnation period in a day and a few random observations included corrosion data from stagnation up to 24 hours. Multicomparisons were made to compare if any of the corrosion rates differed by stagnation time for any of the PDS. The actual comparisons made for each of the three corrosion rates for the entire data from one year is 8144, of which about 3258 were for stagnation up to 6 hours and 4886 for stagnation from 6 to 18 hours. These represent approximately 58 comparisons for each PDS for each stagnation time up to 6 hours, and about 29 comparisons for each PDS for each stagnation time from 6 to 18 hours.

Figure 5.1 shows the results of the multicomparisons with x axis showing the difference in $LPRCR_{Cu}$ (mpy) for any stagnation time with that at 6 hours and y axis showing the stagnation time compared with 6 hour stagnation as (time-6). The dotted line shows the 95 % confidence interval (C.I) in that it compares data from each PDS for each monitoring event of the year by stagnation time, against that at 6 hours stagnation and hence is a simultaneous C.I. The bold dot represents the mean corrosion rate which is the average of all PDSs. The data indicate no statistical difference at 95 % confidence between $LPRCR$ corrosion rates with stagnation time. This is shown in Figure 5.1 by the overlap in all the simultaneous C.I's; hence $LPRCR_{Cu}$ did not vary significantly with stagnation time.

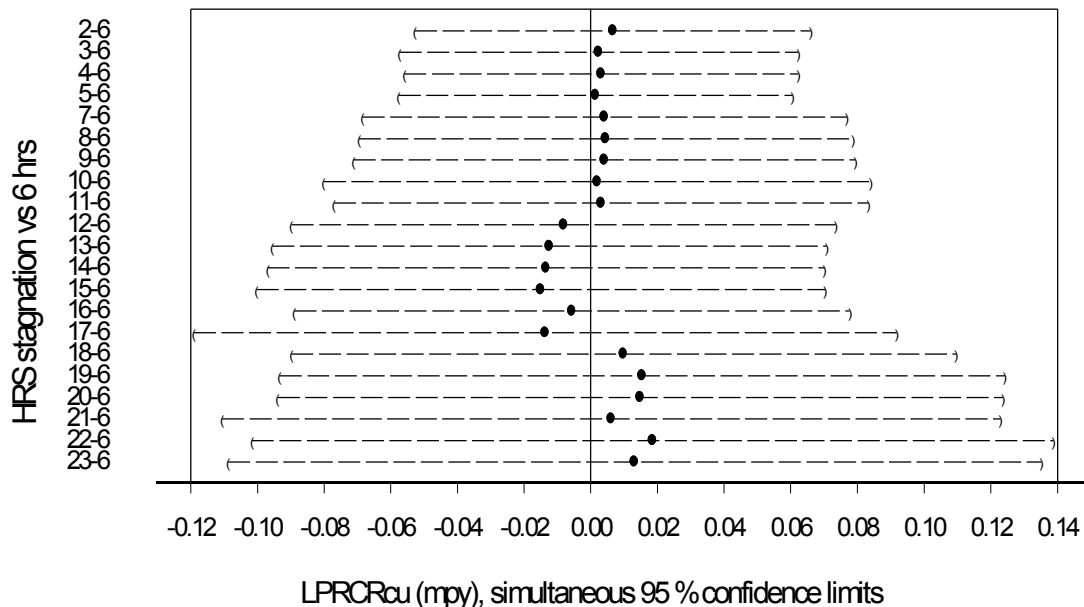


Figure 5.1 Comparison of LPRCR_{Cu} with stagnation time

Similar observations were also made for HMCR_{Cu} and ECNCR_{Cu} for Cu. This showed that corrosion rates for this study did not vary with time period up to 18 hours stagnation and hence it is unlikely that they were limited by the diffusion of oxygen or chlorine. The models developed from this study hence included the cumulative averaged 6 hour EN parameters including corrosion rates.

5.3.2 Cu corrosion rates

The output from the EN equipment2 used consists of 12 parameters which are shown in Table 5.3. Table 5.4 presents corrosion rate from all the three methods used, averaged for all inhibitors and pH controls. The data shows that corrosion rates from LPRCR and HMCR tended to be of the same magnitude while that from ECNCR tended to be much higher. Similarly LPRCR and HMCR from pH controls tended to be similar to the values from inhibitors while ECNCR for the inhibitors tended to be much larger

than that from pH controls. Corrosion rates for individual inhibitor doses followed this generic trend. TBW II data is consistent with the findings of Duranceau et al., (2004) that corrosion rates (ECNCR) may increase when inhibitors are used.

Table 5.3 Output parameters from electrochemical noise monitoring

Symbol	Parameter name	mpy
LPRCR	Linear Polarization Resistance Corrosion Rate	mpy
HMCR	Harmonic Distortion Analysis Corrosion Rate	mpy
ECNCR	Electrochemical Noise Corrosion Rate	mpy
PF	Pitting Factor- evaluated from electrochemical noise & harmonic distortion analysis	-
<i>B</i>	Stearn Geary constant -evaluated from the Harmonic Distortion Analysis	Volts
<i>Ba</i>	Anodic tafel slope	Volts/decade
<i>Bc</i>	Cathodic tafel slope	Volts/decade
PSKW	Skew of potential	-
PKRT	Kurtosis of the potential	-
ISKW	Skew of current	-
IKRT	Kurtosis of the current	-
RSOL	Solution resistance	ohms

Table 5.4 Summary of water quality and Cu corrosion rates from various studies

Method for corrosion rate (mpy)	Phase I	Phase II	Phase III	Phase IV
LPRCR _{Cu} control	0.13	0.11	0.13	0.1
HMCR _{Cu} control	0.15	0.32	0.27	0.38
ECNCR _{Cu} control	0.69	0.89	1.16	0.47
LPRCR _{Cu} inhibitors	0.16	0.07	0.15	0.06
HMCR _{Cu} inhibitors	0.24	0.32	0.27	0.38
ECNCR _{Cu} inhibitors	4.4	23.17	23.71	12.32

In review of the observations of Duranceau et al., (2004) it is obvious that numerous reactions are expected to occur on a metal surface in drinking water environment. Metal scale formation, oxygen consumption, hydrogen generation, chlorine reduction, biological oxidation etc are examples of reactions that change surface potential (voltage) and result in current flow, which generates electrochemical noise (ECN) but are not direct measurements of Cu release. Hence ECNCR can over estimate the actual corrosion rate of metal dissolution because ECNCR represents the total current activity on a metal surface. The Correlation amongst the EN parameters was evaluated for possible confounding effects with simultaneous use of such parameters. No confounding effect was anticipated for copper EN parameters and the highest correlation (Pearson's R^2) was 0.292 between $LPRCR_{Cu}$ and $HMCR_{Cu}$; hence EN parameters may be used in regression models as independent variables.

5.3.3 Development of transient Cu release models

Variation of water quality was achieved by blending finished GW, SW and RO. Phase I & III water quality was typical of high GW blends, and had high alkalinity, low chloride and low sulfate. Phase II had a higher SW and hence sulfate were relatively higher, and alkalinity and chlorides were lower, the Phase IV blend had a relative higher fraction of RO finished water, which had relatively higher chlorides, lower sulfates and moderate alkalinity. The actual variation in phase water quality was 84 mg/L-175 mg/L as $CaCO_3$ alkalinity, 35.4 mg/L to 122.9 mg/L Cl and 136 mg/L-252 mg/L as $CaCO_3$ total hardness. Maximum cooper release was observed in the pHs PDS. All other corrosion control strategies: pHs_{+0.3}, BOP, OP and ZOP at 0.5, 1.0 and 2.0 mg/L as P and

SiO₂ at 3.0, 6.0 or 12 mg/L as SiO₂ mitigated dissolved (DCu) and total (TCu) copper release in all phases. Transient models can be developed from the steady-state metal release concentrations before and after a water quality change. The development of the general transient model for total metal release was initiated by defining total metal release as shown in Equation 5.1, as the sum of present total metal release and change in total metal release. The change in total metal release was defined as the sum of total unreleased metal and the total released metal, both as functions of time as defined in Equation 5.2. The unreleased total metal at time zero was defined as equal to the released total metal at time infinity as shown in Equation 5.3. The unreleased total metal at any time was defined as nth order differential equation as shown in Equation 5.4 which was integrated with respect to time as shown in Equation 5.5. Identification of the steady-state metal release was done by plotting the time-series data of metal release.

$$C_{total} = C_p + C_{change} \quad \text{Equation 5.1}$$

where C_{total} = total metal (copper), mg/L
 C_p = present total metal, mg/L
 C_{change} = change in total metal, mg/L

$$C_{change} = C_{unrel} + C_{rel} \quad \text{Equation 5.2}$$

where C_{unrel} = unreleased total at time t (days) in mg/L
 C_{rel} = released total at time t (days) in mg/L

$$C_{unrel(t=0)} = C_{rel(t=\infty)} = C_o \quad \text{Equation 5.3}$$

$$\frac{dC_{unrel}}{dt} = -k C_{unrel}^n \quad \text{Equation 5.4}$$

$$k \times t = \frac{1}{n-1} \left[\left(\frac{1}{C_{unrel}} \right)^{n-1} - \left(\frac{1}{C_o} \right)^{n-1} \right] \quad \text{Equation 5.5}$$

Figure 5.2 shows such time series plots for TCu release from 3 copper loops. As discussed above Phases I & III with highest alkalinity show an increasing trend of TCu release with time where as Phases II & IV with lower alkalinity showed a decreasing trend with time. Figure 5.2 shows that Cu release was highest for pHs and lower for pHs+0.3. The BOP dosed (0.5 mg P/L) loop shown in Figure 5.2 also followed the same behavior as with pH controls, except that both mean Cu concentration and the variability about the mean were significantly reduced. This was typical behavior of all inhibitor dosed loops. A closer inspection of these plots revealed that Cu release trend continued for all PDSs and all phases for the entire duration of each phase which ranged from 84 to 98 days. Hence steady-state Cu concentration for each PDS was defined as the average of last two observations in each phase.

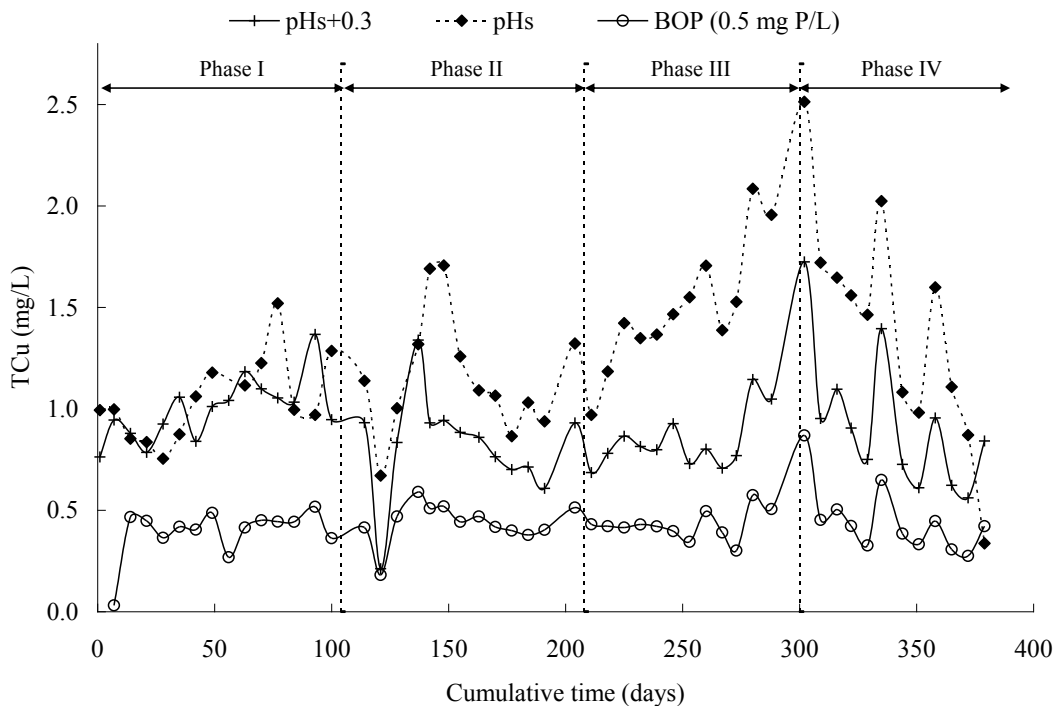


Figure 5.2 Time-series plots of TCu release

The steady-state metal concentration by phase and PDS for TCu is presented in Table 5.5, the steady-state defined as the average of last two observations in a phase for each PDS. Transient Cu release models as defined in Equation 5.1 can be developed for data wherein steady-state concentrations can be estimated i.e. models for Phases II, III and IV can be developed. From Table 5.5 it is observed that steady-state TCu release changed by water quality (Phase) for all PDSs, however Phase II data showed a lower variation in TCu release than Phase III & IV when the data were compared with the one from proceeding phases. Hence transient models were developed from data of Phase III & IV and were verified on data from Phase II. Data analysis showed that the models converged only for a first order response for all PDSs and each phase implying that Cu release followed a first order transient response. The models reduce to the one shown in Equation 5.6 for a first order response and was modified to include temperature effects as shown in Equation 5.7.

$$C_{rel} = C_1 + (C_2 - C_1)(1 - e^{-kt}) \quad \text{Equation 5.6}$$

where C_1 = steady-state total metal release before water quality change
 C_2 = steady-state total metal release after water quality change
 $C_2 - C_1$ = driving force due to a water quality change
 k = 1st order reaction rate constant
 t = time after water quality change

$$C_{rel} = C_1 + (C_2 - C_1)(1 - e^{-k_1 t \theta^{T - T_0}}) \quad \text{Equation 5.7}$$

θ = temperature correction factor
 T = temperature in °C

Table 5.5 Average of last two observations by phase for total Cu release

Inhibitor	BOP	BOP	BOP	OP	OP	OP	ZOP	ZOP	ZOP	Si*	Si*	Si*	pHs	pHs+0.3
PDS #	1	2	3	4	5	6	7	8	9	10	11	12	13	14
Target	0.5 mg	1.0 mg	2.0 mg	0.5 mg	1.0 mg	2.0 mg	0.5 mg	1.0 mg	2.0 mg	3 mg	6 mg	12 mg		
dose	P/L	P/L	P/L	P/L	P/L	P/L	P/L	P/L	P/L	SiO ₂ /L	SiO ₂ /L	SiO ₂ /L	-	-
Steady state Cu conc. (mg/L)														
Phase I	0.48	0.36	0.37	0.46	0.44	0.23	0.56	0.37	0.34	0.74	0.72	0.47	0.98	1.20
Phase II	0.39	0.29	0.26	0.37	0.31	0.22	0.41	0.39	0.22	0.60	0.53	0.42	0.98	0.66
Phase III	0.54	0.38	0.33	0.49	0.41	0.24	0.62	0.42	0.19	0.79	0.69	0.47	2.02	1.09
Phase IV	0.34	0.28	0.25	0.33	0.27	0.20	0.42	0.33	0.44	0.48	0.38	0.32	0.60	0.70

5.3.4 Transient Cu release models

The variation of Cu release depends on the driving force (C_2-C_1) as shown in Equation 5.7 and is the difference in the steady-state metal concentrations in subsequent phases in this study. This driving force was small for all inhibitors since they did not show a significant difference in metal levels by phase. The maximum driving force was observed for pH_s and was 1.416 mg/L TCu for phase IV, while the next largest one was for $pH_{s+0.3}$ loop and was 0.395 mg/L TCu also for phase IV. All other loops had a driving force (TCu difference between phases) less than 0.32 mg/L for TCu. Hence transient models could not be developed for other loops (PDSs) than that shown in Table 5.6. The TCu models presented in Table 5.6 were statistically significant at 95 % confidence and were obtained for pH_s for Phases III & IV and SiO_2 at 6 mg/L for Phase IV. $LPRCR_{Cu}$ and $ECNCR_{Cu}$ were identified as the EN parameters which correlated with Cu release (Taylor et al., 2007). LPRCR represents general corrosion and TCu release was found to depend more on general corrosion than on localized corrosion (ECNCR) in this study (Taylor et al., 2007). Since Cu release was observed to increase or decrease exponentially with time, the EN models were developed by using LPRCR in an exponential form to predict transient TCu release. Various empirical regression models using LPRCR and time (t) in an exponential form were tried and the best-fit generic form of the EN model for transient TCu release is shown in Equation 5.8. The significant EN models are also shown in Table 5.6 along with transient TCu models from actual data.

$$C_{rel} = e^{(b.LPRCR^a + t)} \quad \text{Equation 5.8}$$

where e = exponential
 a = exponent for LPRCR

b = coefficient for LPRCR
c = coefficient for time
t = time in days

Table 5.6 Transient TCu model results

Inhibitor	Si*	pH _s	pH _s
PDS #	11	13	13
Phase	IV	III	IV
Target dose	6 mg SiO ₂ /L	-	-
WQ Analysis	Tcu=C1+(C2-C1)(1-exp[-k.t.θ ^(T-20)])		
R ²	0.49	0.63	0.64
k	0.016	0.020	0.018
θ	0.85	0.95	0.91
*Predicted % response-WQ	72.2	82.8	76.3
EN Analysis	Tcu=exp(b.LPRCR ^{a+c.t})		
R ²	0.82	0.84	0.69
a	0.51	0.80	0.02
b	-1.30	-0.47	0.89
c	-0.01	0.01	-0.01
*Predicted % response-EN	61.7	62.0	61.7

A comparison of transient model fits from Table 5.6 suggests that the R² from EN model was better than that from actual data fit. This is attributed to the slow response of TCu release in this study, which is evident from the small values of first order decay k and small values of coefficient c for time in Table 5.6. Thus both the actual data fitted model (water quality WQ model) and EN model show that water quality changes required a long response time for TCu release. Hence steady state may not have been achieved in the study duration (84-98 days) for all phases. The predicted percent change in steady-state Tcu release is also shown in Table 5.6 and is about 62 % for the EN models and varies from about 72 to 82 percent for the WQ models. The exponent a of

LPRCR shown in Table 5.6 has the values of 0.80 and 0.02 for pH_s for phases III and IV respectively. Hence LPRCR was sensitive to TCu release in phase III than in phase IV. This is attributed to a higher alkalinity (mg/L CaCO_3) of 154 in phase III than of 127 in phase IV. Comparison of Si and pH_s EN model coefficients shown in Table 5.6 suggests that TCu release decreased with time for both loops to the same extent ($c=-0.01$ for both), but LPR was more sensitive for TCu changes for Si than for pH_s shown by a higher coefficient for a as 0.51 for Si than 0.02 for pH_s . Similarly WQ model fit (R^2) when compared against that of EN models suggests that both models do equally well in moderate alkalinity waters for pH_s (phase IV) but EN model does significantly better ($R^2=0.84$) than WQ model ($R^2=0.63$) for pH_s in higher alkalinity water. For Si inhibitor EN model fit was significantly better ($R^2=0.82$) than WQ model ($R^2=0.49$) for phase IV i.e. in moderate alkalinity water.

Figure 5.3 shows the model predicted TCu release from both the WQ and EN models against actual data. The planes in Figure 5 are for model predicted TCu release and these represent (top to bottom) EN- pH_s , WQ- pH_s , EN-Si and WQ-Si fits respectively. From Figure 5.3 it is observed that the fit of WQ and EN models departs significantly. For pH_s i.e. the top plane representing the EN model fit for both Phase III and IV fits which had an average alkalinity of 154 and 127 (mg/L as CaCO_3) respectively. The EN model for pH_s fits at both high and low values of TCu release observed for the data and range from about 0.33 to 2.08 mg/L. This data range resulted in an action limit violation of TCu release at 90th percentile in excess of 1.3 mg/L. From Figure 5.3 the EN models offer a better visual fit than the WQ models. Similarly for the Si model shown as bottom plane in Figure 5.3 high values of TCu which were observed at low values of time (days)

in Phase IV show a poor fit where as the EN model (second plane from bottom) fits the data better. The WQ model was developed assuming the last two observations in every Phase are the steady-state concentrations, but both models predict about 62-83 % of this response is actually achieved. LPRCR for Cu responds to a change in TCu release over time without assuming any steady-state Cu concentration and hence can explain the better fit of EN model.

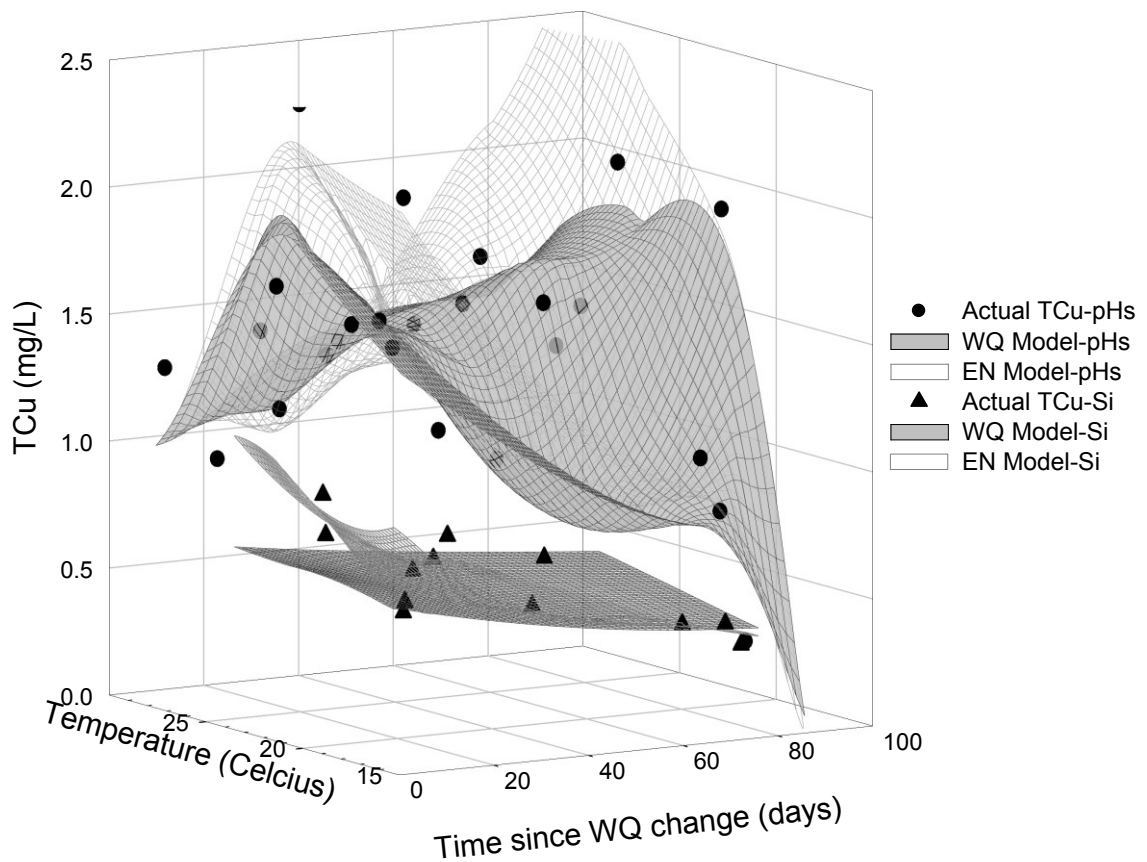


Figure 5.3 Model predicted transient TCu release against actual data

5.3.5 Model verification

The data in Phase II was not used in model development and hence was used to verify the transient WQ and EN models. Alkalinity and chlorides were found to have an adverse impact whereas sulfates did not have a significant impact on TCu release in this study (Taylor et al., 2007). Decrease in alkalinity (mg/L as CaCO₃) from 163 to 109 from phase I to II is likely to have a similar impact on Cu release in phase II as did the decrease in alkalinity from 154 to 127 from phase III to IV. Hence the models developed for phase IV were used to verify the TCu release in phase II. The difference in phases II & IV were in that II had a higher SW while IV had higher RO. The average sulfates and chlorides (mg/L) in phase II were about 112 and 59 and in phase IV were 84 and 56.

Figure 5.4 shows the fit of both WQ and EN transient TCu release models for copper loops exposed to Si (6 mg/L SiO₂) and pH_s. The actual phase II data for Si is represented by filled triangles and for pH_s by filled spheres. The two flat planes are the WQ models which show little sensitivity to TCu release except that Si inhibitor dosed loop is predicted to have a lower TCu release than that for pH_s, and is consistent with the data. The clear plane on top is the EN model for pH_s and the clear plane on bottom is the EN model for Si. EN models provide a better visual fit than from WQ models for phase II model verification data. The deviation of actual TCu from the WQ fitted model plane was approximately within 0.3 mg/L and was even less for the EN models.

Statistical hypothesis testing of the actual and simulated transient Cu release was made using paired t-tests between means and is presented in Table 5.7. A total of 13 data points were used for each paired t-test from phase II data. The results were interpreted as there being no significant difference at 95 % confidence between the mean of actual and

predicted values for both WQ and EN models. Note the p values for some comparisons is approximately 0.05. Hence the models are considered to be adequate to explain transient Cu release. In all cases EN models provided a better fit than assuming a steady-state TCU release concentration in this study.

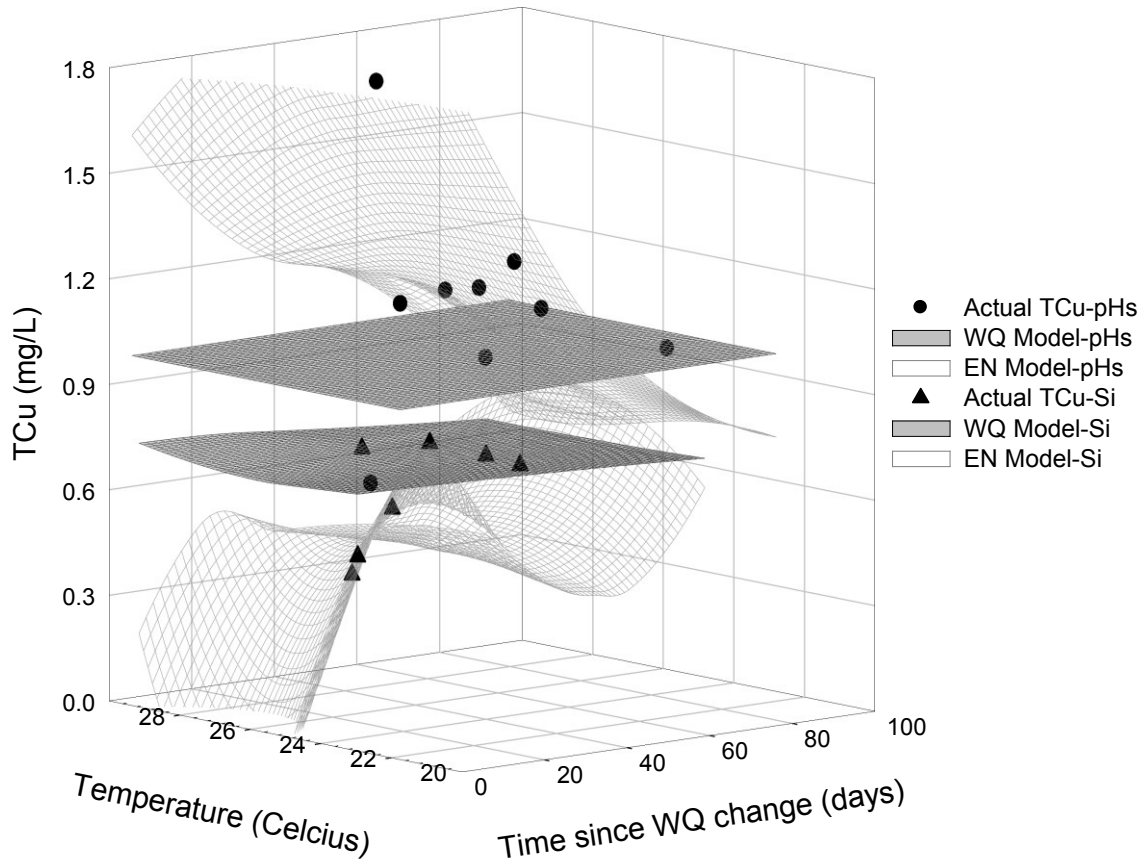


Figure 5.4 Transient TCU release model verification for phase II

Table 5.7 Summary of paired t-test for model verification

PDS	Data	Mean (mg/L)	Significantly different	p value
	Actual Tcu	0.59	-	-
Si	EN model	0.43	N	<0.001
	WQ model	0.68	N	0.022
	Actual Tcu	1.16	-	-
pH _s	EN model	1.29	N	0.054
	WQ model	0.98	N	0.055

Transient TCu release models developed from this study showed a good fit and were verified on independent data. The models suggest that a significant transient time exists before the impact of water quality change on TCu release is fully realized. A short transient time occurs when kinetics of metal release are fast and equilibrium with a new steady-state water quality is quickly achieved, whereas a long transient time indicates a slow achievement of a steady-state and a prolonged period before metal release levels would change significantly. Inhibitor addition is expected to reduce metal release and if the inhibited surfaces have mechanical strength and not easily destabilized by water quality change, then a subsequent water quality change would require a long transient time. Utilities can take advantage of this period to implement desired measures to reduce the full impact of adverse water quality by implementing mitigatory measures as pH adjustment, inhibitor dose increase etc.

5.4 Conclusions

- EN monitoring of strategically placed electrodes could provide instantaneous monitoring of corrosion rates and a baseline over the order of a few weeks can be used to correlate with Cu release. EN parameters can be used in the same way than water quality parameters as they are descriptive of general redox water quality.
- Development of transient Cu release models in real distribution systems is expected to suffer from kinetic limitations in that Cu release response to water quality changes is kinetically limited and may not achieve a true equilibrium over a period of several weeks; however EN parameters respond in real-time to existing redox reactions occurring on metal surfaces. Data from this pilot scale study shows that $LPRCR_{Cu}$ can be used to correlate with TCu release and EN models were successfully demonstrated to predict transient Cu release in a changing water quality environment.

5.5 Recommendations

- Utilities can use EN monitoring to quantify corrosion rates and identify the potential for Cu release in drinking water on a real-time basis. The use of EN at field scale to measure corrosion parameters and correlate with Cu release must be undertaken to encompass a wider range of water quality parameters than used in this study). This would increase the difference in steady-state Cu concentrations i.e. the driving force and help achieve better regression fits due to enhanced variability in the data.

- EN monitoring which is a real-time, remote access technology is applicable in drinking water systems to predict Cu release in changing water quality conditions.

5.6 Acknowledgements

The University of Central Florida (UCF) and UCF project team wish to express their sincere gratitude to Tampa Bay Water (TBW); Hillsborough County, Fla.; Pasco County, Fla.; Pinellas County, Fla.; City of New Port Richey, Fla.; City of St. Petersburg, Fla.; and City of Tampa, Fla. which are the Member Governments of TBW and the American Water Works Association Research Foundation (AwwaRF) for their support and funding for this project. Special thanks to Dr. John D. Dietz who is an Associate Professor in the University of Central Florida Civil (UCF) Civil & Environmental Engineering (CEE Department) in Orlando, Florida. Dr. Dietz initially developed water quality models for transient Cu release in TBW I and also coordinated field operations for TBW projects.

5.7 References

1. Broo, A.E., B. Berghult and T. Hedberg. 1998. Copper Corrosion in Water Distribution Systems – The Influence of NOM on the Solubility of Copper Corrosion Products. *Corrosion Science.*, 40(9):1479-1489.
2. Cottis .R and Turgoose .S, 1999. *Electrochemical impedance and noise.* NACE international. *Corrosion testing made easy.* ISBN 1-57590-093-9.
3. Drogowska M, Brossard L and Ménard H. 1992. Copper Dissolution in NaHCO₃ and NaHCO₃ + NaCl aqueous solutions at pH 8. *J. Electrochem. Soc.* 139(1).
4. Edwards M, Himdi L and Gladewell D. 2002. Phosphate inhibition of soluble corrosion-byproduct release. *Corrosion science.* 44(5), 1057.

5. Edwards M, McNeill L.S, Holm T.R and Lawrence M.C. 2001. Role of phosphate inhibitors in mitigating lead and copper corrosion. American Water Works Association (AWWA) and AWWA Research Foundation, Denver CO.
6. Edwards M, Jacobs S and Taylor R. 2000. The blue water phenomenon. American Water Works Association Journal. 92(7), 72-82.
7. Edwards M, Schock M. Rand Meyer T.E. 1996. Alkalinity, pH, and copper corrosion by-product release. American Water Works Association Journal. 88(3), 81-94.
8. Edwards M, Meyer T. and Rehring J. 1994. Effect of selected anions on copper corrosion rates. American Water Works Association Journal. 86(12), 73-81.
9. Feng Y, Teo W.K, Siow K.S, Tan K.L and Hsieh A.K. 1996 . The corrosion behaviour of copper in neutral tap water. Part II: Determination of corrosion rates. Corrosion science. 38(3), 387-395.
10. Lee, R.G., W.C. Berker and D.W. Collins. 1989. Lead at Tap: Sources and Control. *Jour. AWWA*, 81(7):52-62.
11. Monticelli C, Fonsati M, Meszaros G, and Trabanelia G. 1999. Copper corrosion in industrial waters a multimethod analysis. *Journal of the Electrochemical Society*. 146(4) 1386-1391.
12. Pisigan, R.A., and J.E. Singley. 1987. Influence of Buffer Capacity, Chlorine Residual, and Flow Rate on Corrosion of Mild Steel and Copper. *Jour. AWWA*, 79(2): 62-70.
13. Qiu J and Dvorak B.I. 2004. The impact of phosphate treatment on copper corrosion in two Nebraska public water supply systems. Proceeding of 2004 AWWA WQTC, San Antonio TX.
14. Riber S. 1989. Copper plumbing surfaces: An electrochemical study. American Water Works Association Journal. 81(7), 114-122.
15. Royuela J.J and Otero E. 1993. The assessment of short term data on pipe corrosion in drinking water-II Copper. *Corrosion Science*. 34(10) 1595–1606.
16. Stone, A., D. Spyridakis, M. Benjamin, J. Ferguson, and S. Osterbus. 1987. The Effect of Short-term Changes in Water Quality on Copper and Zinc Corrosion rate. *Jour. AWWA.*, 79(2):75-82.
17. Taylor, J.S., J.D. Dietz, A.A. Randall, C.D. Norris, A. Alshehri, J. Arevalo, X. Guan, P. Lintereur, D. MacNevin, E. Stone, R. Vaidya, B. Zhao, S. Glatthorn and A. Shekhar. 2007. Control of distribution system water quality in a changing water quality environment using inhibitors. Draft final report submitted to

AWWA Research Foundation Denver CO and Tampa Bay Water. (TBW II report)

18. Taylor, J.S., J.D. Dietz, A.A. Randall, S.K. Hong, C.D. Norris, L.A. Mulford, J.M. Arevalo, S. Imran, M. Le Puil, S. Liu, I. Mutoti, J. Tang, W. Xiao, C. Cullen, R. Heaviside, A. Mehta, M. Patel, F. Vasquez, and D. Webb. 2005. Effects of Blending on Distribution System Water Quality. AWWA Research Foundation Denver CO and Tampa Bay Water. (TBW I report).
19. Zhang X, Pehkonen S, Kocherginsky N and Ellis G.A.2002. Copper corrosion in mildly alkaline water with the disinfectant monochloramine. Corrosion Science. 44(11) 2507–2528

¹ All coupons were obtained from Metal samples, Munford, Alabama 36268.

² SmartCET is the commercial name of the EN equipment used to monitor corrosion parameters.

6 CORRELATING ELECTROCHEMICAL CORROSION MONITORING FOR IRON WITH WATER QUALITY

ABSTRACT

This one year study investigated the use of electrochemical corrosion monitoring (EN) to correlate with iron release in presence and absence of phosphate (P) and silicate (Si) inhibitors using pilot distribution systems (PDSs). Iron release was mostly in particulate form and Pitting Factor (PF_{Fe}) correlated with alkalinity, chlorides, sulfates and modified Larson's ratio. Variation in corrosion current which was represented by PF_{Fe} in this study correlated with chlorine residual loss in the PDSs. Empirical regression models using EN parameters were developed for chlorine residual loss, dissolved and total iron; these showed that both general and localized corrosion were important. The EN models are in agreement with the water quality models developed from this study and offer an advantage in being an on-line tool to identifying the potential of adverse Fe release and estimate chlorine residual loss in real systems.

6.1 Introduction

Preventing corrosion and mitigating corrosion product (CP) release is an important task facing the drinking water community. Iron (Fe) release has significant aesthetic and economic impacts with complex chemistry. USEPA (1993) states that electrochemical techniques though are not a cumulative measure of changes occurring on a metal surface do provide a snapshot of the change at a particular time and are

particularly useful for many process control operations or screening programs. Monitoring corrosion rates using methods that take advantage of electrochemical processes are typically fast compared to alternatives of weight loss coupons, electrical resistance probes, or direct inspection by visual, ultrasonic, or nuclear means (Duranceau et al., 2004). However, correlating corrosion rate monitoring information to CP concentration, although highly desirable, is not yet fully understood. This article demonstrates the use of EN parameters that can be correlated to water quality and can be used to estimate chlorine residual loss and Fe release for a wide variety of distributed water qualities.

6.1.1 Background

Tampa Bay Water (TBW) manages drinking water resources for six member governments (MGs) on the west coast of central Florida: the cities of New Port Richey, St. Petersburg, and Tampa, and Hillsborough, Pasco, and Pinellas counties. TBW serves nearly two million consumers at a 250 MGD average daily demand. Historical use of ground water (GW) by TBW had mandated the use of alternative sources as desalinated seawater and treated surface water for limiting GW withdrawals for aquifer protection. TBW manages two alternative supplies: a 66 MGD (2.5×10^5 m³ per day) surface water treatment facility, which utilizes enhanced coagulation, ozone, and biological filtration; and a 25 MGD (9.5×10^4 m³/day) desalination plant.

The impact of new source waters and their blends on water quality changes were evaluated Taylor et al.(2005) under a tailored collaboration project (TCP) called as TBW I, conducted by the University of Central Florida (UCF) and funded by TBW and

American water works association research foundation (AwwaRF). In this follow up one-year TCP called TBW II, the effect of corrosion inhibitors to mitigate adverse impacts in distribution systems that receive blended finished waters produced from ground, surface and saline sources was investigated. Four different corrosion inhibitors were selected and added to the pilot distribution system (PDS) built in 2001 during TBW I. These were blended ortho-phosphate (BOP), ortho-phosphate (OP), zinc ortho-phosphate (ZOP), and silicate. Each phosphate based inhibitor was used at three target doses of 0.5, 1, and 2 mg/L as P and the silicate inhibitor was applied at targets of 3, 6, and 12 mg/L as SiO₂.

6.1.2 Literature on Fe corrosion monitoring

Corrosion monitoring techniques either apply an external signal of current and or voltage and study the response or just evaluate the natural fluctuations in current/voltage. The former is used in linear polarization resistance (LPR) and harmonic distortion analysis (HDA); while the latter is employed in electrochemical noise (ECN) technique. Naturally occurring fluctuations of current or potential are termed as noise when referring to ECN measurements. Various corrosion processes are reported to generate distinct noise characteristics in the time domain (Eden, 1998). ECN technique has been used to study ferrous and ferrous alloy corrosion. Some studies which used carbon steel in various aqueous solutions and are listed as follows: de-aerated bicarbonate solutions (Haruna et al., 2003); drinking water (Sun & Yang, 2006) and artificial potable water (Takasaki & Yamada 2006). These studies showed that ECN can be used to monitor corrosion rates in low conductivity aqueous environments similar to drinking water.

Vatankhah et al., (1998) studied Fe corrosion in mixtures of sodium sulfate and bicarbonate at pH of 8. They reported uniform corrosion in presence of sulfate only with sulfate ions being aggressive and increasing corrosion while bicarbonate addition reduced the aggressive effect of sulfate. Frateur et al., (1999) studied free chlorine consumption during cast Fe corrosion in drinking water and found that Fe corrosion depended on the presence or absence of free chlorine but was not sensitive to the chlorine dose in the study, and concluded the suitability of linear polarization technique for on-line measurements in drinking water.

Norton and LeChevallier (1997) reported corrosion rates from 0.5 to 6.1 mpy (0.01 to 0.15 mm/yr) and 1.2 to 11.4 mpy (0.03 to 0.29 mm/yr) in two distribution systems. The corrosion rate exhibited a close relationship with temperature and lagged by a month or two with maximum and minimum temperatures. The corrosion rate from plant effluent dropped from a range of 4.9-5.6 mpy (0.12-0.14 mm/yr) to 1.3-1.4 mpy (0.03-0.04 mm/yr) after increasing zinc orthophosphate levels from 0.5 to 2.0 mg/L as P. Subsequent increase in the distribution system resulted in a sustained corrosion rate below 4.0 mpy with no coliform detection. They also reported proactive monitoring of daily corrosion rates using on-line ECN monitoring equipment would reduce decrease the operating expenses by optimizing corrosion inhibitor feed rates.

Volk et al., (2000) studied the influence of corrosion control programs on Fe corrosion rates using chloraminated surface water with ZOP inhibitor and found that temperature had a significant adverse effect on Fe corrosion rates and CP release. The study recommended monitoring of corrosion rates for utilities on a regular basis to determine seasonal changes in corrosivity and adjust corrosion inhibitor feed rates. A

quote from the conclusions of this study are included “A linear polarization probe (located at the point of entry and one site of the distribution system) is very useful for measuring relative changes in the corrosion process over time.” In summary monitoring of Fe corrosion rates has been demonstrated to be worthy of investigation but has not been correlated with CP release or with water quality. Table 6.1 summarizes Fe corrosion rates from studies similar to drinking water environment.

Table 6.1 Summary of water quality and corrosion rates for iron from various studies

Water/Study	pH	Cl (mg/L)	SO ₄ (mg/L)	Ca (CaCO ₃ mg/L)	Alkalinity (CaCO ₃ mg/L)	Fe Corrosion rate (mpy)	Method
Various utilities (Duranceau et al., 2004)	7.8	28	288	44	117	14.7 to 14.9	ECN
	7.9	69	154	121	94	4 to 8	
	7.6	8	44	141	162	1.7 to 6.5	
	7.7	12	21	199	202	2.3 to 2.5	
SW. ^{inh} (MacQuarrie et al., 1997)	6 to 6.3				1.5 to 3.7	14.6	LPR
	8				20	15.7	
	8				20	16.6	
	8		Not available		20	12.4	
	8				20	16.1	
	8				20	6.3	
	7.5				10 to 12	8.3	
SW. (Vatankhah et al. 1998)	0.3 to 1 M Na ₂ SO ₄ +0.1 to 0.3 M NaHCO ₃ at pH=8.0					2.24 to 4.46 *	LPR
Simulated drinking water. (Frateur et al., 1999)	not reported	4.5	10	97.5	292.6	0.08 to 0.15 *	LPR
Simulated tap. (Takasaki & Yamada 2006)	8.2	<1	<1	39	74	1.83*	LPR
	7.9	8	17	40	44	4.03*	
	7.9	27	39	40	40	12.81*	
SW. ^{inh} (Volk et al., 2000)	7.3 to	10.6 to	46.3 to	169 to	116 to	0.9 to 7	LPR
	7.6	49.9	97.8	275 ^a	183		
SW. (Chen et al., 2002)	Pond water used in cooling heat exchangers was tested. No water quality data available.					1 to 6	LPR

*denotes the corrosion current density was converted to corrosion rate (mpy)

^{inh} denotes that P or Si were used in this study

SW denotes surface water

LPR & ECN denote linear polarization resistance and electrochemical noise technique respectively.

^a Total hardness as CaCO₃.

6.2 Materials and methods

6.2.1 Field facility

The facility was built in 2001 and consists of 14 hybrid pilot distribution systems (PDSs), copper loops, cradles and treatment processes to obtain finished waters. To maintain integrity of the system finished ground water was fed to the PDSs and copper loops when the facility was not used after TBW I and before start of this study i.e. from 2003 till Fall 2005. The PDSs were constructed of aged pipes that were obtained from existing utility distribution systems to represent the pipe materials used in the TBW Member Government's (MG's) distribution systems and were identified sequentially (PDS01 to PDS14).

The PDSs were operated to maintain a two-day hydraulic residence time (HRT). Standpipes made from translucent plastic pipes 60 inches (1.5 m) long and of 4 inches (0.1 m) diameter were located at the beginning and end of each PDS. To avoid bacterial growth, the standpipes were wrapped in a non-transparent material to eliminate direct light exposure and cleaned regularly with a plastic brush and a 0.1% solution of sodium hypochlorite. The PDSs were constructed with a sampling port after each pipe segment to allow an assessment of water quality changes associated with each pipe material and were composed of four materials, laid out sequentially as:

- Approximately 20 feet (6.1 m) of 6-inch (0.15 m) diameter polyvinylchloride (PVC) pipe,
- Approximately 20 feet (6.1 m) of 6-inch (0.15 m) diameter lined cast iron (LCI) pipe,

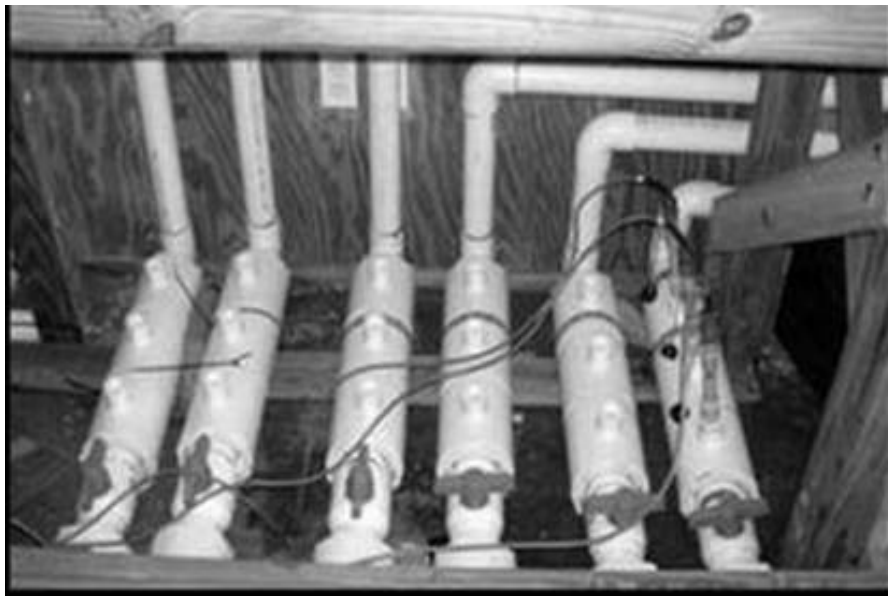
- Approximately 12 feet (3.7 m) of 6-inch (0.15 m) diameter unlined cast iron (UCI) pipe,
- Approximately 40 feet (12.2 m) of 2-inch (0.05 m) diameter galvanized steel (G) pipe

Photograph 6.1 shows the layout of the PDSs. The total hydraulic retention time (HRT) in each hybrid PDS was 2 days to simulate dead-ends in a distribution system, of which PVC, LCI, UCI and G segments had an individual HRT of 17, 17, 10.3 and 3.7 hours respectively. The effluent from the PDSs was split in two parts, one part was directed to the copper corrosion loops and the other part was directed to the Electrochemical Noise Trailer. The effluent Fe concentration was measured from the copper loops to mimic Fe CP release concentrations at tap.

The Fe EN probes and corrosion coupons were housed in 4 inch diameter PVC pipes that were located in the EN trailer. These PVC pipes were referred to as Nadles. EN probes were used to monitor corrosion rates of Fe, Cu & Pb-Sn. The probes were placed with the more noble metal upstream (Cu>Fe>Pb-Sn) to minimize any galvanic corrosion from particulate release and subsequent deposition on the downstream metal. Photograph 6.2 shows the connection of a typical EN probe in a Nadle. The Nadles were flushed daily and before each monitoring event with 5 pipe volumes of water at an average velocity of 1 ft/s (0.3 m/s).



Photograph 6.1 Pilot Distribution Systems



Photograph 6.2 EN probe connection in Nadle

6.2.2 Operation

Prior to this study, field monitoring was resumed in the fall of 2005 to verify uniformity between the PDS effluent for all PDSs. Introduction of a blend of ground water (GW), surface water (SW), and desalinated simulated reverse osmosis (RO) was initiated in December 2005. This project was divided into 4 phases; each of three months duration started from February 2006. All PDSs received the same blend composition for a three month period or phase. At the end of each three month period the blend composition was changed.

The average water quality of the blends and corrosion rates are shown by phase in Table 6.2. Similar blends were used during phases I and III to evaluate the effect of seasonal conditions on the PDS. The individual sources were chloraminated to produce a residual of approximately 4.5 to 5.0 mg/L, and additions were made to the blend to maintain the desired combined monochloramine residual of about 5 mg/L.

The target doses of the inhibitors were defined as: 0.5, 1.0, and 2.0 mg/L as P for the phosphorus-based inhibitors (approximately zero background) and 10, 20, and 40 mg/L as SiO₂ above the background concentration for the silicate-based inhibitor. After 1 month of operation, the doses of the silicate inhibitor were changed to 3, 6, and 12 mg/L because the 20 and 40 mg/L doses were causing CaCO₃ precipitation within the PDS. The equipment connection to the EN probes was switched manually between the Nadles every 6 hours to allow data collection from all Nadles.

Table 6.2 TBW II Water quality by phase

Parameter	Project Minimum	Project Maximum	Phase I	Phase II	Phase III	Phase IV
Alkalinity (mg/L as CaCO ₃)	84	175	163	109	154	127
Calcium (mg/L as CaCO ₃)	53.8	220	202	105	206	168
Chloride (mg/L)	35	123	47	59.2	64.5	56
Dissolved Oxygen (mg/L)	6.6	10.9	8.7	8	8	9.1
pH	7.4	9.1	7.9	7.9	7.9	7.8
Silica (mg/L)	4	65.0*	10.9	5.1	10.2	6.4
Sodium (mg/L)	5	53	7	37	40	32
Sulfate (mg/L)	52	119	72.1	112.2	73.7	84.5
TDS (mg/L)	338	436	365	388	413	378
Temperature (°C)	10.4	29.7	21.2	25.5	24.7	19.6
Total Phosphorus (mg/L as P)	0	3.36*	0.2	0	0	0.1
UV-254 (cm ⁻¹)	0.007	0.105	0.071	0.069	0.077	0.063
Zinc (mg/L)	0.001	0.793	0.031	0.023	0.04	0.037
LPRCR _{Fe} (mpy)	0.001	6.757	0.121 to 5.190	0.007 to 1.077	0.298 to 2.665	0.114 to 1.123
HMCR _{Fe} (mpy)	0.007	14.242	0.198 to 6.137	0.225 to 2.711	0.417 to 2.087	0.303 to 0.811
ECNCR _{Fe} (mpy)	0.024	178.03	0.456 to 61.148	0.478 to 29.962	5.028 to 63.002	0.501 to 81.305
PF _{Fe}	0.006	9.813	0.017 to 0.086	1.846 to 3.522	0.126 to 0.388	0.065 to 0.312

6.2.3 Electrochemical corrosion rate measurement

The Nadles were flushed 5 pipe volumes of water at 1 foot per second average velocity and then monitored continuously for at least a 6 hour standing period. Each Fe probe had three electrodes with an area of 4.67 cm² (0.72 in²) each, atomic weight of 55.46 and a density of 7.84 g/cm³. Electrodes were numbered sequentially as A, B, and C on the probe body for identification. EN monitoring was conducted using commercially

available equipment¹ which monitored corrosion rates continuously, with cycles of 430 seconds. Within each cycle 100 seconds were used for LPR, 30 seconds for HDA and 300 seconds for ECN. The corrosion rates from these three techniques are abbreviated as LPRCR, HMCR and ECNCR respectively and are reported in units of mils/yr, mpy (1 mpy = 0.0254 mm/yr). The parameters obtained from EN monitoring as output are displayed in Table 6.3. Fe electrodes from all 14 PDSs were exposed to varying blends for the project duration of one year and subsequently examined by Scanning Electron Microscope (SEM) and Energy Dispersive Spectroscopy (EDS) for surface characterization of chemical scales. SEM visually magnifies the physical structure of the scale surface for identification of the morphology of the corrosion products. EDS identifies the elemental composition of the surface layer.

Table 6.3 TBW II Water quality by phase

Symbol	Parameter name	mpy
LPRCR	Linear Polarization Resistance Corrosion Rate	mpy
HMCR	Harmonic Distortion Analysis Corrosion Rate	mpy
ECNCR	Electrochemical Noise Corrosion Rate	mpy
PF	Pitting Factor- evaluated from electrochemical noise & harmonic distortion analysis	-
<i>B</i>	Stearn Geary constant -evaluated from the Harmonic Distortion Analysis	Volts
<i>Ba</i>	Anodic tafel slope	Volts/decade
<i>Bc</i>	Cathodic tafel slope	Volts/decade
PSKW	Skew of potential	-
PKRT	Kurtosis of the potential	-
ISKW	Skew of current	-
IKRT	Kurtosis of the current	-
RSOL	Solution resistance	ohms

6.2.4 Quality assurance & control

Samples were collected and analyzed in the field and at the UCF laboratory. Quality assurance and quality control of both the laboratory and field determinations of water quality parameters was established by duplicating analyses of at least 10% of the samples. Blind duplicates and spikes were also used to determine the accuracy of measurements. Dynamic control charts were used to determine whether the results were acceptable. A comprehensive overview of quality control procedures, analytical results and supplementary discussion of associated PDS sampling events and process sampling events over the duration of this entire project is given elsewhere (Taylor et al., 2007).

6.3 Results and discussion

6.3.1 Water quality variations by phase

Variation of water quality was achieved by blending finished GW, SW and RO as shown in Table 6.2. Phase I & III water quality was typical of high GW blends, and had high alkalinity, low chloride and low sulfate. Phase II had a higher SW and hence sulfate were relatively higher, and alkalinity and chlorides were lower. The Phase IV blend had a relative higher fraction of RO finished water, which had relatively higher chlorides, lower sulfates and moderate alkalinity. The actual variation in phase water quality was 84 mg/L to 175 mg/L as CaCO₃ alkalinity, 35.4 mg/L to 122.9 mg/L Cl and 136 mg/L to 252 mg/L as CaCO₃ total hardness. Maximum Fe release was observed in the pH_s PDS. All other corrosion control strategies: pH_{s+0.3}, BOP, OP and ZOP at 0.5, 1.0 and 2.0 mg/L as P and SiO₂ at 3.0, 6.0 or 12 mg/L as SiO₂ mitigated dissolved (DFe) and total (TFe) iron

release relative to pH_s in all phases. Unless otherwise noted, data is reported as weekly averages for each PDS over one year, which produced 717 observations.

From Table 6.2 it is observed that the magnitude of LRRCR_{Fe} and HMCR_{Fe} from this study were similar with the corrosion rates shown in Table 6.1; whereas the magnitude of ECNCR_{Fe} was higher. Duranceau et al., (2004) investigated the application of electrochemical corrosion monitoring using the electrochemical noise (ECN) method at four utilities along with some water quality sampling. Their study concluded that ECN can be used to derive practical information for assessment of corrosion susceptibility of metals and the type of corrosion process. A quote from the report reads, “the usefulness of this type of testing is demonstrated in this project by the conclusion that for some conditions, ‘inhibition’ increases the corrosion rate”. Inhibition herein was referred to as addition of the corrosion inhibitor ZOP at 1 mg/L as P and the corrosion rate referred to was from ECN. This study (TBW II) data is consistent with the findings of Duranceau et al., (2004) in that ECN corrosion rates increased in presence of inhibitors.

In review of the observations of Duranceau et al., (2004) it is obvious that numerous reactions are expected to occur on a metal surface in drinking water environment. Metal scale formation, oxygen consumption, hydrogen generation, chlorine reduction, biological oxidation and metal oxidation are examples of possible reactions that change surface potential (voltage) and result in current flow, which generates ECN and are not direct measurements of metal release. Hence ECNCR can over estimate the actual corrosion rate of metal dissolution because ECNCR represents the total current activity on a metal surface with all activity assumed to cause metal corrosion.

6.3.2 Iron release by inhibitor and phase

Paired data t-tests (one tailed) were used to compare the total Fe concentration between pH controls (either PDS13 at pH_s or PDS14 at $\text{pH}_{s+0.3}$) and a PDS that received a corrosion control treatment (pH elevation or inhibitor). A comparison of the PDS influent and effluent total iron (TFe) concentrations obtained from corrosion loops was also conducted. All tests of significance used an alpha value of 0.05. This analysis permits an assessment of the significance of any increase in Fe concentration after a 2-day HRT in the hybrid PDS. The increase in Fe concentration was significant for every comparison: for each of the four phases, for the composite assembly of data, for every PDS. These results confirm a potential problem with Fe release (red water) in unlined cast iron or galvanized pipes if the HRT is excessive.

A separate set of paired t-tests was used to compare the corrosion loop total Fe concentrations for the corrosion treatments (inhibitor addition or pH elevation) with the pH_s control (PDS13) and are presented in Table 6.4. Entries shown in bold font indicate that the concentration associated with the corrosion treatment was actually greater than the concentration of the pH_s control. In general, the inhibitors or pH elevation did achieve a reduction in TFe concentration relative to operation at pH_s . A total of 65 such comparisons were made (13 PDS, 4 separate phases, and one composite data set). In 51 of the comparisons, the difference was significantly lower ($\alpha = 0.05$), in 9 comparisons the difference was not significant, and in 5 comparisons the difference was significantly higher. Of the 5 comparisons in which inhibitor addition had an increase in Fe, 4 were from PDS07 (low ZOP dose at 0.5 mg P/L) and one was from PDS09 (medium ZOP dose at 1.0 mg P/L).

Table 6.4 Paired t-tests for iron concentrations compared with pH_s.

Treatment Inhibitor (mg/L)	PDS 13 pH pH _s	PDS 01 BOP P	PDS 02 BOP P	PDS 03 BOP P	PDS 04 OP P	PDS 05 OP P	PDS 06 OP P	PDS 07 ZOP P	PDS 08 ZOP P	PDS 09 ZOP P	PDS 10 Silicate SiO ₂	PDS 11 Silicate SiO ₂	PDS 12 Silicate SiO ₂	PDS 14 pH pH _{s+0.3}
Phase I														
Average	0.15	0.14	0.09	0.12	0.12	0.14	0.11	0.18	0.14	0.16	0.14	0.12	0.17	0.11
StDev	0.03	0.07	0.02	0.05	0.04	0.03	0.06	0.03	0.05	0.12	0.09	0.04	0.14	0.04
Significant		No	Yes	Yes	Yes	No	Yes	Yes	No	No	No	Yes	No	Yes
P-Value		0.315	< 0.001	0.039	0.04	0.158	0.034	0.005	0.27	0.362	0.367	0.047	0.309	0.008
Avg inhibitor dose	-	0.58	1.08	1.82	0.49	1.04	1.84	0.65	0.99	1.76	2.81	6.33	11.66	-
Phase II														
Average	0.28	0.21	0.15	0.15	0.16	0.2	0.17	0.34	0.23	0.16	0.17	0.13	0.19	0.19
StDev	0.06	0.12	0.05	0.05	0.04	0.06	0.04	0.13	0.06	0.04	0.04	0.02	0.07	0.07
Significant		No	Yes	Yes	Yes	Yes	Yes	Yes	Yes	Yes	Yes	Yes	Yes	Yes
P-Value		0.06	< 0.001	< 0.001	< 0.001	< 0.001	< 0.001	0.021	0.008	< 0.001	< 0.001	< 0.001	0.001	0.003
Avg inhibitor dose	-	0.57	1	1.95	0.55	0.9	1.91	0.54	0.89	1.77	2.69	6.57	12.06	-
Phase III														
Average	0.27	0.12	0.10	0.12	0.14	0.2	0.14	0.21	0.22	0.11	0.11	0.09	0.11	0.14
StDev	0.06	0.03	0.02	0.04	0.03	0.04	0.03	0.06	0.05	0.01	0.02	0.01	0.01	0.03
Significant		Yes	Yes	Yes	Yes	Yes	Yes	Yes	Yes	Yes	Yes	Yes	Yes	Yes
P-Value		< 0.001	< 0.001	< 0.001	< 0.001	0.018	< 0.001	0.016	0.022	< 0.001	< 0.001	< 0.001	< 0.001	< 0.001
Avg inhibitor dose	-	0.49	0.9	1.73	0.54	0.99	1.87	0.49	0.88	1.82	2.79	6.54	12.05	-
Phase IV														
Average	0.19	0.12	0.13	0.09	0.13	0.13	0.20	0.28	0.24	0.11	0.11	0.09	0.12	0.14
StDev	0.09	0.05	0.05	0.04	0.06	0.06	0.13	0.08	0.13	0.05	0.03	0.02	0.04	0.05
Significant		Yes	Yes	Yes	Yes	Yes	No	Yes	Yes	Yes	Yes	Yes	Yes	Yes
P-Value		< 0.001	0.002	< 0.001	< 0.001	0.003	0.404	0.011	0.043	< 0.001	< 0.001	< 0.001	0.003	0.006
Avg inhibitor dose	-	0.68	1.31	2.66	0.47	0.82	1.69	0.46	0.88	1.58	2.95	6.79	11.39	-
Composite														
Average	0.22	0.15	0.12	0.12	0.14	0.18	0.16	0.25	0.21	0.14	0.13	0.11	0.15	0.14
StDev	0.08	0.08	0.04	0.05	0.04	0.06	0.08	0.10	0.08	0.07	0.06	0.03	0.08	0.05
Significant		Yes	Yes	Yes	Yes	Yes	Yes	Yes	No	Yes	Yes	Yes	Yes	Yes
P-Value		< 0.001	< 0.001	< 0.001	< 0.001	< 0.001	< 0.001	0.016	0.087	< 0.001	< 0.001	< 0.001	< 0.001	< 0.001
Avg inhibitor dose	-	0.58	1.07	2.04	0.51	0.94	1.83	0.53	0.91	1.73	2.81	6.56	11.79	-

The notable, and consistent, treatment that did not achieve a reduction in Fe was PDS07 (low ZOP dose). This observation may be attributed to the absence of any benefit associated with a low ZOP dose or to some factor associated with the particular construction of PDS07. The former argument is supported by the absence of a significant benefit from the medium ZOP dose in PDS08. The data suggest that all of the inhibitors and pH elevation yield potential benefits to address red water issues. The data is less compelling for ZOP.

For this dataset a Fe concentration of 0.16 mg/L corresponded with the secondary color standard of 15 CPU. Paired t-tests were also used to compare the corrosion loop TFe concentrations for the inhibitor treated PDSs (PDS01 to PDS12) with the elevated $\text{pH}_{\text{s}+0.3}$ control (PDS14); and these tests indicate that many of the inhibitor dosed PDSs had an Fe concentration greater than the concentration of the elevated $\text{pH}_{\text{s}+0.3}$ control. Elevation of pH to 0.3 units greater than pH_{s} appears to be about as effective as use of an inhibitor.

There were 12 possible comparisons for each of the four phases and 12 more possible comparisons for the composite data set. For the comparisons by individual phase, one half i.e. 24 out of 48 of the inhibitor treatments had an average Fe concentration that was less than the elevated pH control and only 17 of these were statistically significant. For the composite data set, one half i.e. 6 out of 12 of the inhibitor treatments had a reduction in average Fe concentration vs. the elevated pH control and only 3 of these were statistically significant.

Examination of the results by inhibitor type for the composite data suggest that the BOP inhibitor may be more effective than the other inhibitors. The BOP achieved a

significant improvement at dose of 1 mg P/L or higher. The Silicate achieved a significant improvement at the medium dose of 6 mg SiO₂/L. The OP and ZOP inhibitors did not result in a statistically significant improvement vs. the elevated pH control at any dose. Overall elevation of pH was as effective as the inhibitors studied for mitigating TFe release in the PDSs.

6.3.3 Observations by photographs and SEM/EDS

Digital images were taken of all Fe electrodes after exposure to blended waters for one year. All electrodes show dark brown to blackish scale with areas of orange scale. The scale appeared to be distinct in at least two layers with the outer layer porous and dull in color mostly orange to brown while the inner layer was dense and dark from grey to black. Photograph 6.3 shows the electrodes for BOP, ZOP and two pH controls at pH_s and pH_{s+0.3}. The BOP scale at low dose (0.5 mg P/L) shown in top left part of Photograph 6.3 shows the porous and flaky scale with voluminous corrosion products (CPs).

The CPs on BOP scale appeared to decrease in volume with an increase in dose and PDS03 with the highest BOP dose (2 mg P/L) had a dark brown to black scale with no visible loose CPs. There appeared to be no relationship of CP volume with dose for the OP inhibitor and the general scale was orange brown with some dark brown areas. ZOP had a dull orange and dark grey scale. The volume of CPs also decreased with increasing ZOP dose, and the scale on ZOP appeared to be the hardest amongst all inhibitors and was not flaked easily even when rubbed with a plastic scraper. The scale on silicate electrodes varied from orange to dark brown to grey color with reduced CP volume with increasing dose. The pH_s control PDS13 had an orange to brown scale with

significant patches of light grey color which was the region of underlying bare metal. The scale on $\text{pH}_{\text{s}+0.3}$ control i.e. PDS14 was darker orange and brown with respect to PDS13.

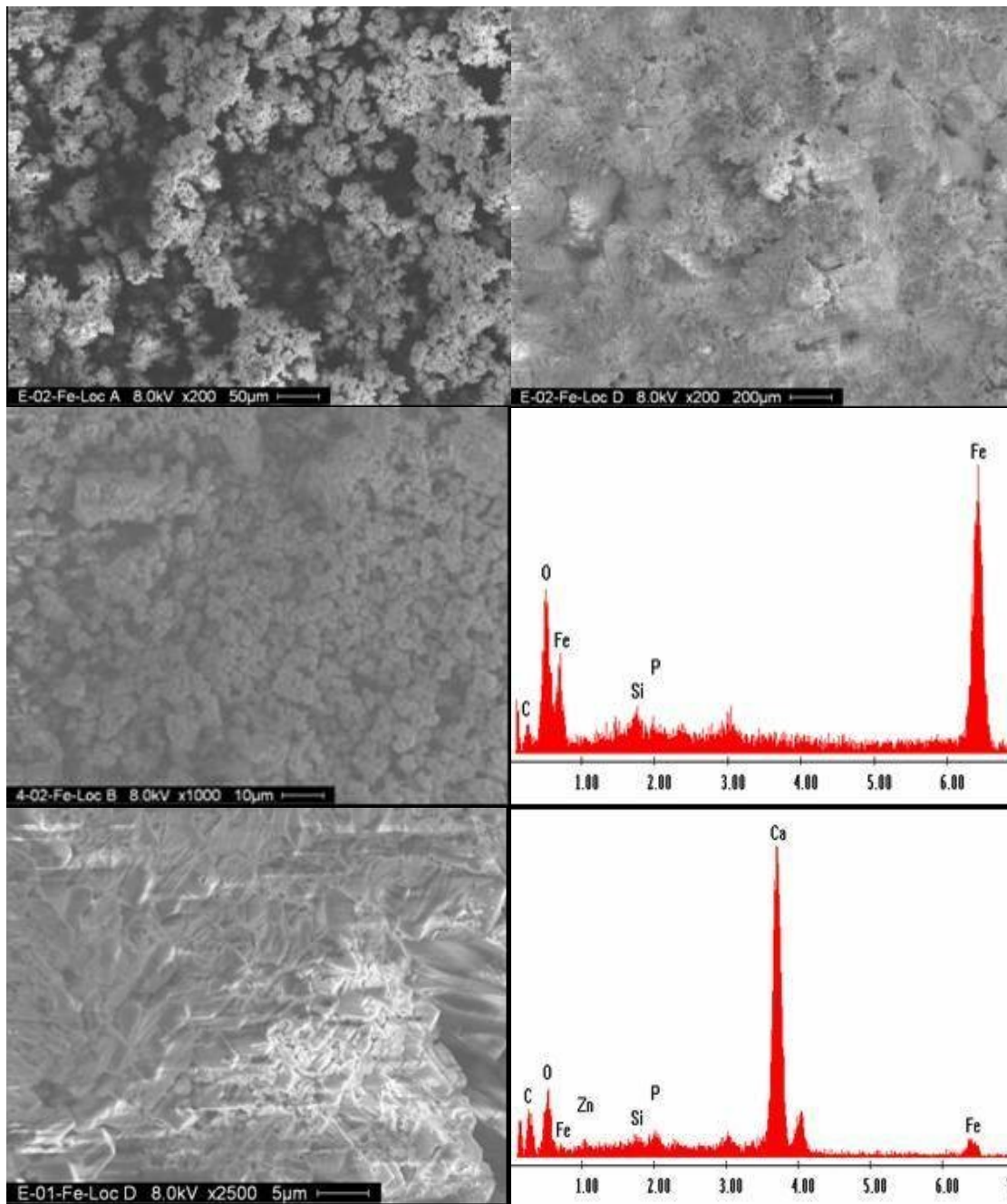


Photograph 6.3 Fe electrodes, clockwise from top left BOP (0.5 mg P/L), ZOP (2 mg P/L), pH_{s} and $\text{pH}_{\text{s}+0.3}$.

The electrodes had distinct areas of scale occurrence with the electrode tips being relatively free of scale and the EN probe ends of electrodes having the bulk of CPs and

scales. The areas on electrodes near the probe end of electrodes and were labeled as A and B while areas near the tips were labeled as C and D for identification. The SEM/EDS showed distinct structures and composition for areas A & B against areas C & D. This is attributed to the thinner accumulation of CP near the tips where the velocity of water used in daily flushing was expected to be higher and hence erode any loose CPs. EDS revealed that areas A and B had porous, spongy looking structures and scales with more Fe content where as areas C & D had denser and more compact scales richer in Ca and P or Si. The P or Si content of the scales increased with increasing amount of the P or Si dose respectively.

Photograph 6.4 shows SEM micrographs for electrodes exposed to BOP which represent the general observation for the phosphate inhibitors used. Top left and right images show areas A and D respectively for exposure to 1 mg P/L and show spongy porous scales for A and dense looking smoother scales for D. The middle left image in Photograph 6.4 shows the SEM micrograph for electrode exposed to 1 mg P/L BOP area B which is near the probe with loose porous looking scales. EDS shown in middle right image shows it to be composed of Fe and O and with small amounts of C, P, and Si. The bottom left image in Photograph 6.4 show the SEM micrograph for electrode exposed to 0.5 mg P/L BOP area D which is near the electrode tip with dense smooth looking scales. EDS shown in bottom right image shows it to be composed of predominantly of Ca and O and with less amounts of Fe and small amounts of C, P, and Si. EDS showed the presence of trace amounts of Zn, Cl, SO₄ and Al. For the pH controls pHs+0.3 showed a high Ca & O surface content and low Fe. In summary SEM of EN electrodes shows presence of P & Si which appeared to increase with inhibitor dose.



Photograph 6.4 SEM & EDS of Fe electrodes exposed to BOP. Top & middle are for exposure to 1 mg P/L and bottom is for exposure to 0.5 mg P/L.

Distinct scale morphology and chemical composition was observed on each of the 14 electrodes with loose porous looking CPs having more Fe content and dense smooth

scales having less Fe and more Ca & O content. A statistical comparison of elemental composition for the major elements i.e. Fe, Ca, O, C, Si & P which made up for approximately 98 % of the surface composition as detected by EDS was made. T-tests (one tailed) assuming unequal variances were used to compare means of elemental composition of areas A & B combined against areas C & D combined and a summary is presented in Table 6.5. These allowed comparison of means of unequal sample numbers for the 14 electrodes tested. Comparison of variances of elemental composition was made using F tests and is also presented in Table 6.5, individual F test p values are shown with standard deviation (Std. Deviation) since it a generally used statistic rather than the variance.

F tests presented in Table 6.5 showed that that the variability in elemental composition was not significantly different (95 % confidence) by location. Hence variability in elemental composition detected by EDS is statistically insignificant by location and may represent the natural variation on electrode surfaces and or EDS method variability. T-tests presented in Table 6.5 showed that Fe, Ca, O and C composition was similar in areas A & B and in areas C & D, but that A & B composition was significantly different than C & D composition. This suggests that Fe surfaces exposed to standing conditions developed loose porous looking scales with less Ca and O (areas A & B) whereas compact and smooth looking scales were higher in Ca and O and were located near electrode tips (areas C & D). The daily flushing had flushed away any loose CPs near the electrode tips. These observations were consistent for the inhibitors. For the pH controls tested, the electrodes exposed to a pH elevation of $\text{pH}_{s+0.3}$ formed scales similar to areas C & D where as the lower pH control ones exposed to pH_s had scale composition

of areas A & B. No significant difference in P or Si content was found by location for the inhibitors and hence it is likely that stagnation did not result in limiting the inhibitor availability on Fe surfaces by mass transfer i.e. by diffusion.

Table 6.5 Comparison of surface elemental composition from EDS by areas

Statistic	Element	Areas A & B	Areas C & D	N	p value	Significantly Different
Mean	Fe	61.5	37.1	37 &	1.98E-05	Y
Std. Deviation		24.81	27.23	50	2.82E-01	N
Mean	Ca	17.39	30.96	37 &	1.55E-03	Y
Std. Deviation		21.66	17.66	45	9.86E-02	N
Mean	O	15.82	20.22	38 &	3.01E-03	Y
Std. Deviation		7.04	7.45	49	3.64E-01	N
Mean	C	9.34	11.36	34 &	1.69E-02	Y
Std. Deviation		3.76	4.6	46	1.15E-01	N
Mean	Si	1.6	1.39	31 &	1.46E-01	N
Std. Deviation		0.84	0.88	45	4.07E-01	N
Mean	P	3.4	2.59	24 &	1.05E-01	N
Std. Deviation		2.58	2.1	34	1.40E-01	N

where N denotes number of EDS measurements for areas A & B and C & D respectively.

6.3.4 Water quality correlations with EN

Correlations between Fe EN parameters were assessed to determine if the parameters were independent. The highest Pearson's linear correlation (R^2) amongst the 12 EN parameters for Fe was 0.45 for the correlation of $LPRCR_{Fe}$ and $HMCR_{Fe}$, which indicates that confounding of EN parameters for Fe is not an issue. Alkalinity was observed to be modestly correlated with $LPRCR_{Fe}$ ($R^2=0.47$) and PF_{Fe} ($R^2=0.27$). EN parameters would correlate with water quality as both are global measures of the same environment. Both $LPRCR_{Fe}$ and $HMCR_{Fe}$ measure a general corrosion rate and were positively correlated with alkalinity. In contrast, the PF, which has been proposed as a measure of localized corrosion, is negatively correlated with alkalinity. Since a higher

alkalinity mitigated Fe release in this study (Taylor et al., 2007), a negative correlation between PF_{Fe} and alkalinity is theoretically sound. PF_{Fe} was positively correlated with chlorides, sulfates and temperature which are historically known to induce pitting. From previous studies a $PF \ll 1$ is considered to be an indication of a more or less constant general corrosion rate where as PF consistently approaching one may indicate actual pitting or a widely varying general corrosion (Cottis & Turgoose, 1999; Eden, 1994). The values of PF_{Fe} calculated by this EN equipment ^{CET} do not limit the values to unity, but PF_{Fe} herein is the ratio of the standard deviation of naturally occurring current from ECN to the mean current from HDA technique and is shown in Equation 6.1. From Equation 6.1, it is observed that for a low mean general corrosion current density I_{corr} near zero, misleadingly high values of PF_{Fe} would be generated, although aggressive localized corrosion may not be occurring. Hence a high PF_{Fe} from this study may or may not have indicated localized corrosion but likely indicated a widely varying general corrosion rate. The values of PF_{Fe} obtained in this study are within a range from 0.001 to 10.

$$PF = \frac{\sigma_i}{(I_{corrHDA})} \quad \text{Equation 6.1}$$

where σ_i = standard deviation of corrosion current density from ECNCR
 I_{corr} = mean corrosion current density from HDA

Plots of PF_{Fe} versus alkalinity, chlorides and sulfates are shown in Figure 6.1. The plots show that there is no direct linear correlation between these variables over the data range and there appear to be threshold values of alkalinity, chlorides, and sulfates that correspond with a sudden increase in PF_{Fe} values. The relatively high PF_{Fe} for alkalinities

less than 120 mg/L (as CaCO₃) correspond to the same range of alkalinity that was noted for high release of TFe during the TBW I project (Taylor et al., 2005). Similarly relatively high PF_{Fe} were observed for chlorides or sulfates concentrations above 60 and 90 mg/L respectively. Consequently, the data presented in Figure 6.1 support the use of PF_{Fe} for monitoring water quality and predicting high Fe release.

The traditional Larson's ratio was modified to incorporate the effect of alkalinity, chlorides, sulfates and temperature and is shown LR1T in Equation 6.2. The data and linear regression of Log₁₀(PF_{Fe}) versus LR1T is also shown in Figure 6.1 for all data (N=717). The R² is 0.63 with a p value<0.001 and F =835.1, which show the trend of the data is statistically significant. This shows that a slight change in LR1T would change PF_{Fe} values considerably since it is on a Log (base 10) scale in Figure 6.1.

$$LR1T = \frac{[SO_4^-] + [Cl^-]}{[HCO_3^-]} \times \frac{Temp}{25} \quad \text{Equation 6.2}$$

where [] = concentration (meq/L)
 LR1T = Larson's ratio one including temperature effect
 Temp = Influent Temperature (° C)

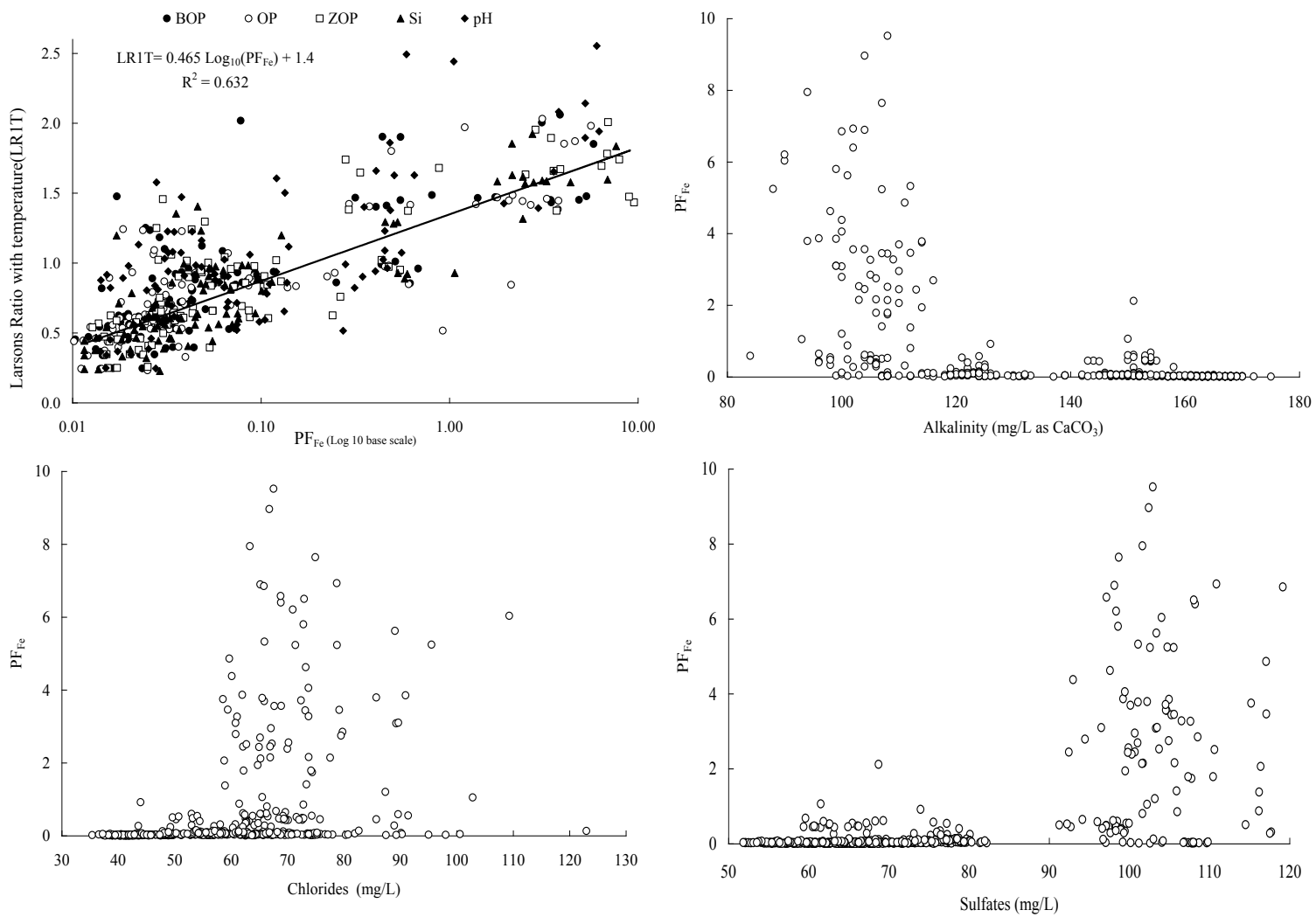


Figure 6.1 PF_{Fe} graphs with water quality
 Clockwise from top left: Alkalinity, Chlorides, Sulfates and LRIT.

Dissolved oxygen (D.O) and chlorine residual are oxidants in drinking water. Statistical analysis was made by Pearson's correlation, linear regression and ANOVA to evaluate correlation of EN parameters with D.O and (monochloramine) total chlorine residual(TCl₂) The influent D.O to the PDSs in this study varied from 6.6 to 10.9 (mg/L), while the lowest PDSs effluent D.O which was directed to the Cu corrosion loops was 4.1. Hence D.O was not considered to be low or rate limiting for Fe release and Fe corrosion was independent of D.O for this work. TCl₂ appeared to have a trend with PF_{Fe}, hence statistical models were developed for predicting TCl₂.

Regression models were developed for TCl₂-loss using TCl₂ influent (Cl₂INF) to the PDSs and PFFe. The effluent temperature was monitored continuously in the EN trailer and was averaged over the 16 hour period prior to water quality sampling and is denoted by T16. This period of 16 hours corresponds to the combined hydraulic retention time in unlined cast iron and galvanized steel sections of each PDS of 14 hours and approximately 2 hours for the PDS effluent to reach the EN trailer. Grab water quality samples taken from the PDS influent and effluent were also used to measure temperature and are denoted as INFTEMP and EFFTEMP respectively.

The models which were found statistically significant are shown in Table 6.6. Models with T16 or INFTEMP or EFFTEMP did equally well. Models with temperature only (# 9) did poorly than models with PFFe only (# 3).The model (# 7) shown in bold font in Table 6.6 is considered to be a representative model for use of Cl₂INF and PF_{Fe} to predict TCl₂-loss in the PDSs. The negative exponents a1 and Z for PFFe and INFTEMP respectively suggest that increase in either parameter would increase the TCl₂-loss with

the term $A \cdot PF^{a1} \cdot INFTEMP^Z$ representing the fraction of Cl_2INF coming out as the effluent (Cl_2EFF). The models indicate an increase in PF_{Fe} or $INFTEMP$ or both tends to decrease Cl_2EFF which is physically sound. This suggests that corrosion current variation as represented by PF_{Fe} results in a direct consumption of chlorine residual for the combined chlorine used in this study. The model shown in bold font in Table 6.6 is shown with actual data in Figure 6.2 for comparing a visual fit of the model.

Table 6.6 Total chlorine loss PF_{Fe} models

#	Model- TCl ₂ -loss =	a1	A	Z	R ²	S.E (mg/L)	p value
1	Cl ₂ INF*(1-(A*PF ^{a1} *T16 ^Z))	0.0279	0.0609	0.7093	0.23	0.64	<0.0001
2	Cl ₂ INF *(A*PF ^{a1} *T16 ^Z)	0.0279	0.0609	0.7093	0.67	0.64	<0.0001
3	Cl ₂ INF *(A*PF ^{a1})	0.0632	0.6224	-	0.6	0.7	<0.0001
4	Cl ₂ INF *(1-A*PF ^{a1})	-0.0832	0.3743	-	0.6	0.7	<0.0001
5	Cl ₂ INF *(1-PF ^{a1} *T16 ^Z)	-0.0708	-	-0.3035	0.64	0.66	<0.0001
6	Cl ₂ INF *(1-A*PF ^{a1} *T16 ^Z)	-0.0448	3.2757	-0.6624	0.67	0.64	<0.0001
7	Cl₂INF *(1-A *PF^{a1}*INFTEMP^Z)	-0.0593	2.1203	-0.5392	0.66	0.64	<0.0001
8	Cl ₂ INF *(1-A*PF ^{a1} *EFFTEMP ^Z)	-0.0652	1.3968	-0.4162	0.65	0.65	<0.0001
7	Cl ₂ INF *T16 ^Z *(1-A*PF ^{a1})	0.435	-0.269	-0.2336	0.54	0.75	0.0013
8	Cl ₂ INF *(1-A*PF ^{a1} *INFTEMP ^Z)	-0.0593	2.1203	-0.5392	0.66	0.63	<0.0001
9	Cl ₂ INF *T16 ^Z	-	-	0.184	0.42	0.84	<0.0001
10	Cl ₂ INF *PF ^{a1} *T16 ^Z	0.0736	-	-0.1427	0.57	0.73	<0.0001
11	Cl ₂ INF *(1- PF ^{a1} *T16 ^Z *(A1*BOP+A2*OP+A3*ZOP+A4*SI+A5*pH))	-0.0437	3.04 to 3.43	-0.6643	0.68	0.63	<0.0001

where * represents multiplication and a1 and Z are exponents.

- A1 = Coefficient for BOP
- A2 = Coefficient for OP
- A3 = Coefficient for ZOP
- A4 = Coefficient for SI
- A5 = Coefficient for pH controls
- BOP = BOP inhibitor dummy variable (0, 1)
- OP = OP inhibitor dummy variable (0, 1)
- ZOP = ZOP inhibitor dummy variable (0, 1)
- SI = Silica inhibitor dummy variable (0, 1)
- pH = pH controls dummy variable (0, 1)

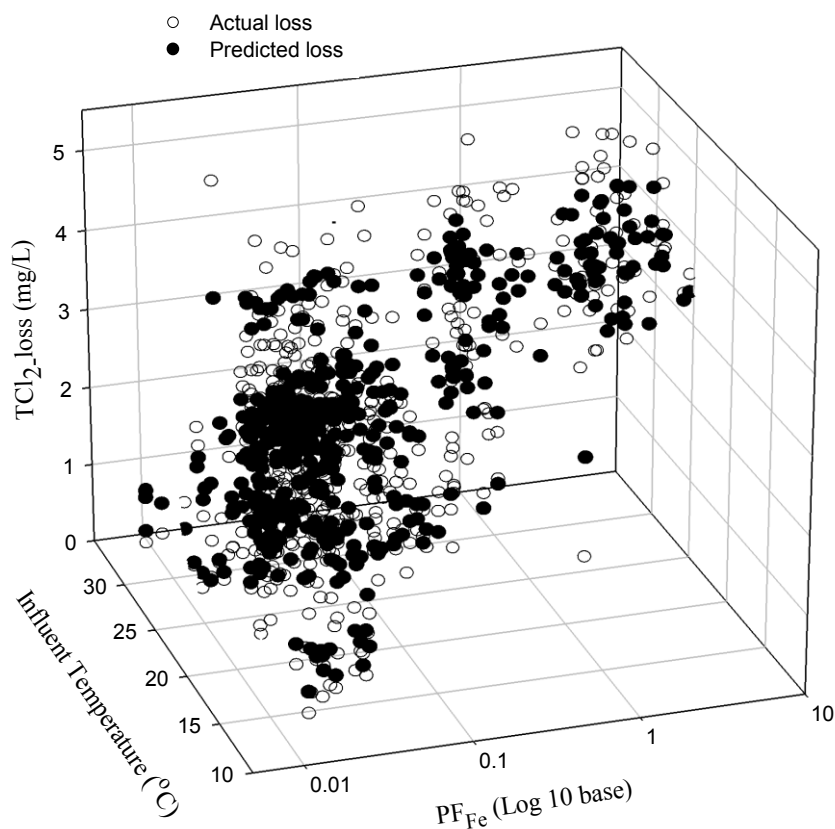


Figure 6.2 PF model predicted versus actual TCl₂-loss

The visual fit shown in Figure 6.2 suggests that though a wide scatter in actual TCl₂-loss occurred the model fitted the data well enough without any wide gaps for the range of temperature and PF_{Fe} in this study. These results are similar in nature to those of Frateur et al., (1999) wherein the authors showed that corrosion of cast iron correlated with consumption of free chlorine. Evaluation of the effect of inhibitor type for the model (# 11 in Table 6) showed that no improvement was obtained by considering inhibitor effects separately and PF_{Fe} alone was sufficient to correlate with TCl₂-loss. This is a tremendous advantage for potential field application of PF_{Fe} since this study had a

wide variation of water quality with respect to silicate and phosphate inhibitor types and doses likely to be encountered in real systems.

6.3.5 Statistical Fe release model development

Regression models were developed using EN parameters to predict both total (TFe) and dissolved (DFe) iron release. The models used dummy variables to segregate the effect of inhibitor dose by inhibitor type. The effects of the EN parameters and temperature were included in the model without regard to inhibitor type. Models using all 12 EN parameters did not converge. Subsequent modeling attempts using reduced sets of EN parameters eventually produced a model based on LPRCR, HMCR, HMCR and PF. The general form of the EN power model with dummy variables for inhibitor type is shown in Equation 6.3. The remaining 8 EN parameters were added one at a time and are represented by EN^{ai} in Equation 6.3, where EN represents either B, B_a, B_c, PSKW, PKRT, ISKW, IKRT or RSOL. The dummy variables shown in Equation 6.3 represent the effects of influent concentrations of total phosphate or silicate. The temperature used for all EN models was T16. The resulting models have the dummy variables abbreviated as DV for convenience, and are shown in Equation 6.4.

$$Me = (LPRCR_{Me}^{a1} \times HMCR_{Me}^{a2} \times ECNCR_{Me}^{a3} \times PF_{Me}^{a4} \times EN_{Me}^{ai}) \times (a \times \text{OP} \times P^f + b \times P \times P^g + c \times \text{OP} \times P^h \times n^i + l \times i \times iO_2^j + d \times H_s) \times emp^o \quad \text{Equation 6.3}$$

where Me = Fe
 $a1$ = LPRCR_{Me} exponent
 $a2$ = HMCR_{Me} exponent
 $a3$ = ECNCR_{Me} exponent
 $a4$ = PF_{Me} exponent

EN_{Me}^{ai}	= One of the terms associated with exponents a5, a6, a7, a8, a9, a10, a11 or a12
a5	= B_{Me} exponent
a6	= Ba_{Me} exponent
a7	= Bc_{Me} exponent
a8	= $PSKW_{Me}$ exponent
a9	= $PKRT_{Me}$ exponent
a10	= $ISKW_{Me}$ exponent
a11	= $IKRT_{Me}$ exponent
a12	= $RSOL_{Me}$ exponent
BOP	= BOP inhibitor dummy variable (0, 1)
OP	= OP inhibitor dummy variable (0, 1)
ZOP	= ZOP inhibitor dummy variable (0, 1)
Si	= Silica inhibitor dummy variable (0, 1)
pH _s	= pH control dummy variable (0, 1)
TP	= total phosphorus, mg/L
Zn	= zinc, mg/L
SiO ₂	= silica, mg/L as SiO ₂
Temp	= Temperature (T ₁₀), °C
a	= BOP dummy variable coefficient
b	= OP dummy variable coefficient
c	= ZOP dummy variable coefficient
d	= Silica dummy variable coefficient
e	= pH control dummy variable coefficient
f	= TP exponent associated with BOP dummy variable
g	= TP exponent associated with OP dummy variable
h	= TP exponent associated with ZOP dummy variable
i	= Zn exponent associated with ZOP dummy variable
j	= SiO ₂ exponent associated with Silica dummy variable
o	= Temperature exponent

$$DV = (a \times BOP + b \times OP + c \times ZOP + d \times Si + e \times pH_s + f \times TP^f + g \times TP^g + h \times TP^h + i \times Zn^i + j \times SiO_2^j + o \times Temp^o) \quad \text{Equation 6.4}$$

The statistically significant (p<0.05) empirical EN models developed for TFe and DFe release in this study are shown in Table 6.7. These models were reduced by discarding any independent variables with p >0.05, which generated the TFe model shown in bold font in Table 6.7. The model fit for TFe was with a R² of 0.27 which is poor but is similar to the fit with a R² of 0.29 from the water quality model developed from this study (Taylor et al., 2007) This suggests that EN parameters can be used as well

as water quality to predict TFe release in this work. The best fit EN and water quality models for TFe release in their full forms are presented in Equation 6.6 and Equation 6.7 respectively.

Table 6.7 Iron release EN models

Model	R ²	S.E (mg/L)	Model p value	Parameter** of highest p value	p value**
TFe=(ECNCR _{Fe} ^{a3} *PF _{Fe} ^{a5})*DV	0.27	0.07	<1e-4	ECNCR _{Fe}	0.054
TFe=(PF_{Fe}^{a5})*DV	0.27	0.07	<1e-4	PF_{Fe}	<1e-4
DFe=(LPRCR _{Fe} ^{a1} *HMCR _{Fe} ^{a2} *ECNCR _{Fe} ^{a3} *RSOL _{Fe} ^{a12})*DV	0.46	0.03	<1e-4	ECNCR _{Fe}	0.043
DFe=(LPRCR _{Fe} ^{a1})*DV	0.43	0.03	<1e-4	LPRCR _{Fe}	<1e-4
DFe=(HMCR_{Fe}^{a2})*DV	0.43	0.03	<1e-4	HMCR_{Fe}	<1e-4
DFe=(ECNCR _{Fe} ^{a3})*DV	0.42	0.03	<1e-4	ECNCR _{Fe}	<1e-4

where * represents multiplication
DV= Dummy Variable terms shown in (4).
S.E is the standard error of prediction.
Bold font indicates model evaluated as the best fit.

$$\begin{aligned}
TFe = & (PF_{Fe}^{0.0694}) \times 0.240 \times BOP \times TP^{-.071} + 1.277 \times OP \times TP^{0.047} \\
& + 1.239 \times ZOP \times TP^{-.088} \times Zn^{-.157} + 1.071 \times Si \times SiO_2^{0.456} \\
& + 1.334 \times pH_s \times Temp^{-.144}
\end{aligned}
\tag{Equation 6.5}$$

where TFe = total iron, mg/L
PF_{Fe} = pitting factor for iron (unit less)
BOP = BOP inhibitor (0, 1)
OP = OP inhibitor (0, 1)
ZOP = ZOP inhibitor (0, 1)
Si = Silica inhibitor (0, 1)
pH_s = pH controls (0, 1)
TP = total phosphorus, mg/L as P
Zn = zinc, mg/L
SiO₂ = silica, mg/L as SiO₂

Temp = Temperature (T_{16}), °C

$$\begin{aligned}
 TFe = & 0.495BOP \times P^{-.104} + 1.593OP \times P^{0.047} & \text{Equation} \\
 & + 1.470ZOP \times P^{-.1073} \times n^{-.180} + 1.122Si \times iO_2^{0.528} + 1.661pH_s) & 6.6 \\
 & \times Alk^{-.457} \times Cl^{0.345} \times Fe_{inf}^{0.136}
 \end{aligned}$$

where *TFe* = total iron, mg/L
Alk = alkalinity, mg/L as CaCO₃
Cl = chloride, mg/L
Fe_{inf} = influent iron, mg/L

The EN models have significant terms for ECNCR_{Fe} and PF_{Fe} both indicate that Fe corrosion was dependent not only on general corrosion but also likely depended on localized corrosion. The exponent for PF_{Fe} is positive, which means that TFe release will increase as PF_{Fe} increases. The exponent on temperature is negative, which means increasing temperature decreases Fe release in this work. A change in temperature from 10°C to 30°C which is the range observed in this study would reduce the temperature effect by the ratio (30/10)^{-0.144} i.e. by 0.85, and decrease the model predicted TFe release by 15 %.

Each corrosion control strategy (inhibitor or pH elevation) has different contributing terms, multiplied by the dummy variables, which adjust the predicted Fe concentration as a function of the corrosion control strategy. Phase I Fe release versus temperature by inhibitor type is shown in Figure 6.3. The data shows that all TFe concentrations exceeding 0.2 mg/L in Phase I were for inhibitors and not for pH controls. The few spikes of Fe exceeding 0.3 mg/L i.e. the secondary standard were for ZOP and Si inhibitors only. Phase I had a blend with high alkalinity which mitigates Fe release. Hence the Phase I TFe release data indicates that the inhibitor addition caused an initial

release of TFe, which did not continue in subsequent phases. Release of materials from distribution systems is not uncommon during an initial period following inhibitor addition. However, the initial release of TFe may have biased the relationship between Fe release and temperature as Fe release was not expected to decrease with increasing temperature.

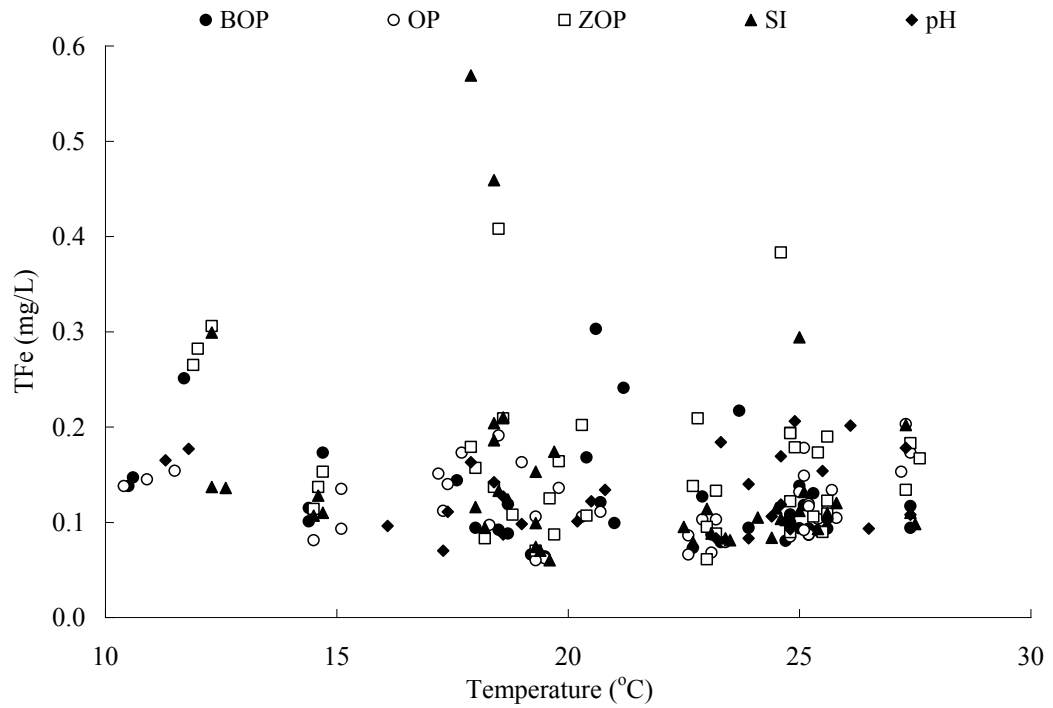


Figure 6.3 Temperature vs TFe by phase

DFe models were also developed using the same form as was used in development of the TFe models. The $HMCR_{Fe}$ model was selected for DFe and had a $0.43 R^2$, which is better when comparable to $0.37 R^2$ from the water quality model. The DFe models using $HMCR_{Fe}$ and water quality are shown in Equation 6.7 and Equation 6.8 respectively. The $HMCR_{Fe}$ model indicates DFe release will increase as $HMCR_{Fe}$ increases and decrease as temperature increases. The water quality model suggests that

alkalinity and influent Fe contribute to DFe concentrations, as shown by the positive exponent on those terms in the model. The model also suggests that increases in chloride concentration and temperature will mitigate DFe concentrations as they increase.

$$\begin{aligned}
 DFe = & (HMCR_{Fe}^{0.486}) \times 246.71 \times BOP \times TP^{-.128} + 57.63 \times OP \times TP^{0.275} & \text{Equation} \\
 & + 142.92 \times ZOP \times TP^{-1.534} \times Zn^{0.109} + 14.79 \times Si \times SiO_2^{0.188} & 6.7 \\
 & + 72.21 \times pH_s \times Temp^{-.22}
 \end{aligned}$$

$$\begin{aligned}
 DFe = & 3.82 BOP \times TP^{-.027} + 1.91 OP \times TP^{0.178} + 1.94 ZOP \times TP^{-.760} \times Zn^{0.313} & \text{Equation} \\
 & + 1.38 Si \times SiO_2^{0.012} + 1.62 pH_s \times Alk^{2.10} \times Cl^{-.76} \times Fe_{inf}^{0.245} \times Temp^{-.36} & 6.8
 \end{aligned}$$

The actual versus predicted DFe release using the $HMCR_{Fe}$ model is shown in Figure 6.4 for all phases. A change in temperature from 10°C to 30°C would reduce the temperature effect by the ratio $(30/10)^{-3.22}$ i.e. by a ratio of 0.03 and decrease the model predicted DFe release by 97 %. This seems counterintuitive but is consistent with Figure 5 which shows DFe release by phase. A detailed analysis of data showed that DFe release increased in the presence BOP, ZOP and Si inhibitors relative to pH control on several occasions in Phase I and was attributed to starting of inhibitor addition which most likely disrupted existing scales in the PDSs.

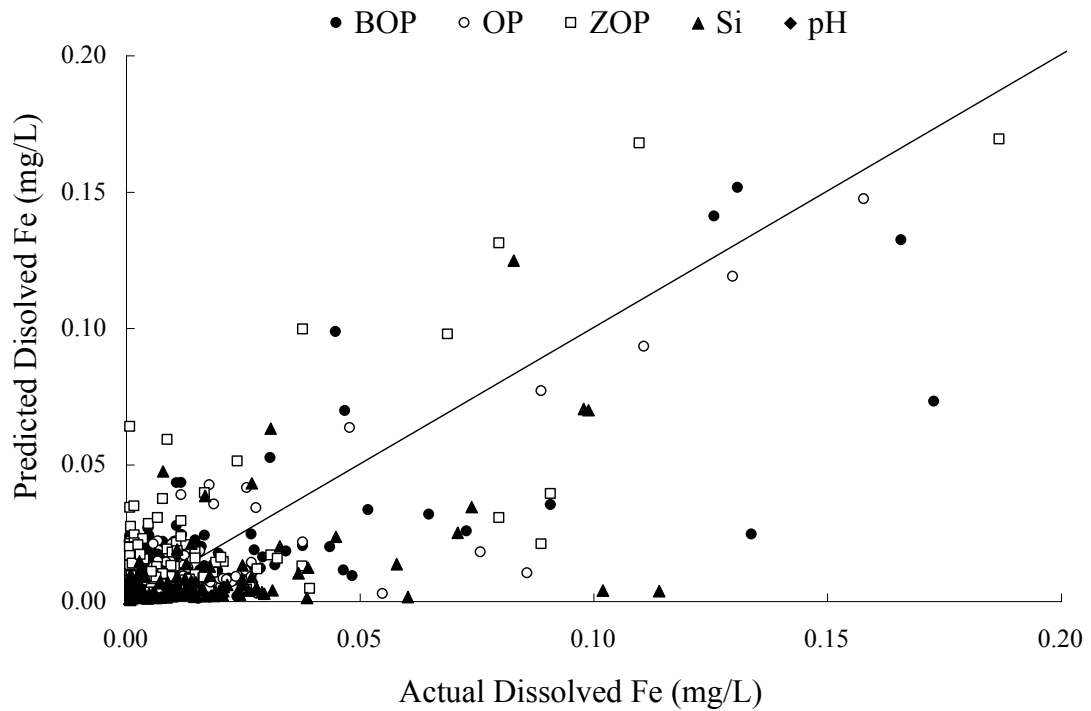


Figure 6.4 EN model predicted versus actual DFe.

6.4 Conclusions

- The EN electrode areas near the probe body (areas A & B) had thick, loose and porous looking corrosion products (CPs) with poor Ca & O surface content while areas near the tips (areas C & D) had significantly higher Ca & O. This was observed irrespective of inhibitor type and dose with pH elevation to pHs+0.3 being as effective as inhibitor addition for Fe release mitigation. This is attributed to ineffective scouring of porous CPs near the EN probe body and effective scouring of loose CPs near the tips, both observations for standing water conditions.
- EN measures the corrosion current which represents electron transfers due to all oxidation reactions on a metal surface, without regard to whether metal is

released to the water or incorporated in an oxidized scale. Hence a direct relation between EN and Fe release in drinking waters may not be possible.

- Fe corrosion was found to be dependent on both general and localized corrosion with the latter likely to be more important for particulate Fe release which comprised of most of the TFe in this study.
- The EN model did equally well as the water quality model developed for TFe release but both models had a poor fit. PF_{Fe} was found to be correlated with alkalinity, chlorides, sulfate, and a modified Larson's ratio.
- PF_{Fe} was used successfully to develop empirical models to predict monochloramine residual loss through the PDSs and the models provided a reasonably good fit. PF_{Fe} may not represent pitting or localized corrosion but represents the variation in general corrosion rate.
- EN regression models were found to provide a reasonable fit to DFe release. The best model used $HMCR_{Fe}$ alone and had a modest fit with a R^2 of 0.43 but did better than the water quality model developed from this study.
- The data indicate there may be a concern for ZOP and SiO_2 inhibitors which increased Fe release during the first few weeks of inhibitor dosing.

6.5 Recommendations

- The use of EN monitoring in actual distribution systems is worthy of investigation to predict chlorine residual loss, estimate Fe release and indicate significant changes in alkalinity, chlorides or sulfates.

- Monitoring periods of a few weeks may be sufficient to establish a baseline for correlation between EN and water quality. EN application with a wider range of water quality parameters than used in this study would enable estimating correlation likely to be encountered in real distribution systems.
- EN monitoring is a real-time, remote access technology and should be used to proactively identify water quality change in distribution systems.

6.6 Acknowledgements

The University of Central Florida (UCF) and UCF project team wish to express their sincere gratitude to Tampa Bay Water (TBW); Hillsborough County, Fla.; Pasco County, Fla.; Pinellas County, Fla.; City of New Port Richey, Fla.; City of St. Petersburg, Fla.; and City of Tampa, Fla. which are the Member Governments of TBW and the American Water Works Association Research Foundation (AwwaRF) for their support and funding for this project. Special thanks to, Robert M. Powell the Pinellas County, Fla. Director of Laboratory for support and grant for EN research; Christine Owen the Water Quality Assurance Officer and TCP project coordinator for TBW and Roy Martinez the AwwaRF Project Officer.

6.7 References

1. Chen T.Y, Banks R.H, Breshears J, Nicolich S.N and Cicero D.M. Ondeco Nalco. 2002. Reprint R-815. Corrosion monitoring techniques for industrial cooling water and process systems. First presented at the International water conference, October 20-24, 2002, Pittsburg PA.
2. Cottis .R and Turgoose .S, 1999. Electrochemical impedance and noise. NACE international. Corrosion testing made easy. ISBN 1-57590-093-9.

3. Duranceau, S.J., D. Townley, and G.E.C. Bell. 2004. Optimizing Corrosion Control in Water Distribution Systems. Awwa Research Foundation Denver, Colorado.
4. Eden D.A 1994. Comments on: Electrochemical noise analysis of iron exposed to NaCl solutions of different conductivity. *Journal of Electrochemical Society*. 141(5), 1402-1404.
5. Eden D.A 1998. Electrochemical Noise-The first two octaves. Corrosion 1998. National Association of Corrosion Engineers (NACE) conference. Paper No 386.
6. Frateur I., Deslouis C., Orazem M.E. and Tribollet B. 1999. Modeling of cast iron/ drinking water system by electrochemical impedance spectroscopy. *Electrochimica Acta*. 44:4445-4356.
7. Haruna T, Morikawa Y, Fujimoto S and Shibata T. 2003. Electrochemical noise analysis for estimation of corrosion rate of carbon steel in bicarbonate solution. *Corrosion science*. 45:2093-2104.
8. MacQuarrie D. M , Mavinic D.S., and Neden D.G. 1997. Greater Vancouver Water District drinking water corrosion inhibitor testing. *Canadian journal of civil engineering*. 24: 34-52.
9. Norton, C.D. and LeChevallier M.W. 1997. Chloramination: It's Effect on Distribution System Water Quality. *Journal AWWA*, 89(7):66-77.
10. Sun X and Yang L. 2006. Real-time monitoring of localized and general corrosion rates in drinking water systems utilizing coupled multielectrode array sensors. Corrosion, NACE Annual conference San Diego CA. Paper No 6094.
11. Taylor, J.S., J.D. Dietz, A.A. Randall, C.D. Norris, A. Alshehri, J. Arevalo, X. Guan, P. Lintereur, D. MacNevin, E. Stone, R. Vaidya, B. Zhao, S. Glatthorn and A. Shekhar. 2007. Control of distribution system water quality in a changing water quality environment using inhibitors. Draft final report submitted to AWWA Research Foundation Denver CO and Tampa Bay Water. (TBW II report)
12. Taylor, J.S., J.D. Dietz, A.A. Randall, S.K. Hong, C.D. Norris, L.A. Mulford, J.M. Arevalo, S. Imran, M. Le Puil, S. Liu, I. Mutoti, J. Tang, W. Xiao, C. Cullen, R. Heaviside, A. Mehta, M. Patel, F. Vasquez, and D. Webb. 2005. Effects of Blending on Distribution System Water Quality. AWWA Research Foundation Denver CO and Tampa Bay Water. (TBW I report)
13. Takasaki S and Yamada S. 2006. Effects of temperature and aggressive ions on carbon steel in potable water. *Corrosion science*.
14. Vatankhah G, Drogowska M and Menard H. 1998. Electrodissolution of iron in sodium sulfate and sodium bicarbonate solutions at pH 8. *Journal of applied electrochemistry*. 28:173-183.
15. US Environmental Protection Agency. 1993. Seminar Publication: Corrosion of lead and copper in drinking water. EPA/625/R-93-001.
16. Volk C, Dundore E, Schiermann J and LeChevallier M. 2000. Practical evaluation of iron corrosion control in a drinking water distribution system. *Water Research*. 54(6)1967-1974.

^{CET} SmartCET is the commercial name of the EN equipment used to monitor corrosion parameters in this study. SmartCET is made by InterCorr international, Houston Texas 77014.

7 CORRELATING Pb RELEASE WITH ELECTROCHEMICAL CORROSION MONITORING IN A CHANGING WATER QUALITY ENVIRONMENT

ABSTRACT

This one year study investigated the use of electrochemical corrosion monitoring (EN) to correlate with Pb release in presence and absence of phosphate (P) and silicate (Si) inhibitors using pilot distribution systems (PDSs). Lead release was mostly in particulate form and EN parameters correlated with chloride to sulfate mass ratio (CSMR). Variation in corrosion current which was represented by PF_{Pb} in this study correlated with sulfates which mitigated Pb release. Empirical regression models using EN parameters were developed for dissolved and total Pb; these showed that both general and localized corrosion were important. The EN models are in agreement with the water quality models developed from this study and offer an advantage in being an on-line tool to identifying the potential of adverse Pb release and estimate water quality changes in real systems.

Keywords CSMR, Electrochemical Corrosion Monitoring, Pb release.

7.1 Introduction

It is generally accepted that Lead (Pb) release in drinking water systems has significant health impacts on consumers. Pb release studies on tap water have been conducted previously to investigate the impacts of stagnation time, pH, alkalinity, and

orthophosphate (Schock 1980, 1989; Schock & Gardels 1983; Schock et al., 1996) and recently by Korshin et al., (2005) for the impact of organic matter. Preventing corrosion and mitigating corrosion product (CP) release is an important task facing the drinking water community. USEPA (1993) states that electrochemical techniques though are not a cumulative measure of changes occurring on a metal surface do provide a snapshot of the change at a particular time and are particularly useful for many process control operations or screening programs. Monitoring corrosion rates using methods that take advantage of electrochemical processes are typically fast compared to alternatives of weight loss coupons, electrical resistance probes, or direct inspection by visual, ultrasonic, or nuclear means (Duranceau et al., 2004). However, correlating corrosion rate monitoring information to CP concentration, although highly desirable, is not yet fully understood. This article demonstrates the use of EN parameters that can be correlated to water quality and can be used to estimate Pb release.

Tampa Bay Water (TBW) manages drinking water resources for six member governments (MGs) on the west coast of central Florida: the cities of New Port Richey, St. Petersburg, and Tampa, and Hillsborough, Pasco, and Pinellas counties; and serves nearly two million consumers at a 250 MGD average daily demand. Historical use of ground water (GW) by TBW had mandated the use of alternative sources as desalinated seawater and treated surface water (SW) for limiting GW withdrawals for aquifer protection. The impact of new source waters and their blends on water quality changes were evaluated Taylor et al.(2005) under a tailored collaboration project (TCP) called as TBW I, conducted by the University of Central Florida (UCF) and funded by TBW and American water works association research foundation (AwwaRF). In this follow up one-

year TCP called TBW II, the effect of corrosion inhibitors to mitigate adverse impacts in distribution systems that receive blended finished waters produced from GW, SW and saline sources (RO) was investigated. Four different corrosion inhibitors were selected and added to the pilot distribution system (PDS) built in 2001 during TBW I. These were blended ortho-phosphate (BOP), ortho-phosphate (OP), zinc ortho-phosphate (ZOP), and silicate. Each phosphate based inhibitor was used at three target doses of 0.5, 1, and 2 mg/L as P and the silicate inhibitor was applied at targets of 3, 6, and 12 mg/L as SiO₂.

7.1.1 Literature on Pb corrosion

Corrosion monitoring techniques either apply an external signal of current and or voltage and study the response or just evaluate the natural fluctuations in current/voltage. The former is used in linear polarization resistance (LPR) and harmonic distortion analysis (HDA); while the latter is employed in electrochemical noise (ECN) technique. Naturally occurring fluctuations of current or potential are termed as noise when referring to ECN measurements. Various corrosion processes are reported to generate distinct noise characteristics in the time domain (Eden, 1998). USEPA (1993) states that electrochemical techniques though are not a cumulative measure of changes occurring on a metal surface do provide a snapshot of the change at a particular time and are particularly useful for many process control operations or screening programs. USEPA (1993) also reports that electrochemical testing techniques work well on lead (Pb) and Pb-Sn solders but the absolute accuracy can be low unless a rather involved potentiodynamic scan is involved. From previous studies a PF \ll 1 is considered to be an indication of a more or less constant general corrosion rate where as PF consistently

approaching one may indicate actual pitting or a widely varying general corrosion (Cottis & Turgoose, 1999; Eden, 1994).

From the TBW I study (Taylor et al., 2005) Pb release increased with an increase in chlorides and temperature and a decrease in sulfates while the effects of pH and alkalinity were not clearly elucidated due to confounding effects (Tang et al., 2006; and Taylor et al., 2005). According to McNeill and Edwards (2004) OP and poly-phosphate (PP) tended to decrease particulate Pb possibly due to formation of lead-phosphate solid. They report that at pH 7.2 and increase in alkalinity from 15 to 45 had no apparent effect on dissolved Pb while particulate Pb release was reduced.

Chlorides and sulfate can also affect Pb corrosion by complex formation and or other mechanism (AWWA, 1996). Edwards et al., (1999) reported from utility data that the 90th percentile Pb concentration was higher when the chloride to sulfate mass ratio (CSMR) was high; CSMR defined as ratio of mg/L of chlorides to sulfates respectively. Dudi and Edwards (2005) investigated the effect of galvanic connections between copper and lead materials and report that a higher CSMR increase galvanic attack on Pb and anodic areas on Pb experienced a local pH drop which increased the galvanic attack. Dodrill and Edwards (1995) reported that 12 out of 12 utilities with a CSMR below 0.58 met the 15 µg/L Pb action limit, where as only 4 out of 11 utilities with a higher CSMR were in compliance. Triantafyllidou and Edwards (2006) reported increased Pb leaching with a higher CSMR for Pb solder galvanically connected to copper and the adverse effect of a higher CSMR were dramatic even in presence of orthophosphate.

7.2 Experimental

7.2.1 Field facility

The facility was built in 2001 and 14 hybrid pilot distribution systems (PDSs), copper loops, corrosion cradles, Electrochemical Corrosion (EN) monitoring trailer and treatment processes to obtain finished waters from this facility were used in this work. To maintain integrity of the system finished GW was fed to the PDSs and copper loops when the facility was not used after TBW I and before start of this study i.e. from 2003 till fall 2005. The PDSs were operated to maintain a two-day hydraulic residence time (HRT) and their complete description can be found elsewhere (Taylor et al., 2005, 2007). The effluent from the PDSs was split in two parts, one part was directed to the copper corrosion loops and the other part was directed to the EN Trailer.

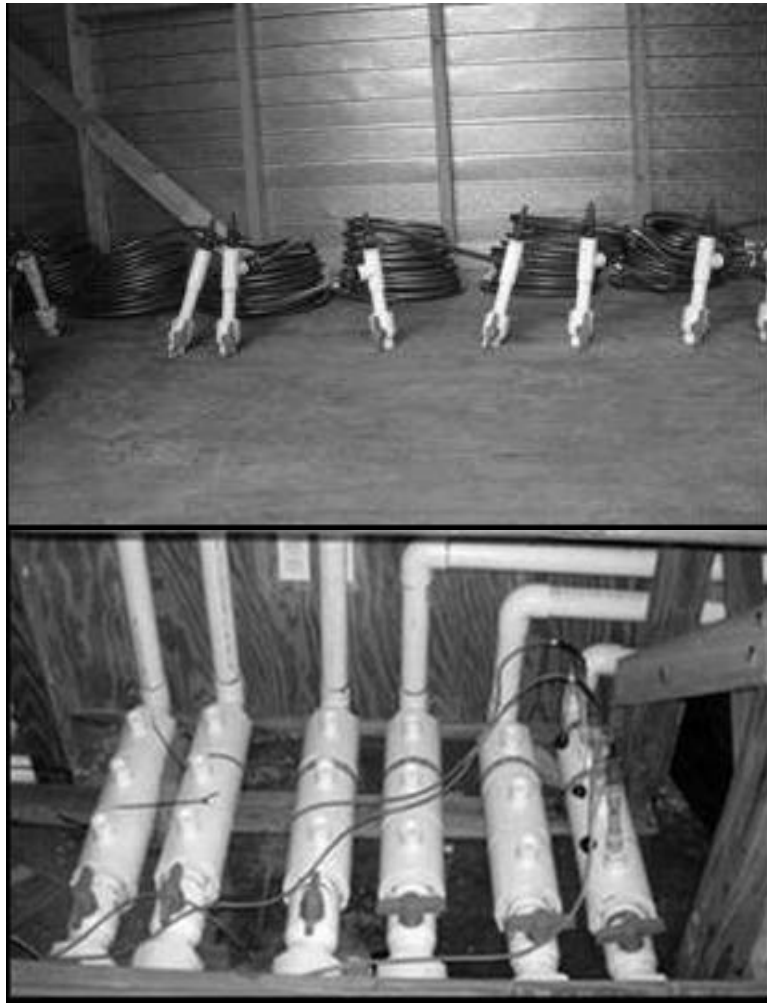
The corrosion loop consisted of 30 feet (9.1 m) copper tubing with a diameter of 1.6 cm (5/8 inch), which could hold approximately 1.8 L of water. One lead-tin (Pb-Sn 50:50 by weight) coupon was placed within the copper tubing between two standard copper tube fittings (brass) for each loop system. All other fittings and materials were PVC or other plastic polymers. The coupons had a surface area of 3.38 square inches (21.8 cm²) and are commonly used for corrosion studies throughout the United States. Assuming that 0.125 inch (3.2 mm) bead on the inside of each 0.5 inch (1.27 cm) diameter joint was the surface area exposed to water using solder, the coupon surface area was equivalent to 17 joint-ends or 7 to 8 fittings and was reasonable for a kitchen sink.

The effluent Pb concentration was measured from the copper loops to mimic Pb CP release concentrations at tap. The Pb-Sn EN probes and corrosion coupons were

housed in 4 inch diameter PVC pipes that were located in the EN trailer. These PVC pipes were referred to as Nadles. EN probes were used to monitor corrosion rates of Fe, Cu & Pb-Sn. The probes were placed with the more noble metal upstream (Cu>Fe>Pb-Sn) to minimize any galvanic corrosion from particulate release and subsequent deposition on the downstream metal. Pb-Sn probes had three electrodes with an area of 4.67 cm² (0.72 in²) each, atomic weight of 162.95 and a density of 7.86 g/cm³. Electrodes were numbered sequentially as A, B, and C on the probe body for identification. A picture of the copper loops and EN probe connection in the Nadles is presented in Photograph 7.1.

7.2.2 Electrochemical corrosion rate measurement

Corrosion data was collected continuously for at least a 6 hour standing period to correlate with samples taken for Cu from the corrosion loops. Each EN probe had three Cu electrodes. All electrodes had an area of 4.67 cm² (0.72 in²) each, atomic weight of 63.54 and a density of 8.89 g/cm³. Electrodes were numbered sequentially as A, B, and C on the probe body for identification. EN monitoring was conducted using commercially available equipment² which monitored corrosion rates continuously, with cycles of 430 seconds. Within each cycle 300 seconds were used for electrochemical noise (ECN), 100 seconds for linear polarization resistance (LPR), and 30 seconds for harmonic distortion analysis (HDA). The corrosion rates from these three techniques are abbreviated as ECNCR, LPRCR and HMCR respectively and are reported in units of mils/yr, mpy (1 mpy = 0.0254 mm/yr).



Photograph 7.1 Copper corrosion loops (top) & EN probe connection in Nadle (bottom)

7.2.3 Operation

This study was conducted over a three year period, which included 12 months of field operations and data collection. Introduction of a blend of GW, SW, and RO was initiated in December 2005. This project was divided into 4 phases; each of three months duration started with inhibitor addition to the blend from February 2006. The PDSs received the same blend composition for a three month period or phase after which the

blend composition was changed. Similar blends were used during phases I and III to evaluate the effect of seasonal conditions on the PDS.

The individual sources were chloraminated to produce a residual of approximately 4.5 to 5.0 mg/L, and additions were made to the blend to maintain the desired combined monochloramine residual of about 5 mg/L. The target doses of the inhibitors were defined as: 0.5, 1.0, and 2.0 mg/L as P for the phosphorus-based inhibitors (approximately zero background). The conditioning doses of 10, 20, and 40 mg/L as SiO₂ above the background concentration for the silicate-based inhibitor were used for about 1 month and were changed to 3, 6, and 12 mg/L because the 20 and 40 mg/L doses were causing CaCO₃ precipitation within the PDS.

The Nadles were flushed daily and before each monitoring event with 5 pipe volumes of water at an average velocity of 1 ft/s (0.3 m/s). The equipment connection to the EN probes was switched manually between the Nadles twice a day with a stagnation time of at least 6 hours. The copper corrosion loops were also flushed with 2 gallons (7.6 L) of water every morning and first flush samples after 6-7 hours stagnation were collected weekly for metal concentration. The first liter sample was shaken to mix thoroughly and split into two parts with one part for total metals and second part for dissolved metals by filtering it on-site through a 0.45 µm membrane filter.

EN monitoring was conducted using commercially available equipment¹ which monitored corrosion rates continuously, with cycles of 430 seconds. Within each cycle 100 seconds were used for LPR, 30 seconds for HDA and 300 seconds for ECN. The corrosion rates from these three techniques are abbreviated as LPRCR, HMCR and

ECNCR respectively and are reported in units of mils/yr, mpy (1 mpy = 0.0254 mm/yr).

The parameters obtained from EN monitoring as output are displayed in Table 7.1.

Table 7.1 Output parameters from electrochemical corrosion monitoring

Symbol	Parameter name	mpy
LPRCR	Linear Polarization Resistance Corrosion Rate	mpy
HMCR	Harmonic Distortion Analysis Corrosion Rate	mpy
ECNCR	Electrochemical Noise Corrosion Rate	mpy
PF	Pitting Factor- evaluated from electrochemical noise & harmonic distortion analysis	-
<i>B</i>	Stearn Geary constant -evaluated from the Harmonic Distortion Analysis	Volts
<i>Ba</i>	Anodic tafel slope	Volts/decade
<i>Bc</i>	Cathodic tafel slope	Volts/decade
PSKW	Skew of potential	-
PKRT	Kurtosis of the potential	-
ISKW	Skew of current	-
IKRT	Kurtosis of the current	-
RSOL	Solution resistance	ohms

Pb-Sn electrodes from all 14 Nadles were exposed to varying blends for the project duration of one year and subsequently examined by Scanning Electron Microscope (SEM) and Energy Dispersive Spectroscopy (EDS) for surface characterization of chemical scales. SEM visually magnifies the physical structure of the scale surface for identification of the morphology of the corrosion products. EDS identifies the elemental composition of the surface layer.

7.2.4 Quality assurance and control

Samples were collected and analyzed in the field and at the UCF laboratory. Metal concentration were measured in the UCF laboratory by inductively coupled plasma (ICP) mass spectrometer and water quality analysis was done in accordance with

Standard Methods (1999). Quality assurance and quality control of both the laboratory and field determinations of water quality parameters was established by duplicating analyses of at least 10% of the samples. Blind duplicates and spikes were also used to determine the accuracy of measurements. Dynamic control charts were used to determine whether the results were acceptable. A comprehensive overview of quality control procedures, analytical results and supplementary discussion of associated PDS sampling events and process sampling events over the duration of this entire project is given elsewhere (Taylor et al., 2007).

7.3 Results and discussion

7.3.1 Water quality variations by phase

The average water quality of the blends and corrosion rates are shown by phase in Table 7.2. Unless otherwise noted, data is reported as weekly averages for each PDS over the study duration, which produced 653 paired observations of Pb release concentration and EN parameters. Similarly unless otherwise stated discussion of alkalinity is in units of mg/L as CaCO₃ and chlorides and sulfates in mg/L and corrosion rates in mpy. From Table 7.2 it is observed that the magnitude of LPRCR_{Pb} and HMCR_{Pb} were similar whereas the magnitude of ECNCR_{Pb} was higher.

Duranceau et al., (2004) investigated the application of electrochemical corrosion monitoring using the electrochemical noise (ECN) method using Pb-Sn solder electrodes at four utilities with some water quality. Their study concluded that that for some conditions, 'inhibition' i.e. addition of the corrosion inhibitor ZOP at 1 mg/L as P increased the ECN corrosion rate.

In review of the observations of Duranceau et al., (2004) it is obvious that numerous reactions are expected to occur on a metal surface in drinking water environment. Metal scale formation, oxygen consumption, hydrogen generation, chlorine reduction, biological oxidation and metal oxidation are examples of possible reactions that change surface potential (voltage) and result in current flow, which generates ECN and are not direct measurements of metal release. Hence ECNCR can over estimate the actual corrosion rate of metal dissolution because ECNCR represents the total current activity on a metal surface with all activity assumed to cause metal corrosion.

Table 7.2 TBW II Water quality by phase

Parameter	Project Minimum	Project Maximum	Phase I	Phase II	Phase III	Phase IV
Alkalinity (mg/L as CaCO ₃)	84	175	163	109	154	127
Calcium (mg/L as CaCO ₃)	54	220	202	105	206	168
Dissolved Oxygen (mg/L)	6.6	10.9	8.7	8	8	9.1
Chloride (mg/L)	35	123	47	59	65	56
pH	7.4	9.1	7.9	7.9	7.9	7.8
Silica (mg/L)	4	65.0*	10.9	5.1	10.2	6.4
Sulfate (mg/L)	52	119	72	112	74	85
Sodium (mg/L)	5	53	7	37	40	32
TDS (mg/L)	338	436	365	388	413	378
Temperature (°C)	10.4	29.7	21.2	25.5	24.7	19.6
Total Phosphorus (mg/L as P)	0	3.36*	0.2	0	0	0.1
UV-254 (cm ⁻¹)	0.007	0.105	0.071	0.069	0.077	0.063
Zinc (mg/L)	0.001	0.793	0.031	0.023	0.04	0.037
LPRCR _{Pb} (mpy)	0.001	4.144	0.036	0.013	0.005	0.003
			to	to	to	to
			3.491	1.077	1.777	0.709
			0.061	0.691	0.962	0.569
HMCR _{Pb} (mpy)	0.001	5.469	to	to	to	to
			3.479	3.434	1.898	1.162
			0.963	0.759	1.737	0.142
ECNCR _{Pb} (mpy)	0.02	723.52	to	to	to	to
			66.643	188.682	63.004	98.635
			0.092	0.682	0.111	0.035
PF _{Pb}	0.012	6.169	to	to	to	to
			0.304	5.005	0.416	0.186

Note: Average values or range of average values reported for Phase I through IV

Silicate start up doses from 20-60 mg/L as SiO₂, maintenance dose from 3-12; background SiO₂ from 4.01 to 13.56 mg/L.

7.3.2 Observations by photographs, SEM and EDS of electrodes

The electrodes showed a distinct lack of general scale but a thin shiny film was apparent on the surface. There were distinct spots or regions on the surfaces which showed

presence of a distinct scale and corrosion products (CPs). The SEM showed structures with specific morphology and composition in distinct areas. EDS showed that the P or Si content of the surface of electrodes increased with increasing amount of the P or Si dose respectively. Thin hexagonal plates which are suspected to be basic lead carbonate i.e. hydrocerussite [$\text{Pb}_3(\text{CO}_3)_2(\text{OH})_2$], were detected in most of the samples.

The presence of hydrocerussite/cerussite as the predominant Pb species was confirmed by X-ray photon spectroscopy (XPS) in this study (Taylor et al., 2007). These plates were not found randomly scattered but were heavily concentrated in distinct growth areas. These results are consistent with those of Korshin et al., (2000). In this study the presence of BOP inhibitor seemed to increase the occurrence of hydrocerussite while OP & ZOP had the opposite effect. These results are consistent with those of Liu et al., (2006) wherein the authors used free chlorine to study oxidation of Pb(II). They reported that hydrocerussite was oxidized to cerussite (PbCO_3) and then to PbO_2 i.e. Pb(IV). The dimensions of hydrocerussite reported by them are of 3-10 μm length thin hexagonal plates. Some of these plates oxidized to quasi prismatic structures which are needle like structures found to be 2-7 μm long and identified as cerussite by Liu et al., (2006). The results in this work are consistent with the above observations in that the dimensions of hexagonal & needle like structures are approximately the same.

Low and medium doses of both phosphate and silicate inhibitors showed presence of both hydrocerussite and cerussite. Except BOP all other inhibitors at high doses resulted in the surface solids to be mostly pencil like crystals of cerussite in the distinct growth areas with only small amounts of hydrocerussite. Figure 5.1 image images on top are for electrodes exposed to 0.5 mg P/L of OP. Top left image shows a typical growth

area on the general surface observed for the inhibitors used in the study while top right image shows the growth area has both hexagonal crystals suspected to be hydrocerussite as well as pencil like crystals suspected to be cerussite. EDS revealed the composition was about 33 % Pb, 54 % Sn ,7 % O, 4 % C, up to 1 % P and Si each and traces of Ca. The image on bottom left shows electrode exposed to medium dose OP (1 mg P/L) with predominant hexagonal structures suspected to be hydrocerussite. The image on right bottom shows the general surface of the electrode exposed to the control at pHs. The pH controls lacked distinct growth areas of scale structures; the numerous holes seen in the image are suspected to be pits and were consistently observed.

In general all P & Si inhibitors used showed abundance of cerussite the longer pencil like crystals for low dose; the medium dose showed presence of both pencil like structures and hexagonal structures, while the high dose showed abundance of the hexagonal structures. Hence both the P & Si inhibitors used appeared to retard the transformation of hydrocerussite to cerussite. The electrodes were ideally 50 % Pb and Sn each when new; and the consistent lower Pb content relative to Sn remaining after the study suggested selective leaching of Pb due to galvanic coupling with Sn the nobler metal.

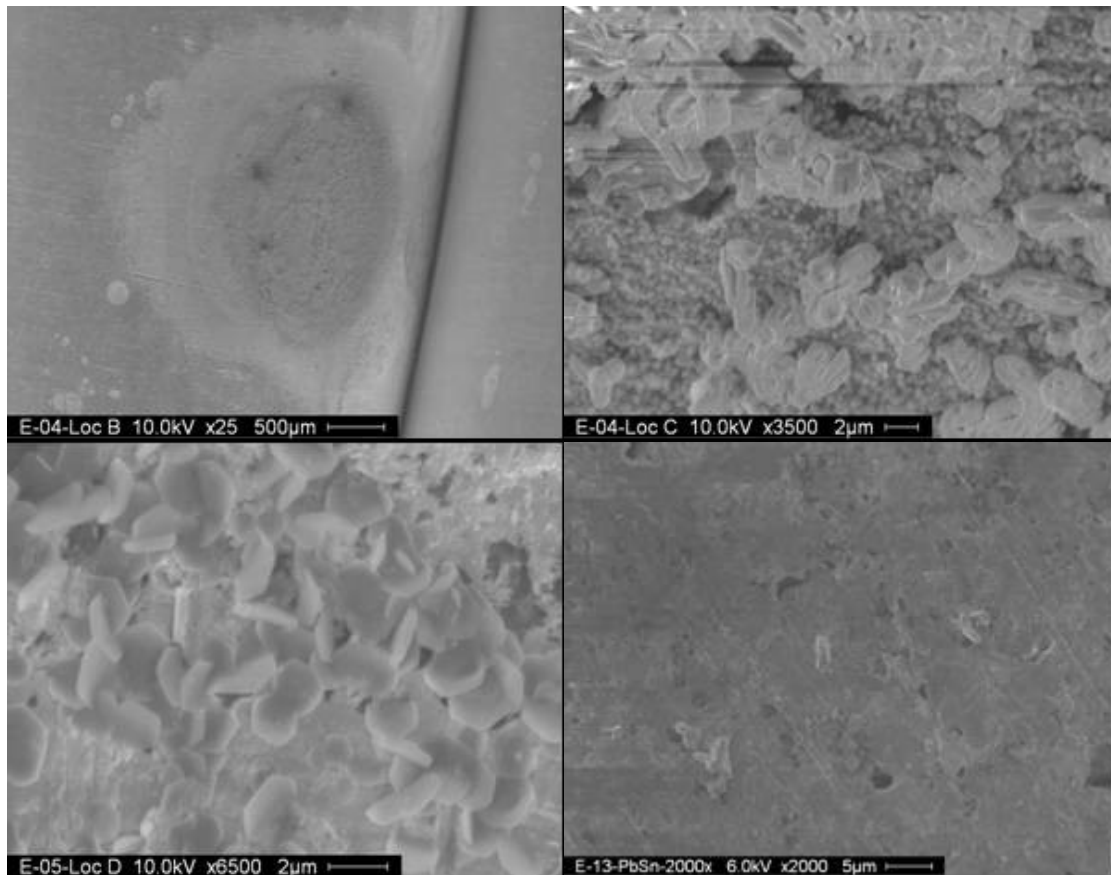


Figure 7.1 SEM of Pb-Sn electrodes

7.3.3 Water quality correlations with EN

With reference to data presented earlier in Figure 7.1 and Table 7.2 the following observations are made. Phase II had highest sulfates and low alkalinity and highest temperature but spikes of high TPb were not observed for this phase. This observation is significant in that a high sulfate and hence low CSMR prevented spikes in TPb release even at the highest temperature in this study which occurred in phase II. Correlations between Pb EN parameters were assessed to determine if the parameters were independent. The highest Pearson's linear correlation (R^2) amongst the 12 EN parameters

was 0.30 for the correlation of $LPRCR_{Pb}$ and $HMCR_{Pb}$, which indicates that confounding of EN parameters was not an issue.

Figure 7.2 shows TPb release and CSMR declined exponentially as $LPRCR_{Pb}$ increased. Hence the higher corrosion rates from this study were associated with low TPb release and a low CSMR. With a high CSMR, TPb release showed an increasing trend and had low corrosion rates. Low corrosion rates were observed to have a wide range of low to high TPb release and CSMR and hence TPb release which was mostly particulate was associated with a high corrosion product (CP) release. Low corrosion rates were inversely proportional to TPb release. These observations were also observed for PF_{Pb} in that high values correlated with low CSMR and low TPb CP release and vice versa.

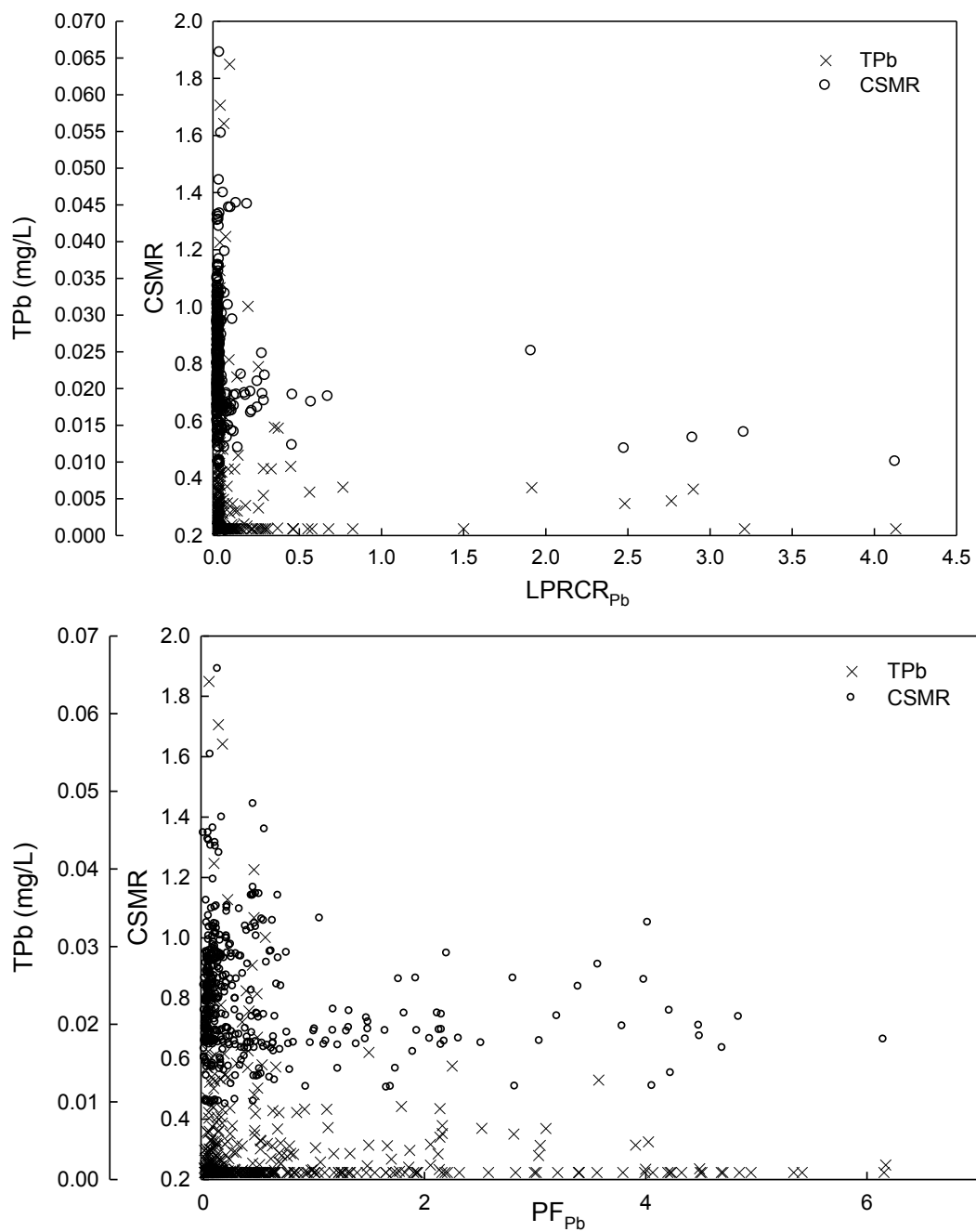


Figure 7.2 Water quality correlations with LPRCR_{Pb} and PF_{Pb}

From previous studies a $PF \ll 1$ is considered to be an indication of a more or less constant general corrosion rate where as PF consistently approaching one may indicate actual pitting or a widely varying general corrosion (Cottis & Turgoose, 1999;

Eden, 1994). The values of PF_{Pb} calculated by the EN equipment (CET) used in this study do not limit the values to unity, but PF_{Pb} herein is the ratio of the standard deviation of naturally occurring current from ECN to the mean current from HDA technique and is shown in Equation 7.1. From Equation 7.1, it is observed that for a low mean general corrosion current density I_{corr} near zero, misleadingly high values of PF_{Pb} would be generated, although aggressive localized corrosion may not be occurring. Hence a high PF_{Pb} from this study may or may not have indicated localized corrosion but likely indicated a widely varying general corrosion rate.

$$PF = \frac{\sigma}{(I_{corrHDA})} \quad \text{Equation 7.1}$$

where σ_i = standard deviation of corrosion current density from ECNCR
 I_{corr} = mean corrosion current density from HDA

7.3.4 Statistical EN models for Pb release

Regression models were developed using EN parameters to predict metal release for both total and dissolved forms of Pb. The models used dummy variables to segregate the effect of inhibitor dose by inhibitor type. The effects of the EN parameters and temperature were included in the model without regard to inhibitor type. Models using all 12 EN parameters did not converge. Subsequent modeling attempts using reduced sets of EN parameters eventually produced a model based on $LPRCR_{Pb}$, $HMCR_{Pb}$, $ECNCR_{Pb}$, PF_{Pb} and $PKRT_{Pb}$. Sequential removal of single EN variables which was statistically insignificant ($p > 0.05$) resulted in a total lead release model based on $LPRCR_{Pb}$, $HMCR_{Pb}$, and PF_{Pb} . The model for TPb using these 3 EN parameters and

dummy variables is presented with all variables in Equation 7.2. This model suggests an increase in phosphate, or silicate from any inhibitor will decrease TPb release due to the negative exponent for TP, and SiO₂. The number of significant EN parameters in this model indicates lead release was caused by general and localized corrosion. This is in agreement with the water quality (WQ) TPb release model developed from this study (Taylor et al., 2007). The WQ TPb release model developed from this study is presented in its full form in Equation 7.3 for comparison. Both models for TPb i.e. EN and WQ were statistically significant at 95 % confidence and had a R² of 0.55.

$$\begin{aligned}
 TPb = & LPRCR_{pb}^{0.217} \times HMCR_{pb}^{0.337} \times P_{pb}^{-.347}) \times 1.58 \times 10^{-5} \times BOP \times TP^{-.805} \quad \text{Equation} \\
 & + .53 \times 10^{-5} \times OP \times TP^{-1.188} + 1.49 \times 10^{-5} \times ZOP \times TP^{-1.784} \times Zn^{0.735} \quad 7.2 \\
 & + 1.56 \times 10^{-5} \times Si \times SiO_2^{-1.326} + .83 \times 10^{-5} \times pH_s) \times Temp^{3.67}
 \end{aligned}$$

where TPb = total lead, mg/L
 LPRCRPb = Corrosion rate from linear polarization for lead (mpy)
 HMCRPb = Corrosion rate from harmonic distortion for lead (mpy)
 PFPb = pitting factor for lead (unit less)
 BOP = BOP inhibitor (0, 1)
 OP = OP inhibitor (0, 1)
 ZOP = ZOP inhibitor (0, 1)
 Si = Silica inhibitor (0, 1)
 pHs = pH control (0, 1)
 TP = total phosphorus, mg/L as P
 Zn = zinc, mg/L
 SiO₂ = silica, mg/L as SiO₂
 Temp = Temperature, oC
 1 mpy = 0.0254 mm/year

$$\begin{aligned}
 TPb = & 6.64 \times 10^{-5} BOP \times TP^{-.283} + 1.94 \times 10^{-5} OP \times TP^{-.47} \quad \text{Equation 7.3} \\
 & + 1.08 \times 10^{-5} ZOP \times TP^{-.892} \times Zn^{-.824} + 1.80 \times 10^{-5} Si \times SiO_2^{-.16} \\
 & + 1.14 \times 10^{-5} pH_s) \times H^{-.75} \times T^{1.98} \times O_4^{-.54} \times Temp^{2.94}
 \end{aligned}$$

where pH = -Log [H⁺]

Alk = alkalinity, mg/L as CaCO₃
Cl = chloride, mg/L
SO₄ = sulfate, mg/L
Temp = Temperature, oC

The TPb WQ model suggests that elevation of pH and sulfate concentration both reduce total lead concentration. This effect is expressed by the negative exponent on these water quality variables. Increases in chloride and temperature are associated with increases in total lead concentration due to the positive exponent on these variables. Inhibitor addition would result in an increase in the concentration of total phosphorus, zinc, and and/or silica. The exponents associated with these water quality variables are all negative, supporting a beneficial effect of all study inhibitors. The temperature exponent (3.67) for the total lead release EN model Equation 7.2 suggests that lead release is very sensitive to temperature and higher temperature will increase total lead release. A change in temperature from 10°C to 30°C which was the range for this study would increase the temperature effect by the ratio $(30/10)^{3.67}$ i.e. by 56 times all other factors being equal.

Figure 7.3 shows TPb release for the entire study with symbols for each phase. All the highest Pb release data occurred in Phase III. Though both Phase II and III had the higher temperatures in this study, phase II had the highest sulfates due to higher surface water in the blend and consequently a lower CSMR of 0.527 compared with that of III which was 0.875. Since EN parameters correlated with CSMR the EN model predictions are consistent with the data in that the highest PF_{Pb} values were consistently observed in phase II, and from Equation 7.2 the negative exponent for PF_{Pb} suggests a reduction in TPb release. For this study PF_{Pb} correlated negatively with sulfates. The WQ

TPb release model presented in Equation 7.3 had a negative exponent for sulfate and suggests TPb release would be higher in phase III than phase II as was observed.

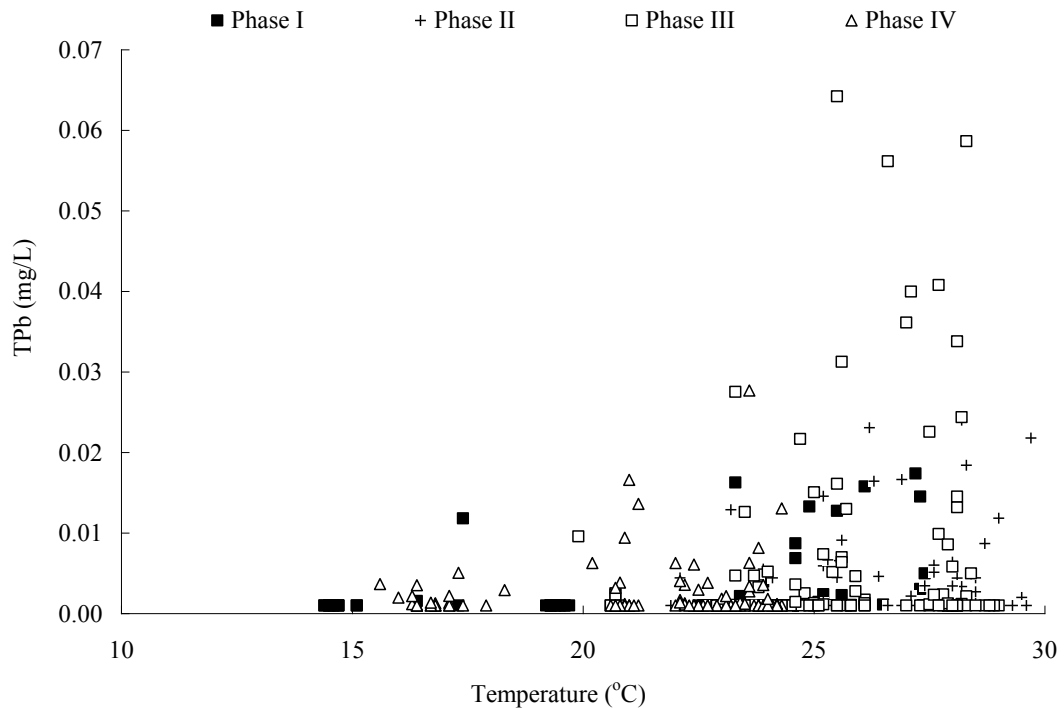


Figure 7.3 Temperature vs TPb by phase

Figure 7.4 top image shows the fit of the TPb EN model predictions with the actual observations for all phases with a diagonal line for perfect fit. The model fits decently at the higher concentrations of lead. The model also shows that lead release is highest for pH controls and all inhibitors reduced TPb release. Dissolved lead (DPb) EN and WQ models were developed from this study and were very similar to the TPb model. The best fit model for DPb using these 3 EN parameters and dummy variables is presented with all variables in Equation 7.4, and the best fit WQ DPb model is presented in Equation 7.5. Observations were similar to the TPb EN model in that inhibitors

mitigated Pb release. The best fit DPb models by EN and WQ were statistically significant at 95 % confidence and had a R² of 0.57 and 0.44 respectively.

Figure 7.4 bottom image shows the fit of the DPb EN model predictions with the actual observations for all phases with a diagonal line for perfect fit. The DPB WQ model had alkalinity term as statistically significant. Elevation of pH and sulfate both are shown in the model to offer a reduction in dissolved lead concentration. This effect is evidenced by a negative exponent on those variables. In contrast, increases in alkalinity, chloride, and temperature all contribute to increased DPb release.

$$\begin{aligned}
 DPb = & LPRCR_{pb}^{0.189} \times IMCR_{pb}^{0.281} \times F_{pb}^{-.297} \times 1.09 \times 10^{-7} \times BOP \times P^{-.115} \quad \text{Equation 7.4} \\
 & + 1.78 \times 10^{-7} \times OP \times P^{2.550} + 1.72 \times 10^{-7} \times ZOP \times P^{-.690} \times n^{0.580} \\
 & + .92 \times 10^{-7} \times Si \times SiO_2^{-.088} + 1.3 \times 10^{-7} \times pH_s \times emp^{2.96}
 \end{aligned}$$

where TPb = total lead, mg/L

$$\begin{aligned}
 DPb = & 1.69 \times 10^{-7} BOP \times P^{0.252} + .63 \times 10^{-7} OP \times P^{-.545} \quad \text{Equation 7.5} \\
 & + .37 \times 10^{-7} ZOP \times P^{0.083} \times n^{-.108} + 1.45 \times 10^{-7} Si \times SiO_2^{-.11} \\
 & + 1.76 \times 10^{-7} pH_s \times H^{-.35} Alk^{0.882} \times Cl^{2.00} \times SO_4^{-.52} \times emp^{2.84}
 \end{aligned}$$

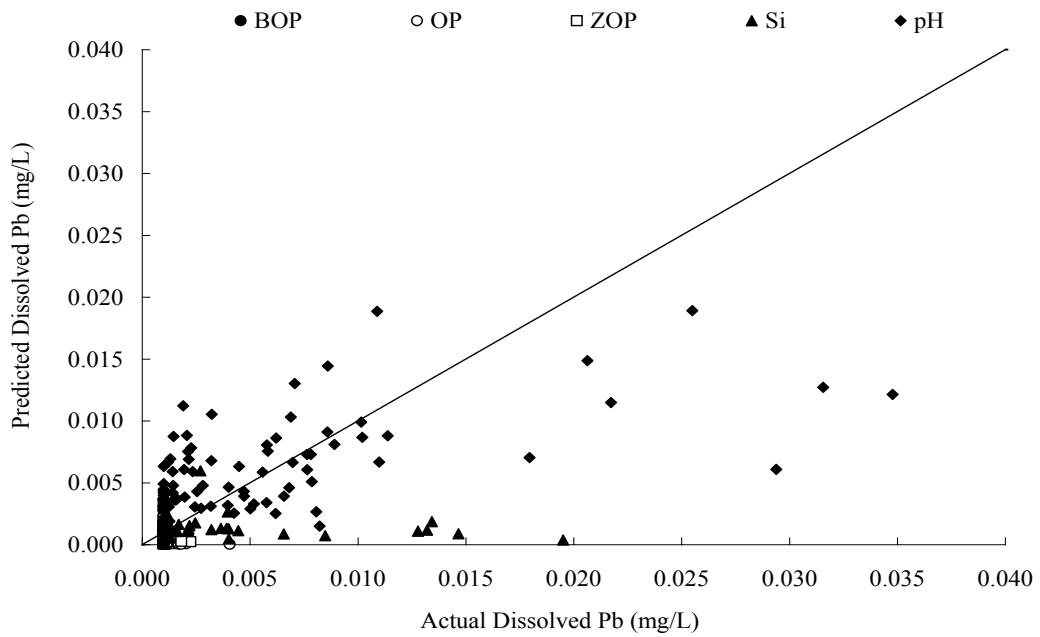
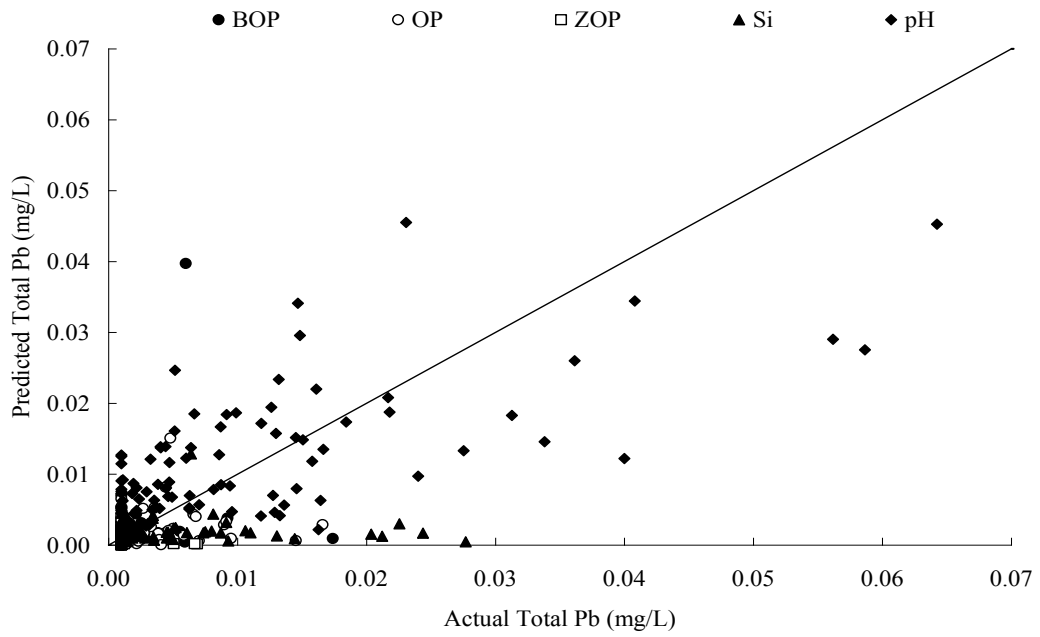


Figure 7.4 EN model predicted TPb (top) and DPb(bottom) against actual data.

7.4 Conclusions

The primary inferences from this study are summarized below:

- The Pb-Sn electrodes showed a distinct lack of general scale but had distinct growth areas with hydrocerussite and cerussite scales; both P & Si inhibitors used appeared to retard the transformation of the former to the latter with increasing dose. Though both P & Si inhibitors mitigated TPb release possibly due to formation of phosphate or silicate films the long term oxidation to Pb(IV) oxides may be hindered by inhibitors.
- $LPR_{CR_{Pb}}$ and PF_{Pb} were correlated with water quality in that correlations between corrosion rates and PF for Pb were meaningful with CSMR. Corrosion rates were negatively correlated with Pb release for this study which was due to the release of Pb CP after Pb had already been oxidized.
- EN empirical regression models were developed from this study to predict Pb release and did equally well as the water quality models developed from this study. This suggests the potential advantage of using EN which has a rapid turn around and offers remote monitoring capability to proactively identify adverse water quality changes for Pb release.

7.5 Acknowledgements

The University of Central Florida (UCF) and UCF project team wish to express their sincere gratitude to Tampa Bay Water (TBW); Hillsborough County, Fla.; Pasco County, Fla.; Pinellas County, Fla.; City of New Port Richey, Fla.; City of St. Petersburg, Fla.; and City of Tampa, Fla. which are the Member Governments of TBW and the American Water Works Association Research Foundation (AwwaRF) for their support and funding for this project.

7.6 References

1. AWWA (American Water Works Association), 1996. Internal Corrosion of Water Distribution Systems, second ed. AWWA, Denver CO.
2. Cottis, R., and Turgoose, S., 1999. Electrochemical impedance and noise. NACE international. Corrosion testing made easy. ISBN 1-57590-093-9.
3. Dodrill, D.M., and Edwards, M., 1995. Corrosion control on the basis of utility experience. . Am. Water Works Assoc. 87 (7)74
4. Dudi, A., and Edwards, M., 2005. Galvanic corrosion of lead bearing plumbing devices. (AWWA) Annual Conference and Exposition. San Francisco, CA.
5. Eden, D.A., 1994. Comments on: Electrochemical noise analysis of iron exposed to NaCl solutions of different conductivity. J. Electrochemical Soc. 141(5), 1402-1404.
6. Eden, D.A., 1998. Electrochemical Noise-The first two octaves. Corrosion 1998. National Association of Corrosion Engineers (NACE) conference. Paper No 386.
7. Edwards, M., Jacobs, S., and Dodrill, D., 1999. Desktop guidance for mitigating Pb and Cu Corrosion By-Products. . Am. Water Works Assoc. 91 (5), 66-77. 13.
8. Liu, H., Korshin, G.V., Ferguson, J.F., and Jiang, W., 2006. Key Parameters and Kinetics of Oxidation of Lead (II) Solid Phases by Chlorine in Drinking Water. Water Practice & Technology (1)4. IWA Publishing doi: 10.2166/WPT.2006092
9. Korshin, G.V., Ferguson, J.F., and Lancaster, A.N., 2005. Influence of natural organic matter on morphology of corroding lead surfaces and behavior of lead-containing particles. Water research. 39, 811-818.
10. Korshin, G.V., Ferguson, J.F., and Lancaster, A.N., 2000. Influence of natural organic matter on the corrosion of leaded brass in potable water. Corrosion Sci., 42, 53-66.
11. MacQuarrie, D.M., Mavinic, D.S., and Neden, D.G., 1997. Greater Vancouver Water District drinking water corrosion inhibitor testing. Canadian J. Civil Engg. 24, 34-52.
12. McNeill, L.S., and Edwards, M., 2004. Importance of Pb and Cu particulate species for corrosion control. J. Enviro. Engg. February 2004, 136-144.
13. Schock, M.R., 1980. Response of lead solubility to dissolved carbonate in drinking water. J. Am. Water Works Assoc. 72(12), 695-704.
14. Schock, M.R., 1989. Understanding corrosion control strategies for lead Response of lead solubility to dissolved carbonate in drinking water. J. Am. Water Works Assoc. 81(7), 88-110.
15. Schock, M.R., Gardels, M.C., 1983. Plumbosolvency reduction by high pH and low carbonate-solubility relationships. J. Am. Water Works Assoc. 75(2), 87-91.
16. Standard Methods for Examination of Water & Wastewater., (1999). 20th ed. APHA, AWWA & WPCF. ISBN 0-87553-235-7
17. Tang, Z., Hong, S., Xiao, W., and Taylor, J., 2006. Impacts of blending ground, surface and saline waters on lead release in drinking water distribution systems. Water Research 40, 943-950.
18. Taylor, J.S., Dietz, J.D., Randall, A.A., Norris, C.D., Alshehri, A., Arevalo, J.M., Guan, X., Lintereur, P., MacNevin, D., Stone, E., Vaidya, R., Zhao, B.,

- Glatthorn, S. and Shekhar, A., 2007. Control of distribution system water quality in a changing water quality environment using inhibitors. Draft final report submitted to AWWA Research Foundation Denver CO and Tampa Bay Water. (TBW II report)
19. Taylor, J.S., Dietz, J.D., Randall, A.A., Norris, C.D., Mulford, L.A., Arevalo J.M., Imran, S., Le Puil, M., Liu, S., Mutoti, I., Tang, J., Xiao, W., Cullen, C., Heaviside, R., Mehta, A., Patel, M., Vasquez, F., and Webb, D. 2005. Effects of Blending on Distribution System Water Quality. AWWA Research Foundation Denver CO and Tampa Bay Water. (TBW I report).
 20. Triantafyllidou, S., and Edwards, M., 2006. Effect of coagulant selection on lead leaching: Effect of the chloride to sulfate mass ratio. AWWA Water quality technology conference (WQTC). Denver CO.
 21. US Environmental Protection Agency, 1993. Seminar Publication: Corrosion of lead and copper in drinking water. EPA/625/R-93-001.

8 SUMMARY OF FINDINGS

Electrochemical corrosion monitoring referred to as EN in this dissertation was correlated with Fe, Cu and Pb release in a changing water quality environment with phosphate and silicate inhibitors and pH controls. The water quality parameters of alkalinity, chlorides, sulfates, Larson's ratio modified to include temperature (LR1T), monochloramine residual and chloride to sulfate mass ratio (CSMR) were correlated with EN parameters from either or all of these metals. This suggested that EN parameters can be considered similar to water quality in that they correlated with different concentrations of metal release in this study. Specific inferences from this study are summarized below:

- EN was related to Cu release and can be used to proactively minimize Cu violations of the Lead and Copper Rule. PF_{Cu} consistently correlated with water quality. Development of transient Cu release water quality may have suffered from kinetic limitations of not achieving a true equilibrium during this study period of 3 months per phase; however EN parameters respond in real-time to existing redox reactions occurring on metal surfaces. Data from this pilot scale study shows that LPRCR can be used to correlate with TCu release and EN models were successfully demonstrated to predict transient Cu release concentration in a changing water quality environment.

- Correlations between PF for Fe were meaningful with LRIT. PF for Fe correlated positively with chloramine residual loss in the PDSs in this study and an empirical regression model was developed to predict this chloramine loss using PF_{Fe} .
- Correlations between LPRCR and PF for Pb were meaningful with CSMR. Corrosion rates were negatively correlated with Pb release for this study which suggests that particulate Pb CP release occurred after Pb had already been oxidized.
- EN empirical regression models were developed to predict Fe, Cu and Pb release concentrations and did equally well as the water quality models developed from this study. This suggests the potential advantage of using EN which has a rapid turn around and offers remote monitoring capability to proactively identify adverse water quality changes for metal release.